DISSERTATION

Synthesis of Quinoxaline Dioxocyclams, Analysis of Their DNA Binding and Cleaving Properties and Progress Toward the Synthesis of Ruthenium(II) Terpyridine-Capped Dioxocyclams

Submitted by
Jory James Wendling
Department of Chemistry

In partial fulfillment of the requirements
for the degree of Doctor of Philosophy
Colorado State University
Fort Collins, Colorado
Summer 2003

COLORADO STATE UNIVERSITY

August 7, 2003

WE HEREBY RECOMMEND THAT THE DISSERTATION PREPARED UNDER OUR SUPERVISION BY JORY WENDLING ENTITLED SYNTHESIS OF QUINOXALINE DIOXOCYCLAMS AND ANALYSIS OF THEIR DNA BINDING AND CLEAVING PROPERTIES AND PROGRESS TOWARD THE SYNTHESIS OF RUTHENIUM(II) TERPYRADINE CAPPED DIOXOCYCLAMS BE ACCEPTED AS FULLFILLING IN PART REQUIREMENTS FOR THE DEGREE OF DOCTOR OF PHILOSOPHY.

Committee on Graduate Work

Richard G. Finke

Steven H. Strauss

Yian Shi

Erica L. Suchman

Louis S. Hegedus / Advisor

C. Michael Elliot / Department Head / Director

ABSTRACT OF DISSERTATION

SYNTHESIS OF QUINOXALINE DIOXOCYCLAMS, ANALYSIS OF THEIR DNA BINDING AND CLEAVING PROPERTIES AND PROGRESS TOWARD THE SYNTHESIS OF RUTHENIUM(II) TERPYRADINE CAPPED DIOXOCYCLAMS

A new class of dioxocyclams containing appended quinoxaline chromophores linked in various spacial orientations were synthesized and tested for their ability to bisintercalate and oxidatively cleave plasmid DNA. The circular-DNA unwinding test revealed no evidence for bisintercalation with either the dioxocyclams or their nickel(II) complexes. However, the DNA cleaving ability of these complexes was found to be directly dependent upon both the nature and spacial orientation of the appended quinoxaline moieties. These results imply at least a transient association of the nickel(II) complexes with DNA.

Progress was made in the synthesis of a new class of dioxocyclam structures. These structures feature a terpyradine moiety appended to a "capped" dioxocyclam. Eventually, a variety of metals will be incorporated into these systems and they will be tested for their electrical, magnetic, and photochemical properties.

Jory James Wendling

Department of Chemistry

Colorado State University

Fort Collins, CO 80523

Fall 2003

TABLE OF CONTENTS

CHAPTER 1:

INTRODUCTION

I. Dioxocyclams 1

A. Dioxocyclams as Novel DNA Cleaving/Binding Agents 2

II. DNA oxidation 3

A. Direct vs. Induced Strand Scission 4

B. Transition Metal-Catalyzed Oxidation 6

1. Guanine Oxidation by Transition Metal Complexes 8

a. Nickel(II) Macrocycles as RNA Structure Probes 11

b. Mechanism of DNA Oxidation by Nickel(II) Macrocycles 12

c. Fate of Oxidized Guanine 16

III. Development of DNA Intercalating Agents 17

A. Bifunctional Intercalators 19

1. Conformational Heterogeneity 22

2. Sequence-Selectivity 23

3. The Nature of Binding and Cytotoxicity 25

B. Reaction of Metallointercalators with DNA 28

1. Metallointercalators as Probes for RNA Structure 30

2. Metal Complexes as DNA Bisintercalators 31

3. Combining Bisintercalation and DNA Oxidation 33

IV. Hypothesis and Goals 35

RESULTS AND DISCUSSION

V. Synthesis of Dioxocyclams/Project Background 36

A. Quinoxaline ether cyclam synthesis 41

B. Attempted Synthesis of a 2-Hydroxyquinoxaline Analog 46

C. Extended Quinoxaline Amide Cyclam Synthesis 47

D. Extended Chiral Quinoxaline Amide Synthesis 52

E. DNA Bisintercalation Studies 53

F. DNA Cleavage Studies 54

VI. Conclusion 56

VII. Experimental 57

VII. References 74

CHAPTER 2

INTRODUCTION 78

I. Rational 81

II. Results and Discussion 83

III. Conclusions / Future Plans 88

IV. Experimental 91

V. References 92

Appendices 93

CHAPTER 1

Introduction

1. Dioxocyclams

Considered intermediate between cyclams and cyclic peptides, dioxocyclams are 14-membered tetraazamacrocycles with two amides and two amines within the ring (Figure 1). Tabushi synthesized the first dioxocyclams; however, the amides were reduced to form a cyclam, leaving the dioxocylams virtually unstudied. Kimura later saw the potential of these tetraazamacrocycles and has extensively studied various dioxocyclams and their metal complexes. Although the starting materials were generally inexpensive, these syntheses were inefficient, multiple component condensations.[1-4]

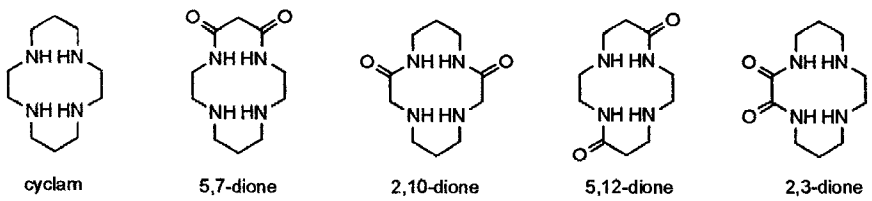

Figure 1. A cyclam and various dioxocyclam isomers.

In contrast, a very efficient synthesis of dioxocylams has been developed in the Hegedus laboratories.[5-8] Hegedus's method for synthesis of 5,12-dioxocyclams was discovered accidentally, while attempting to synthesize penicillin analogs using chromium carbene complexes. The assumed mechanism involves an acid-catalyzed ring opening of the azapenam to form a seven-membered ring imine (Scheme 1). Dimerization followed by reduction of the ring imines produced a stable, saturated dioxocyclam. Like cyclams, dioxocyclams also form stable complexes with a range of transition metals, including nickel. Upon metal complexation, the amide protons of the

dioxocyclam become acidic; deprotonation of the amide protons produces an overall neutral complex.

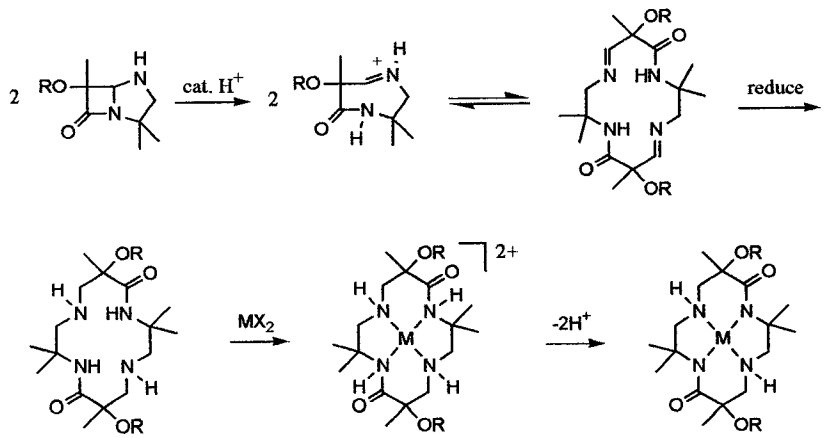

Scheme 1. Hegedus's 5,12-dioxocyclam synthesis and metal complexation.

A. Dioxocyclams as Novel DNA Cleaving/Binding Agents

An interesting feature of the 5,12-dioxocyclams produced in the Hegedus group is that they can contain alkoxy groups in the apical positions (-OR groups in Scheme 1). The research presented below is based upon the idea that attachment of DNA binders to these positions could potentially give rise to novel DNA cleaving/binding agents (Scheme 2). Many attempts have been made to find compounds that combine strong DNA affinity with slow dissociation from DNA. These properties, especially the latter, are considered to be important for antitumor activity.[9-12] Since the regulation of gene expression is based upon the sequence-selective recognition of nucleic acids by repressor, activator, and enhancer proteins, small molecules that selectively bind DNA and activate or inhibit gene expression hold significant promise as therapeutics. Unfortunately, the discovery of such agents has been slow, mainly because of the complexity associated

with understanding small molecule-DNA interactions, and the technically demanding techniques involved in the determination of their binding affinity for a given sequence.

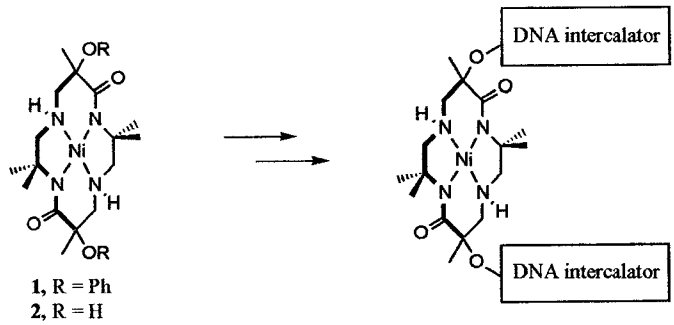

Scheme 2. Original idea for creating novel DNA cleaving/binding agents.

II. DNA Oxidation

The electron-rich purine and pyrimidine heterocycles of DNA (Figure 2) are prime targets for reaction with electrophiles (alkylating agents, halogens, and oxidizing agents). Some of the best-known electrophiles for reaction with DNA are the mustard gases. These historically significant alkylating agents caused over 400,000 casualties in World War I. It wasn't until after World War II however, that their mutagenic activity was investigated.[13-16] Early studies showed that the mustards readily react with the electron-rich sites of nucleobases, especially guanine's N7. It was later discovered that guanine N7 alkylation can lead to depurination of the nucleobase and ultimately strand scission at that site.[17,18] This information led to the use of one of the war gasses, dimethyl sulfate, as a reagent for the Maxam-Gilbert G-specific sequencing reaction.[19,20]

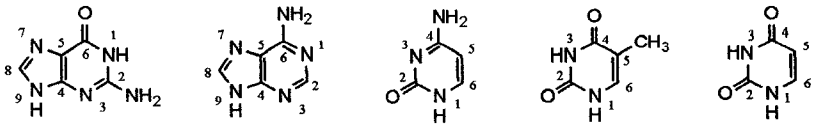

Figure 2. Numbering scheme for the nucleobases.

A similar story exists for nucleobase oxidation. Although radiation-induced illness was known in the early 1900's (indeed, Pierre and Marie Curie both suffered from it) it wasn't until after World War II that the effects of ionizing radiation on DNA were investigated.[21,22] As with alkylation, oxidation chemistry is often focused on the nucleobase guanine; in fact, the analogies between nucleobase oxidation and alkylation are what led to the term "radiomimetic" being applied to the mustard mutagens.[23]

A. Direct vs. Induced Strand Scission

Although oxidizing agents rarely lead to direct strand scission, they do allow DNA or RNA cleavage to occur site-specifically in a second chemical step that can involve base or treatment with an enzyme (Scheme 3). Alkaline conditions are convenient because nucleobases are relatively stable to these conditions unless they have been chemically modified. This allows unmodified nucleosides to remain intact in the polymer, and strand scission to occur only at specifically modified sites.[24]

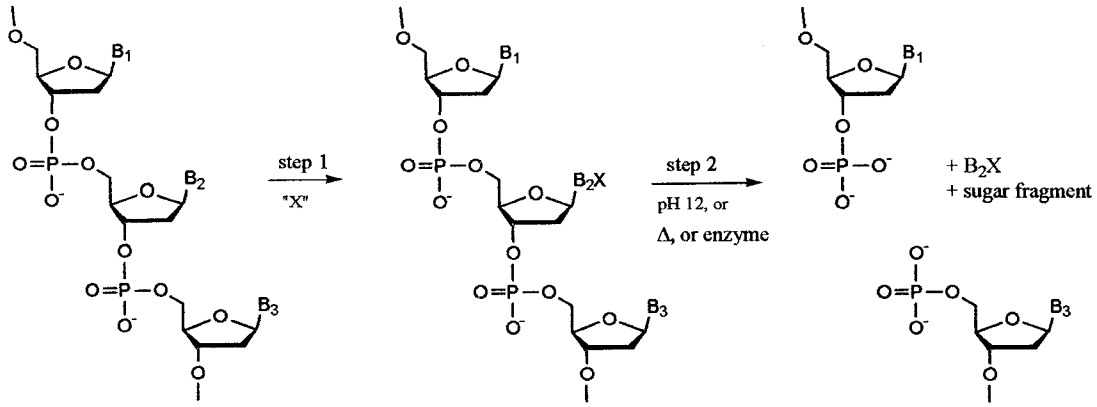

Scheme 3. General scheme for nucleobase modification by reagent "X" followed by strand scission.

In general, oxidation, alkylation, and other electrophilic reagents acting on nucleobases will remove electron density from the heterocycle, making the modified nucleobase a better leaving group.[24] When this happens, the amine can displace the nucleobase, forming a Schiff base (Scheme 4). Schiff base formation facilitates the elimination reaction by increasing the acidity of the $H^{2'}$ proton. In principle, any primary or secondary amine can catalyze phosphate elimination; in practice, piperidine and aniline are the most commonly used.

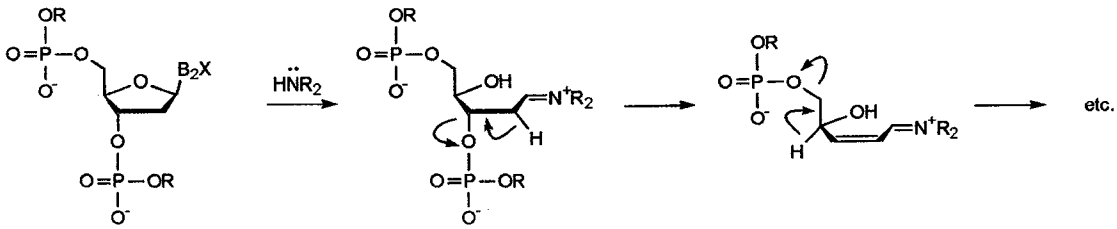

Scheme 4. Amine participation in strand scission.

If a chemical reagent demonstrates no direct DNA strand scission but does show nucleobase-specific, piperidine-labile scission, it is a good indication that nucleobase modification is the primary event. Alternatively, if piperidine only serves to enhance the strand scission already observed in its absence, the chemical modification is most likely

on the ribosyl or deoxyribosyl units. Reactions that modify the nucleobases are inherently more site-specific than those targeting the ribosyl or deoxyribosyl units since each of the nucleobases reacts differently with electrophiles. Additionally, in a structure-probing experiment it can be helpful to have the DNA or RNA polymer remain intact during the first chemical step in which nucleobases are modified so that the polymer structure is not altered until the cleavage step.[17,19]

B. Transition Metal-Catalyzed Oxidation

Most of the nucleobase modification research has been inspired by the investigations of highly toxic metals.[25] This is particularly true for the extremely carcinogenic metals, nickel and chromium. Despite their overall low concentration in biological tissues, both nickel and chromium show high accumulation in genetic material and are known carcinogens. Insoluble, particulate nickel species (such as Ni_2S_3) are especially carcinogenic because of their ability to enter a cell by phagocytosis, slowly dissolve, and eventually localize on the chromatin, mediating oxidative DNA damage (via oxidative DNA strand breaks, DNA-DNA cross-links, and DNA-protein cross-links).[26-31]

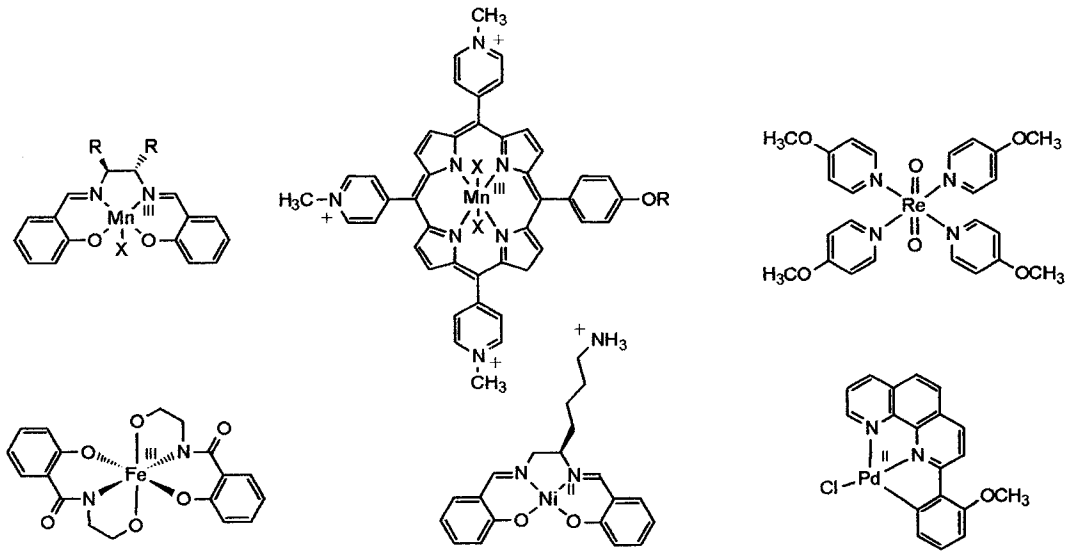

Figure 3. Various transition metal complexes capable of mediating nucleobase oxidation.

Although many transition metal complexes are capable of mediating oxidative DNA damage (several are shown in Figure 3; more will be discussed later), nickel seems to be the metal ion that is most subject to control of its redox behavior by the surrounding organic ligand. One example comes from comparing the reactivity of simple nickel(II) salts with the reactivity of simple cobalt(II) salts. With hydrogen peroxide as the oxidant, studies on isolated DNA showed that these salts react quite similarly (via guanine oxidation), although nickel is much less reactive. On the other hand, coordination of nickel(II) to polydentate ligands, especially histidine and histidine-containing peptides, greatly increases the metal's reactivity, while coordination of cobalt(II) to polydentate ligands actually decreases the metal's reactivity. *In vivo*, proteins are the principle chelators of nickel(II). The N-terminal tripeptides Asp-Ala-His of human serum albumin and Val-Ile-His from desangiotensinogen have been identified as nickel binding sites. Nickel has also been shown to bind to the Cys-Ala-Ile-His sequence of histone H3, and the resulting complex promotes oxidative damage to DNA in the presence of H_2O_2.[32-35]

1. Guanine Oxidation by Transition Metal Complexes

The versatility of nickel(II) as a DNA cleaving agent has been demonstrated by Burrows and coworkers who showed that square planar nickel complexes of tetraazamacrocycles catalytically oxidize DNA in the presence of peracid oxidants (typically monoperoxysulfate—HSO_5^-, sometimes magnesium monoperoxyphthalate or hydrogen peroxide).[35-42] They found that nickel-catalyzed oxidation of DNA by nickel(II) cyclam (Figure 4) was quite selective. When it was exposed to DNA bases paired in a standard Watson-Crick scheme, piperidine workup revealed that oxidation had occurred primarily at guanine bulges, mismatched guanine base pairs, and terminal guanine residues. In a single stranded oligonucleotide, oxidative damage occurred at every guanine in the strand. When other nucleobases were exposed in single stranded regions and coordination to guanine N7 was not possible, the order of reactivity was C > T > A. Thus, exposed C and T residues can be identified when guanines aren't exposed in the same structure. Interestingly, the copper(II) analogue of the cyclam was completely inactive for DNA oxidation under the same conditions.

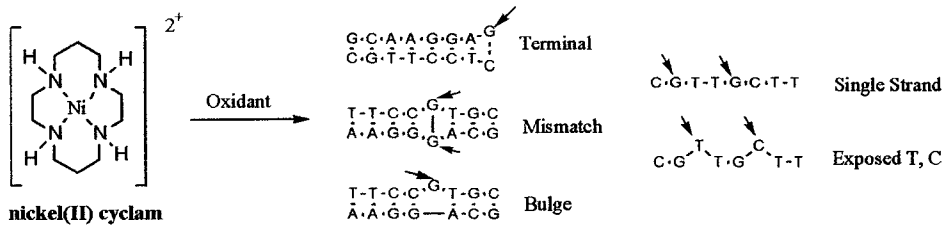

Figure 4. Sites of catalytic DNA oxidation.

Using a 167 base pair restriction fragment from pBR322, Burrows showed that nickel macrocycles such as $NiCR^{2+}$ and the nickel peptide $[NiKGH\text{-}NH_2]^+$ are also capable of mediating oxidative DNA damage when all bases are paired in a duplex

structure (Figure 5). Although oxidation is less efficient than in the above cases, guanines were still the site of oxidation leading to piperidine-mediated strand scission; however, guanines followed by a 3' purine nucleotide (especially G) were more reactive than those followed by a 3' pyrimidine. It is worth noting that single stranded sequences do not show this hyperactivity for guanines flanked by a 3' purine, reinforcing the notion that nucleobase reactivity is affected by base stacking. This 5'-GG-3' effect has been observed elsewhere, including radical, and ionizing radiation reactions, but in all cases only holds true for duplex DNA as the substrate.[37,42]

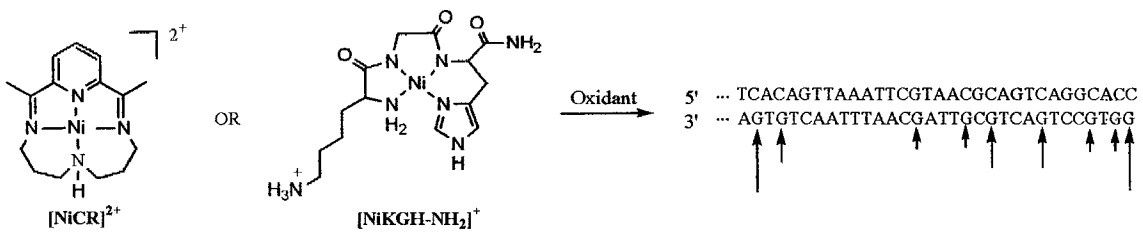

Figure 5. Relative guanine reactivities in duplex DNA.

Although a topic of much debate,[43,44] perhaps the most striking example of the nature of DNA-mediated electron-transfer reactions is from Barton and coworkers who showed that metallointercalators which can oxidize DNA bases appear to do so from a distance.[45] Figure 6 illustrates two oxidative reactions of a Ru(II) intercalator tethered to DNA. Photoexcited ruthenium(II) complexes can sensitize the formation of $^1O_2$, which can then react preferentially at nearby guanine residues, causing damage which marks the binding site (left of figure 6). Alternatively, the photoexcited Ru(II) can also be quenched by electron transfer to a surface-bound quencher such as $[Ru(NH_3)_6]^{2+}$.[46] Once quenched (right of figure 6), the Ru(III) intercalator, generated in situ, becomes a potent

ground-state oxidant, damaging DNA from a distance, by electron transfer, yielding reaction at the 5'-G of 5'GG-3'sites.

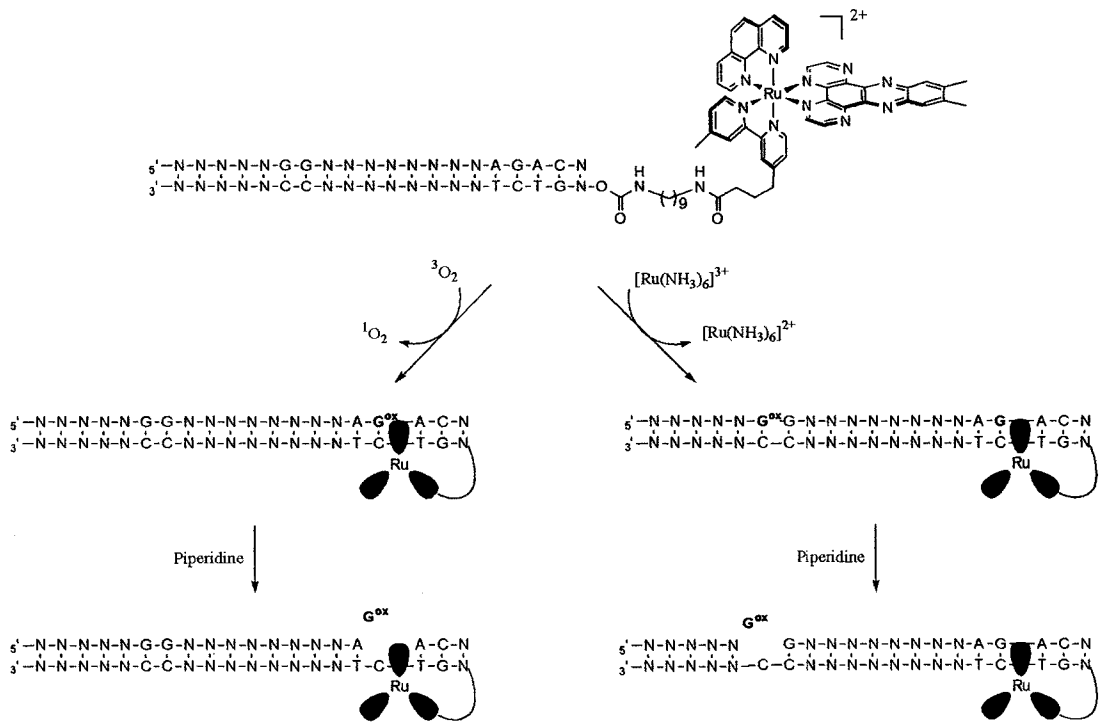

Figure 6. Singlet oxygen-dependent (left) and quencher-dependent (right) pathways to guanine oxidation by a covalently tethered ruthenium(II) complex.

Subsequent studies showed the sensitivity of the reaction to the intervening base pair stack; assemblies containing bulges inserted in the DNA between the site of oxidation and distal 5'-GG-3' doublets showed significantly diminished oxidation at the distal site.[47] In more recent studies, damage was observed at sites up to 200 Å away from the site of intercalation of the metal oxidant![48]

These reactivity patterns closely parallel the sequence dependence of guanine ionization potentials discussed by Saito, who attributes this phenomenon as being due to a π-stacking effect of purines in which the HOMO resides predominantly on the 5'-G in a purine stack.[49,50] The piperidine-sensitive reaction of a range of species at the 5'-G of 5'-

GG-3' sites has come to be regarded as a signature for electron transfer in DNA reactions. That 5'-GG-3' shows higher reactivity implies an electron-transfer mechanism is involved in these reactions and is also evidence for formation of guanine radical cation as the initial product of DNA.

a. Nickel(II) Macrocycles as RNA Structure Probes

This sensitivity to guanine exposure has led to the use of $NiCR^{2+}$ as a probe for DNA and RNA structure.[37] RNA more than DNA structures include a wide variety of conformations that significantly depart from the canonical double helix. Since the biological activity of RNA is directly related to the molecule's tertiary structure (in addition to its primary sequence), the determination of RNA structure is of supreme importance. Crystallographic methods provide the greatest resolution in identifying polynucleotide structure; however, obtaining X-ray quality single crystals is not always possible. NMR spectroscopy is a powerful tool, but its value diminishes the larger and more complicated the biopolymer. When these methods fail or become arduous, one must resort to classical methods of chemical and enzymatic modification to probe the molecule's surface features. Results from chemical and enzymatic modification have led to impressive structural details when combined with computational techniques. Such investigations require the use of a complementary set of reagents to detect solvent exposure of individual regions of the nucleobases and phosphoribose backbone. Ideally, data from a range of reagents could resolve potential ambiguities intrinsic to a particular type of modification. A number of valuable reagents such as hydroxyl radical, DNase, and RNase T1 yield direct cleavage of the backbone, which is very convenient but may

lead to changes in the native conformation during the analysis. Although the guanine-specific reagent NiCR appears to bind to its target, investigations with the well-characterized $tRNA^{Phe}$ (from yeast) showed a dramatic correlation between the electrostatic environment of guanine N7 and oxidation (Figure 7), suggesting that the binding does not perturb the dynamic equilibrium of extrahelical guanine residues. In fact, guanines in bulged or hairpin loop regions of $tRNA^{Phe}$, *Tetrahymena* group I intron, and 5S rRNA (*Xenopus lavis*) were all correctly identified by $NiCR^{2+}$. These modifications agreed with predictions based on crystal structures and most importantly, this nickel complex exhibited greater selectivity than either dimethyl sulfate or RNase T1 for characterizing tRNA.

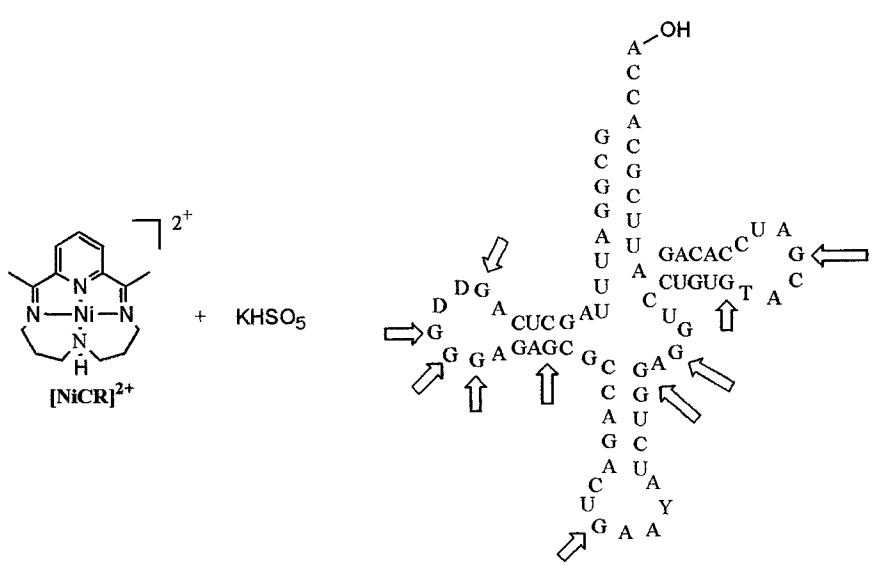

Figure 7. Bulges in tRNA that were correctly identified by $[NiCR]^{2+}$.

b. Mechanism of DNA Oxidation by Nickel(II) Macrocycles

Dervan has shown that Fe-EDTA tethered to sequence-specific DNA-binding agents in the presence of oxidants leads to formation of freely diffusible hydroxyl

radicals that oxidize the sugar and base residues in the general region in which Fe-EDTA is bound (Figure 8).[51] Such clustering of the DNA cleavage sites is the trademark of freely-diffusible oxidants such as HO·. Indeed, the use of HO· as a probe of solvent exposure of sugar moieties in folded nucleic acids has seen widespread application in both DNA[52] and RNA[53] structural studies. In contrast to this, a metal-bound oxidant leads to single site chemistry if the binding of the metal complex is site specific. That square planar nickel(II) complexes show primarily guanine specific, single site cleavage implies a mechanism that involves binding of the metal to guanine's N7. It also implies that freely-diffusing radicals are not involved in the mechanism.

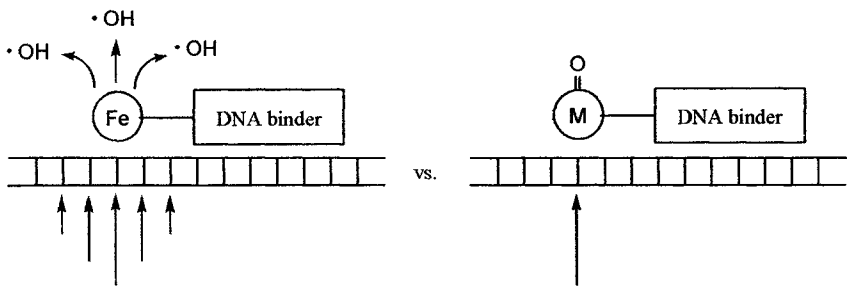

Figure 8. Clustering of DNA cleavage sites vs. single site oxidation.

To gain additional insight into the mechanism of the reaction with $NiCR^{2+}$ or $[NiKGH\text{-}NH_2]^+$ with $KHSO_5$ and DNA, alcohol quenching studies were undertaken. Although it has been shown that $SO_4^{\cdot-}$ reacts readily with the α-hydrogen of ethanol, both $SO_3^{\cdot-}$ and $SO_5^{\cdot-}$ react 10,000-fold slower. Furthermore, *tert*-butyl alcohol reacts about 1,000-fold faster with hydroxyl radical than with sulfur oxy radicals. Consistent with the idea that oxidation of DNA by $NiCR^{2+}$ or $[NiKGH\text{-}NH_2]^+$ with $KHSO_5$ produces a reactive intermediate in which nickel is ligated to $SO_4^{\cdot-}$, effectively producing a caged sulfate radical, the extent of reaction of $NiCR^{2+}$ with DNA and $KHSO_5$ was reduced by

only 20% in the presence of ethanol. Similar results were obtained with $[NiKGH\text{-}NH_2]^+$. In addition, *tert*-butyl alcohol was not able to induce significant levels of quenching.[39,40]

In sharp contrast, when ethanol was added to DNA reactions containing $CoCl_2$ and $KHSO_5$, almost complete quenching was observed. This is similar to the results of ethanol quenching experiments using photolytically-produced sulfate radical; in this case, DNA modification was reduced by 80%. These results, in addition to the lack of direct strand scission, and the guanine-specific nature of the DNA oxidation suggest that hydroxyl radical is not produced, although the production of low levels of caged hydroxyl radical cannot be ruled out.[39]

Direct interaction between nickel and guanine N7 had originally been postulated from the correlations between the efficiency of guanine oxidation and the environment surrounding its N7 position. The initial four-coordinate, square planar compounds are unlikely to be the species that binds to the DNA since they show little propensity for acquiring axial ligands. However, the +3 charge and d^7 electronic configuration of a transient nickel(III) species should have high affinity for guanine N7 since these species strongly favor additional coordination by axial ligation. Such interactions can be observed by a diagnostic conversion of poly(dG-dC) from a B- (right-handed) to Z- (left-handed) helical form. This conversion relocates guanines N7 to the exterior of the helix and facilitates metal binding. Consequently, metal ions such as nickel(II) are thought to promote formation of Z-DNA by stabilizing this structure relative to B-DNA. Circular dichroism experiments showed that neither $Ni^{II}CR$ or Ni^{II}(cyclam) **1** were able to induce a poly(dG-dC) from a B- to a Z-helix, but $Ni^{III}(cyclam)Cl_2ClO_4$ was able to induce the

helical change with greater efficiency than $NiCl_2$! This showed that the macrocyclic ligand did not prevent direct guanine N7-nickel ligation.[41,42]

Later work showed that ^1H and ^{31}P NMR spectra of NiCR ($KHSO_5$ as oxidant) and DNA containing a single, isolated extrahelical guanine are consistent with selective binding of nickel to the N7 of guanine. More evidence came with the characterization of the in situ Ni(III) intermediate generated by oxidation of Ni^{II}(cyclam) **1** by $KHSO_5$ in both the absence and presence of a 17-base pair oligonucleotide containing a guanine-rich hairpin loop d(AGTCTATGGGTTAGACT). Electronic absorption and freeze-quench EPR studies demonstrated that, within the first 30 s of the reaction, a 6-coordinate, axial Ni(III) species is formed which subsequently decays to EPR silent Ni(II) products. These results have lead to the proposed mechanism for guanine oxidation by square planar nickel (II) complexes (Scheme 5), in which the square planar nickel complex is first oxidized by $KHSO_5$ (or another oxidant) generating a nickel(III) intermediate that would be capable of forming a 6-coordinate species with the N7 of guanine as an axial ligand. Oxidation takes place via electron transfer then piperidine work-up reveals the sites of DNA damage.[40-42]

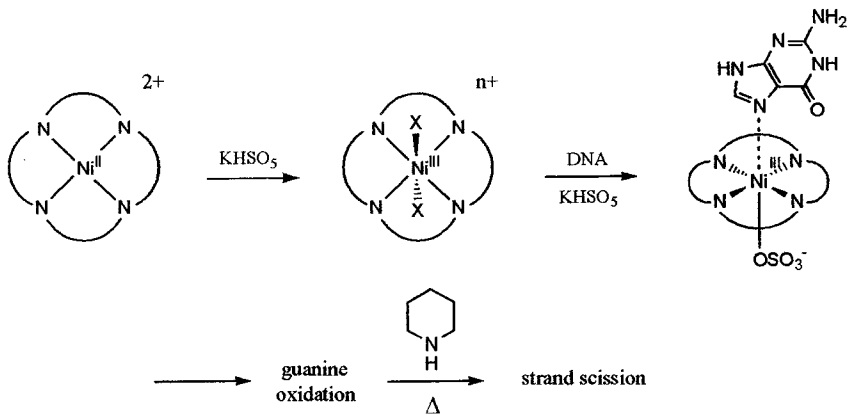

Scheme 5. A proposed mechanism for selective guanine oxidation.

c. Fate of Oxidized Guanine

Although the exact products of guanine oxidation by square-planar nickel(II) complexes are unknown at this point, 8-oxoguanine is the most common oxidative lesion in duplex DNA and is assumed to be a major product. In fact, in the reaction of nickel(II) and H_2O_2, 8-OxoG is the principle product (although other base modifications are observed to a lesser extent). The majority of oxidants are believed to react via a one-electron abstraction pathway to provide $G^{\cdot+}$, which is hydrated and further oxidized to form 8-OxoG (Scheme 6).[42]

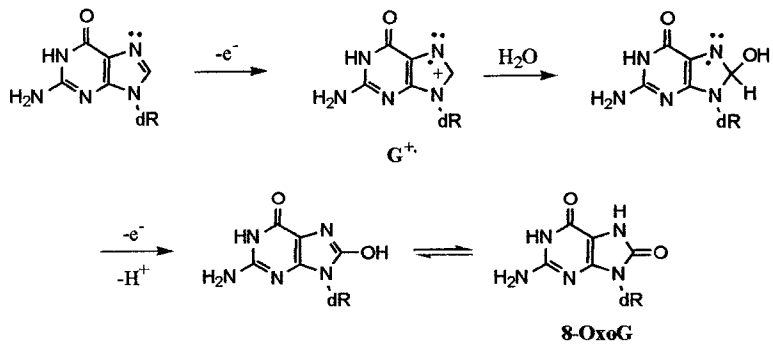

Scheme 6. Possible fate of deoxyguanosine radical cation.

Hailed as the marker of oxidative damage in the cell, 8-OxoG is such a common oxidative lesion in duplex DNA that an entire family of repair enzymes has evolved to deal with it and its mismatches. Studies have suggested that about 1 in 40,000 guanines in the genome is present as 8-oxoG under normal conditions. This means that >30,000 8-oxoGs may exist at any given time in the genome of a human cell! 8-OxoG is a problematic lesion to detect because of its inability to inhibit polymerases and its lack of piperidine sensitivity. Analysis can be further complicated by 8-oxoG's high sensitivity to further oxidation. For example, a redox potential of 0.58V vs NHE has been reported at pH 8 for 8-oxo-2'-deoxyguanosine--substantially lower than the parent nucleoside, 2'-deoxyguanosine, which has a redox potential of 1.29V vs NHE.[54,55]

III. Development of DNA Intercalating Agents

Although cells also make lipids and carbohydrates, DNA does not dictate their structure. DNA only specifies the structure of protein molecules, including enzymes that catalyze the synthesis of all classes of biological molecules. Most of the metabolic machinery of the cell is concerned in some way with protein synthesis. This is not surprising because structural proteins constitute most of the dry cell material, and functional proteins direct and underlie all cellular activities. Essentially, cells are miniature protein factories that synthesize the huge variety of proteins that determine the chemical and physical nature of cells.

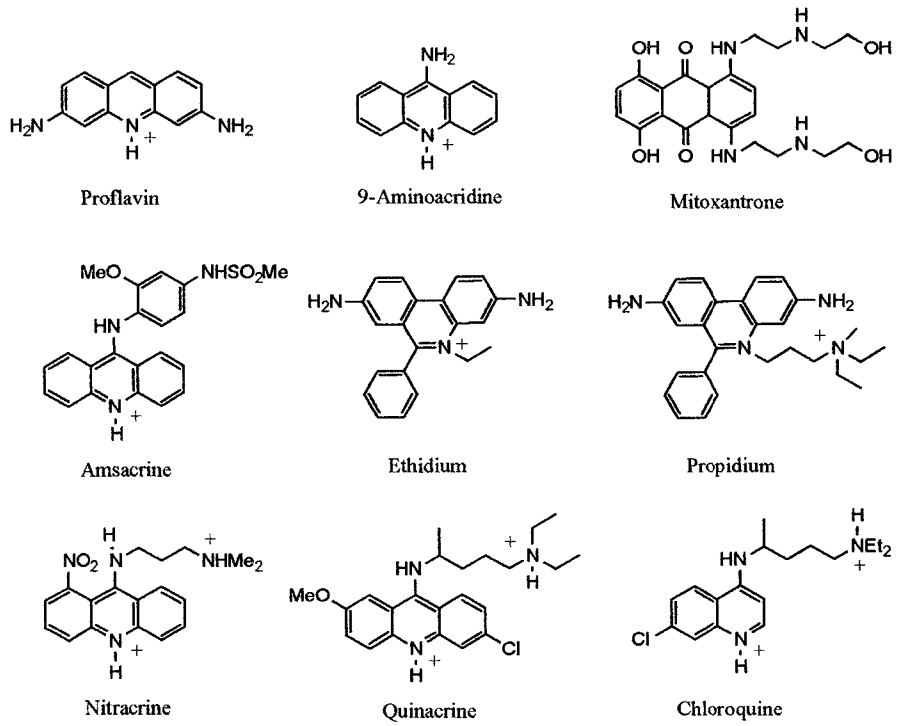

Figure 9. Intercalating agents with therapeutic uses.

Thus, it is not surprising to find that many of the active compounds discovered during the early years of the search for chemotherapeutic agents were later shown to be DNA-binding ligands. It is now known that several important examples belong to classes of compounds identifiable as intercalating agents (Figure 9). Before antibiotics and the sulfonamides, the aminoacridines proflavin and 9-aminoacridine played a significant role in wound asepsis and they still have topical antibacterial uses today. Other aminoacridines, such as quinacrine and its quinoline analogue, chloroquine, were used regularly in antimalarial therapy. Quaternary phenanthridines, such as ethidium, found use as trypanocidal agents in cattle, and the 1940s saw the discovery of the intercalating actinomycin antibiotics, which have since proven useful in the treatment of some childhood cancers.[58-61]

In 1961, Lerman[62] made the landmark contribution of proposing that proflavine intercalates into DNA, a process by which the planar acridine ring becomes inserted between the base pairs of the Watson-Crick helix. He found that proflavine binding enhanced the viscosity of DNA and lowered its sedimentation coefficient; he then proposed that the major structural distortions to the DNA were an increase in length, and a local unwinding of the helix at the intercalation site. Later, the results from his X-ray diffraction and hydrodynamic studies of the proflavine-DNA complex laid the foundation of the intercalation concept.

A. Bifunctional Intercalators

In the 1970's, much attention was devoted to efforts to develop intercalating antitumor agents. Major achievements in this area were with the anilinoacridine amsacrine, the 9-aminoacridine derivative nitracrine (Figure 9), and the broad-spectrum anthracycline antibiotic Adriamycin and its analogues. This period also saw the discovery that the antitumor quinoxaline antibiotics were bifunctional intercalating agents (Figure 10). Although literally dozens of such bisintercalating antitumor/antibiotics are known (including many synthetic analogs), the best-studied examples are echinomycin, triostin A, and sandramycin, and they will be the main focus of this discussion.[59]

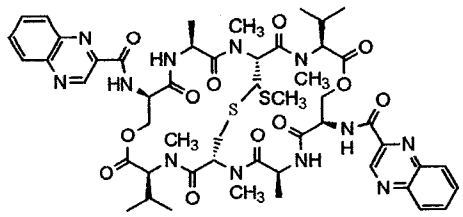

Echinomycin

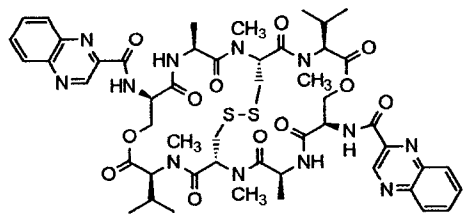

Triostin A

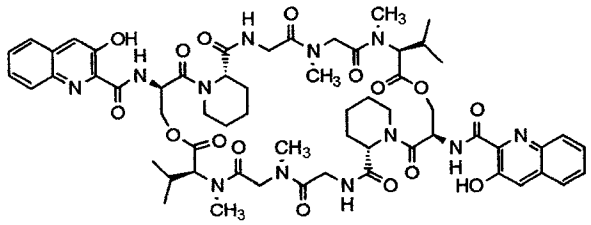

(-)-Sandramycin

Figure 10. Selected bifunctional intercalating antibiotics.

Quinoxaline antibiotics are produced by a variety of streptomycetes that are widely distributed in nature and are highly active against Gram-positive bacteria, viruses, and a variety of experimental tumors. They were first isolated and characterized in the 1950s and were later shown to be powerful inhibitors of DNA-directed RNA synthesis by virtue of their binding to DNA. The mechanism of binding remained unknown until they were subjected to the circular DNA (plasmid) unwinding test, which was then newly-invented for assessing intercalators.[63] The topological character of circular DNA leads to a direct correlation between the winding of the Watson-Crick duplex and the degree of supercoiling. Consequently, in a drug titration, intercalation-induced unwinding is first seen as a reduction in the number of naturally occurring right-handed supercoils (left side of figure 11). As the binding level increases, a point is reached where the supercoiling is completely removed, termed the equivalence point (center of figure 11). This is the point at which the sedimentation coefficient and electrophoretic mobility fall to minimum values and viscosity rises to a maximum. Binding of additional drug causes the

introduction of left-handed supercoils which increases the electrophoretic mobility and decreases the viscosity back to near original levels. These drugs were shown to cause twice the unwinding and elongation of the DNA helix as ethidium (the standard reference intercalator). Later, these effects became well established as diagnostic criteria for bis-intercalation.[64]

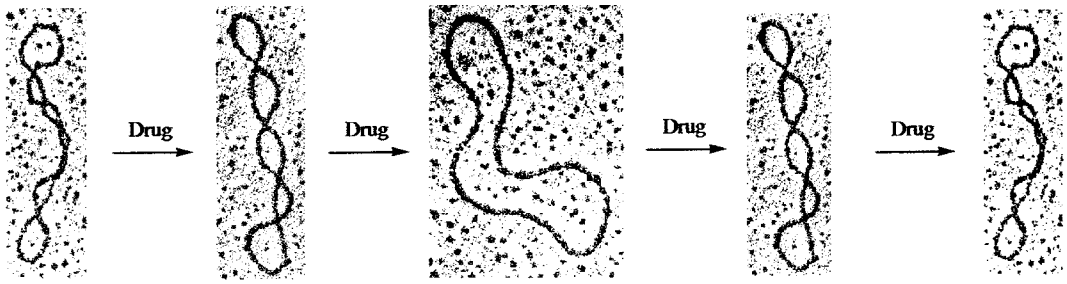

Figure 11. Electron micrographs of circular duplex DNA with various amounts of supercoiling.

It is worth noting that the binding of intercalators to supercoiled DNA has an interesting feature that may be important in the selective toxicity of these compounds towards mitochondria and other organelles containing circular DNA. At low binding densities, (the left side of figure 11) where intercalation is accompanied by progressive removal of right-handed supercoils, affinity is enhanced compared to binding to an equivalent strand of linear DNA because the free energy of ligand binding contains a positive contribution resulting from the release of superhelical strain. On the other hand, when the binding ratios start to introduce left-handed supercoils, (the right side of figure 11) affinity is diminished compared to relaxed circular DNA, since energy is now required to wind up the DNA.[65]

1. Conformational Heterogeneity

Echinomycin and Triostin A (Figure 10) are by far the best-studied examples of the quinoxaline antitumor antibiotics. They differ only in the nature of their sulfur-containing crossbridge (thioacetal for echinomycin, disulphide for triostin). Although echinomycin is active against experimental tumors, clinical trials showed it to be too toxic for use in chemotherapy. Although the exact nature of the biochemical responses to bisintercalation that lead to tumor selective toxicity are largely unknown, much can be gained from the understanding of the interactions between these molecules and DNA.[66]

Initially, it was thought that these molecules were rigid, with the heterocycle chromophores projecting out at the perfect distance to span two base pairs (10-11 Å). Later work showed that these molecules display a surprising degree of conformational heterogeneity in solution. Echinomycin, for example, can be separated into as many as six fractions by HPLC reversed-phase analysis of a solution in methanol. Another striking example of this came in the solution of the crystal structure of sandramycin in which it was found to have an intrachromophore distance of 17-19.5 Å--significantly larger than the 10.1 Å found in the bound state.[67]

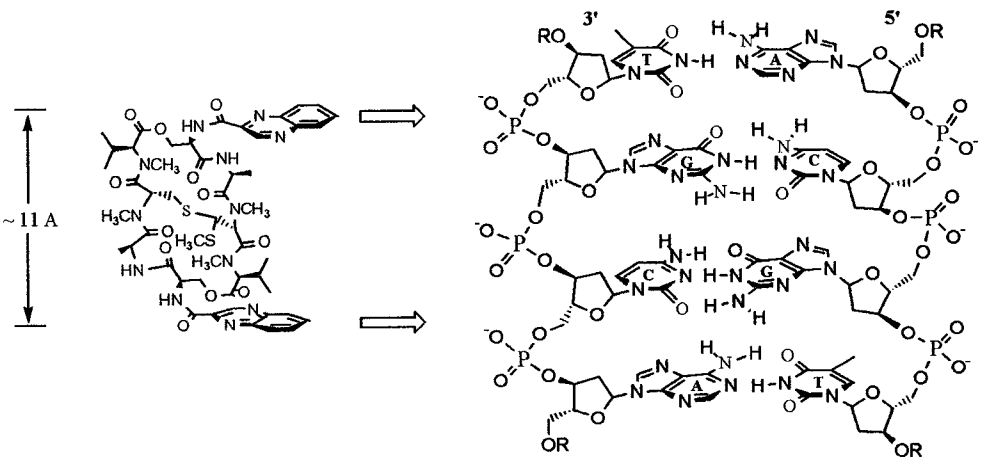

Figure 12. Minor groove DNA binding of echinomycin

2. Sequence-Selectivity

The quinoxaline antibiotics are highly sequence selective. They intercalate from the minor groove, surrounding two base pairs (Figure 12). The preferred binding sites for echinomycin and triostin A in natural DNA were found to be centered largely on CG-rich sites, while sandramycin preferred AT residues. Interestingly, the synthetic depsipeptide des-N-tetramethyl triostin A--TANDEM (Figure 13), which is identical to triostin A except for the lack of methylation of the four peptide bonds, was found to bis-intercalate with a preference for AT-rich residues. This has been attributed to the formation of internal hydrogen bonds within its peptide ring from the NH substituents of the valine residues to the CO groups of the alanines; this displaces the alanine COs from a suitable position to accept hydrogen bonds from guanine.[68]

Clearly, the peptide portion of echinomycin plays an important role in DNA recognition, but its aromatic chromophores are not silent. In one experiment, quinoline-2-carboxylic acid was added to cultures of the producing organism *Streptomyces echinatus*, yielding the bis-quinoline analogue of echinomycin--designated 2QN (Figure

12). This novel antibiotic remained a bisintercalator, but its preferences for binding to DNA were subtly changed from those of echinomycin, notably in respect of stronger binding to the synthetic DNAs poly(dA-dT) and poly(dG-dC) than to natural DNAs. These experiments lead to the assumption that the sequence selectivity comes from both the nature of the peptide ring and the chromophores.[69]

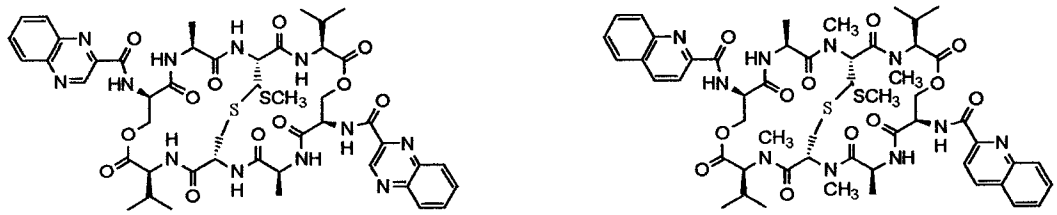

TANDEM 2QN

Figure 13. Echinomycin analogues.

The origins of the sequence selectivity of echinomycin and triostin A were initially revealed in the crystal structures of their complexes with oligonucleotides. The alanine residues of the peptide ring were found to play an important role; their CO and NH groups form hydrogen bonds to the 2-amino groups and N-3 atoms respectively of the sandwiched guanines. In addition to this, many stabilizing van der Waals contacts can be seen elsewhere in the complexes. Drug-induced unwinding in the crystal compares favorably with that determined in solution, and is distributed between all four base pairs forming the binding site.[70]

Definitive evidence for the existence of preferred binding sites in DNA came later with the application of footprinting techniques, allowing experiments to be done on larger fragments of DNA. A variety of probes have been used, including DNAaseI, DNAaseII, and Dervan's methidium-propyl-EDTA·Fe^{II}. All of these studies lead to the same broad conclusion, namely that echinomycin and triostin A bind preferentially to CG rich sites,

while sandramycin prefers AT rich sites. Sometimes, the regions close to strong binding sites became significantly more susceptible to nuclease cleavage in the presence of a bisintercalator, suggesting that antibiotic binding can cause structural distortions of the DNA helix surrounding some of its binding sites.[71,72]

To address the question of how important the 2-amino group of guanine is to the interaction between echinomycin and DNA, footprinting studies were done with inosine substituted for guanine in the DNA strand. Inosine (I) is equivalent to guanosine (G) but lacks the purine 2-amino group. Replacement of G with I in both strands of *tyr* DNA abolished binding of echinomycin within the limits of detectability by DNAaseI footprinting. The same was true for a synthetic 51-mer containing numerous strong echinomycin binding sites, whether inosine is incorporated into one or both strands of the duplex. Clearly the 2-amino group of guanine must be an important determinant of specific binding of echinomycin to DNA since the loss of only one such substituent from the two sandwiched GC base pairs significantly impairs the interaction.[65,72]

3. The Nature of Binding and Cytotoxicity

An interesting phenomenon was noted when echinomycin-DNA complexes were caused to dissociate (using sodium dodecyl sulphate to sequester the echinomycin as it dissociates from DNA) at various times after mixing. Newly formed complexes dissociated relatively fast, whereas complexes allowed to equilibrate for several minutes or hours dissociated much more slowly. This behavior has the characteristics expected for a migration or 'shuffling' phenomenon whereby the antibiotic migrates from low-affinity (fast-dissociating) binding sites to high-affinity (slow-dissociating) binding sites.

However, when this association reaction was probed by stopped-flow kinetic experiments, no spectral changes associated with this putative shuffling process could be observed.[65]

Although there have been numerous studies on DNA sequence recognition by these antibiotics, little is known about the kinetics of their interaction with DNA. This information is important since there is often a correlation between biological activity and persistence time on the DNA lattice. In a recent total synthesis of (-)-sandramycin, Boger deliberately introduced the heteroaromatic chromophores at a late stage to provide access to structural analogs possessing modified intercalation capabilities (Figure 14).[73] Sandramycin itself was found to have an exceptionally high affinity for duplex DNA (K_B = 3.4 x 10^7 M^{-1}, ΔG^o = -10.2 kcal/mol—echinomycin and triostin A exhibit slightly weaker binding, $K_B \sim 10^6$ M^{-1}), which is slightly higher than that of **3** (K_B = 5.7 x 10^6 M^{-1}, ΔG^o = -9.2 kcal/mol), the agent lacking one chromophore, and much more effective than **4** (K_B = 2.4 x 10^4 M^{-1}, ΔG^o = -6.0 kcal/mol), the agent lacking both chromophores. Most importantly, the largest share of the binding affinity is derived from the cyclic decadepsipeptide and the addition of the first and second chromophores incrementally increases binding by approximately 3.2 and 1.0 kcal/mol, respectively.

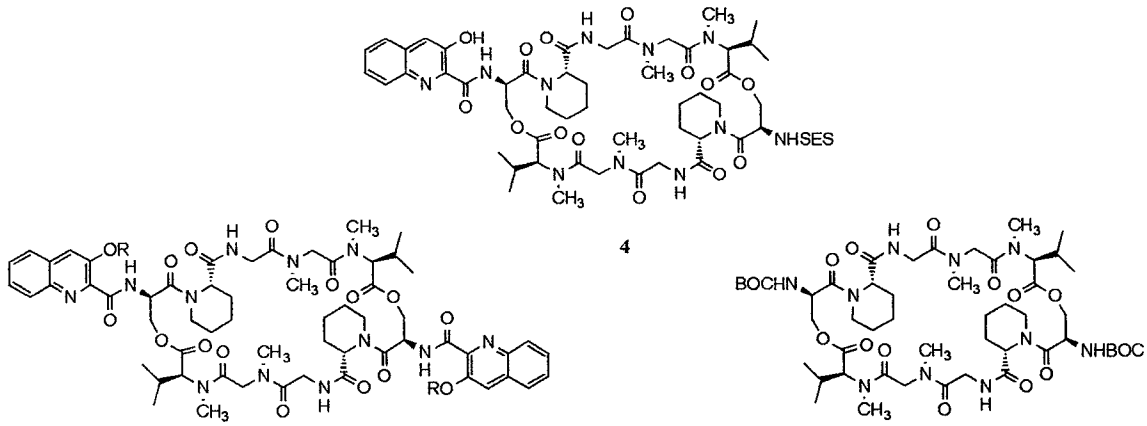

sandramycin, R = H
3, R = Bn

4

5

Figure 14. Sandramycin and various analogs.

The in vitro cytotoxicity studies of sandramycin alongside that of the key partial structures including the bis-benzyl ether **3**, the cyclic decadepsipeptide **4** possessing a single heteroaromatic chromophore, and the cyclic decadepsipeptide **5** are summarized in table 1. Interestingly, the bis-benzyl ether **3** was generally 20-100x less potent than sandramycin, representing a consistent observation that alkylation of the C3 phenol of sandramycin diminishes biological potency. The impact of the introduction of this bulky group is smaller than expected however, but consistent with the subsequent finding that removal of the phenol altogether results in little change in the cytotoxic activity. This implies that the diminished cytotoxic properties of **3** are a result of unfavorable steric interactions rather than loss of hydrogen bonding capabilities. The agent **4** possessing a single chromophore was approximately 500-1000x less potent than sandramycin and the cyclic decadepsipeptide **5** lacking both chromophores was inactive and $\geq 10^5$x less potent than sandramycin! Although the largest share of the binding affinity is derived from the cyclic depsipeptide backbone, the addition of the chromophores appears to be crucial for the cytoxicities of these agents.[73]

	IC_{50}, nM				
agent	Molt-4	L1210	786-0	Ovcar-3	B16
sandramycin	0.8	0.02	4	2	0.4
2	4	20-2	120	60	8
3	400	500	nt	nt	nt
4	$>10^5$	$>10^5$	80 000	80 000	nt

Table 1. Molt-4 (human T-cell leukemia), L1210 (mouse leukemia), 786-0 (human perirenal cell carcinoma), Ovcar-3 (human ovarian carcinoma), B16 (melanoma).

The relatively small contribution to the binding affinity that is attributable to the second intercalation (1.0 kcal/mol) can be rationalized by analyzing the crystal structure of sandramycin with the oligonucleotide 5'-d$(GCATGC)_2$. The agent sandwiches the central two Watson-Crick A-T base pairs and adopts a compact conformation in which the interchromophore distance is 10.1 Å (compared to 17-19.5 Å when not bound). This suggests that the low contribution of the second intercalation might be due to an accompanying destabilizing conformational change in the cyclic decadepsipeptide that offsets much of the gains derived from the second intercalation.[73]

B. Reaction of Metallointercalators with DNA

Historically, Lippard and co-workers were the first to establish that square planar platimum(II) complexes containing an aromatic heterocyclic ligand could bind to DNA via intercalation.[74] Other early experiments describing the interaction of transition-metal complexes with DNA used coordinatively saturated octahedral transition-metal complexes. These studies focused on the binding of tris(phenanthroline) complexes of zinc, cobalt, and ruthenium to DNA (Figure 15). Interestingly, the right-handed Δ-isomers displayed a slight preference for intercalation into right-handed DNA, while a

small preference for the Λ-isomers could be observed for binding in a complimentary fashion against the right-handed groove. The binding interactions of these complexes have been debated; however, consistent enantiomeric preferences have been seen in derivative complexes since prepared.[75-81]

Although the studies on these simple octahedral metal complexes provided a basis for conceptualizing noncovalent interaction with DNA and for exploring how the properties of the metal complexes (photophysical and redox characteristics) might be used in developing new probes for DNA, the binding affinities of these complexes for DNA are unimpressive. The mixture of binding modes, believed to be (i) electrostatic, (ii) hydrophobic binding against the minor groove, and (iii) partial intercalation of one of the phenanthroline ligands, depends upon sequence, salt concentration, and temperature, making them difficult to study. In order for metallointercalators to become useful in biological applications and assays, the intercalative binding affinities needed to be significantly increased.[82]

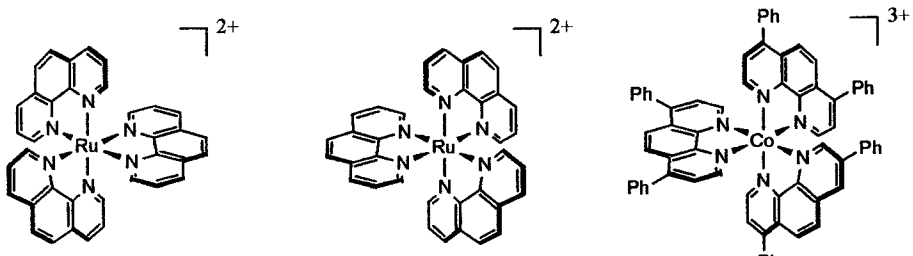

Λ-[Ru(phen)$_3$]$^{2+}$ Δ-[Ru(phen)$_3$]$^{2+}$ Δ-[Co(dip)$_3$]$^{3+}$

Figure 15. Transition metal complexes as early DNA probes.

Phenanthroline and bipyridine ligands are sterically compact, and metal complexes with these ligands have relatively shielded surfaces. This steric shielding is possibly what prevents tris(phenanthroline) complexes from intercalating deeply into the

DNA base pairs. In contrast, metal complexes containing a coordinated dipyrido [3,2-*a*:2',3'-*c*]phenazine (dppz) ligand (Scheme X) would extend a heterocyclic ring system out from the central compact $[Ru(bpy)_3]^{2+}$. Early attempts to increase binding affinities for DNA involved this idea of increasing the surface area for intercalative stacking. The resulting metallointercalators containing an extended aromatic heterocyclic ligand provided encouraging results. By inserting and stacking between the base pairs, octahedral complexes containing the 9,10-phenanthrenequinone diimine (phi) or dppz ligand provided predictable, stable anchors in the major groove with a known orientation of all the functionalities on the metal complex established with respect to the DNA duplex (Figure 16).[83-85]

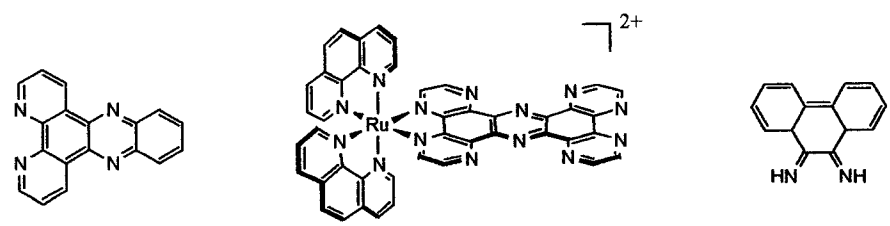

Figure 16. Intercalating ligands with increased surface area, and a PHEHAT complex of Ru(II).

1. Metallointercalators as Probes for RNA Structure

The observation that the site selectivity for $[Rh(phen)_2phi]^{3+}$ depends on relatively open major grooves has been used in probing RNA structure. Metallointercalators that target major groove sites bind poorly to double-stranded RNA.[86] This observation is believed to be based on the fact that A-form RNA duplexes contain a very deep and narrow major groove, making it largely inaccessible for intercalation. Changes in the tertiary structure of the RNA that serve to open the major groove are prime targets for

$[Rh(phen)_2phi]^{3+}$. This notion of shape-selective recognition led to the development of a novel probe for RNA structure. Using well-characterized structures, $tRNA^{Phe}$ and $tRNA^{Asp}$, Barton and coworkers found that photoactivation of $[Rh(phen)_2phi]^{3+}$ resulted in a striking similarity in cleavage on these tRNAs and the sites of cleavage were primarily in regions of tertiary folding.[87,88]

2. Metal Complexes as DNA Bisintercalators

Though there are innumerable examples of bisintercalators (natural and synthetic) that don't contain a metal center, surprisingly little work has been done on metal complexes designed to act as bisintercalators for DNA, although a few examples do exist.[89-91] One example involved the two enantiomers of the diruthenium compound $[\mu C4(cpddppz)_2(phen)_4Ru_2]^{4+}$ (Figure 17). These complexes were found to bisintercalate with extremely high affinity, having a binding constant of ~1.7×10^{10} M^{-1} (considerably higher than the natural product sandramycin, ~3.4×10^7 M^{-1}). The mono ruthenium complex (parentheses in Figure X) was found to have a significantly weaker binding constant of ~3.2×10^6 M^{-1}. The diruthenium complex on the right had similar binding affinity with a binding constant of ~5×10^{11} M^{-1}. Unfortunately, no DNA cleaving studies were done with either of these complexes.

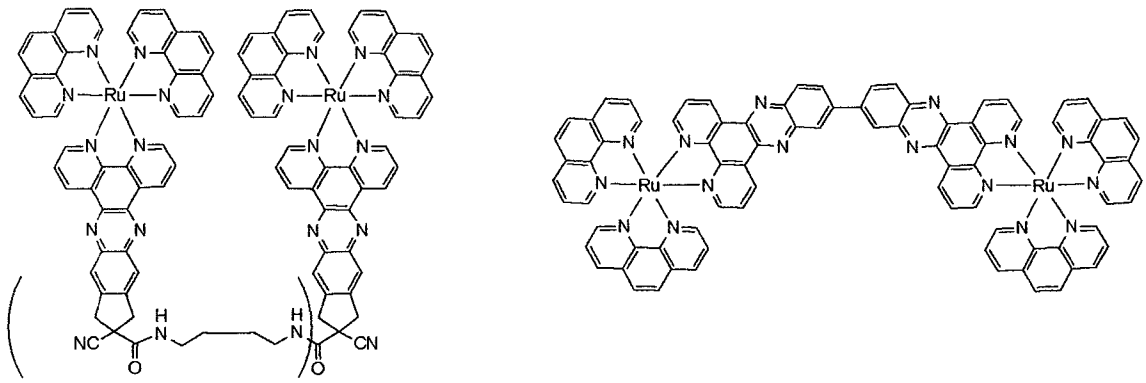

$[\mu$-C4(cpdppz)$_2$(phen)$_4$Ru$_2]^{4+}$ $\Delta\Delta$-$[L_2Ru\{dppz(11\text{-}11')dppz\}RuL_2]^{4+}$

Figure 17. Metal complexes designed for bisintercalation. L= 1,10-phenanthroline.

In another approach, Meunier and coworkers designed a porphyrin complex containing two amino acid spacers attached to two 9-aminoacridine intercalators (Figure 18).[92] A plasmid DNA nicking study with ΦX174 DNA was done using the manganese(III) complex of the porphyrin. A nicking study monitors the conversion of intact supercoiled plasmid DNA (form I) to the nicked open circular molecule (form II). When circular plasmid DNA is subject to agarose gel electrophoresis, relatively fast migration will be observed for the intact supercoiled form (form I). If scission occurs on one of the strands (nicking), the supercoils relax to generate a slower-moving open circular form (form II). If a second nick occurs within approximately twelve base pairs of the first nick, a linear form (form III) will be generated that usually migrates between form I and form II (Figure 19). Multiple nicks causes multiple strand breaks and appears as streaking on an agarose gel.

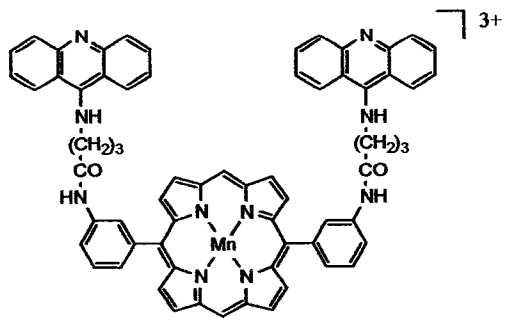

Figure 18. Meunier's mangenese(III) porphyrin complex bearing two acridine moieties.

Unfortunately, very little work was done to assess the DNA binding/cleaving properties of this 9-aminoacridine appended manganese(III) porphyrin. A nicking study with 1 μM Mn^{III}-porphyrin in the presence of 10 mM $KHSO_5$ resulted in conversion of 90% of form I into forms II and III. This is below that of the Mn^{III}-porphyrin complex lacking the acridine moieties, which was able to effect the same conversion at 5 nM in the presence of 10 μM $KHSO_5$. No direct evidence for bisintercalation was found.[92]

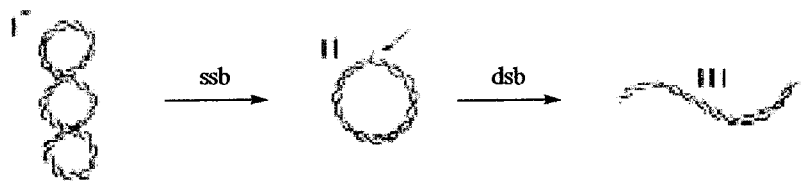

Figure 19. Plasmid DNA nicking diagram.

3. Combining Bisintercalation and DNA Oxidation

While analyzing an X-ray crystal structure of one of Hegedus's C-2 nickel dioxocyclam complexes, it was noticed that these complexes might be capable of acting as a substitute for the cyclic peptide ring structure of the bifunctional intercalating antitumor antibiotics discussed above (Figure 20). Molecular modeling studies (Molecular Simulations Inc. Discover™ program, CFF91 Force Field) of the nickel

complex were done by computationally inserting quinoxaline carboxylic acid groups into a known (methoxy)(methyl)cyclam crystal structure.[8b] Minimization of the energy suggested that the bis-quinoxaline groups preferred to be disposed roughly parallel to each other with only a minor difference in energy for interquinoxaline ring distances between 7 Å and 12 Å. These results also showed that the gem-dimethyls are in a suitable location for hydrophobic interactions analogous to the valine isopropyl groups in echinomycin. Additionally, the bound N-H's were in approximately the right location for hydrogen bonding to DNA. Although the unbound intrachromophore distance in the dioxocyclam is significantly smaller than the corresponding unbound distance in the natural antibiotics (i.e. sandramycin: 17.5-19Å), it is thought that the relatively small contribution from the intercalation of the second chromophore of sandramycin (~1 kcal/mol) is from an accompanying destabilizing conformation change to achieve the correct ~11 Å needed to surround two base pairs. That accompanying destabilizing energy would not be necessary for a dioxocyclam that is already at the desired ~11 Å.

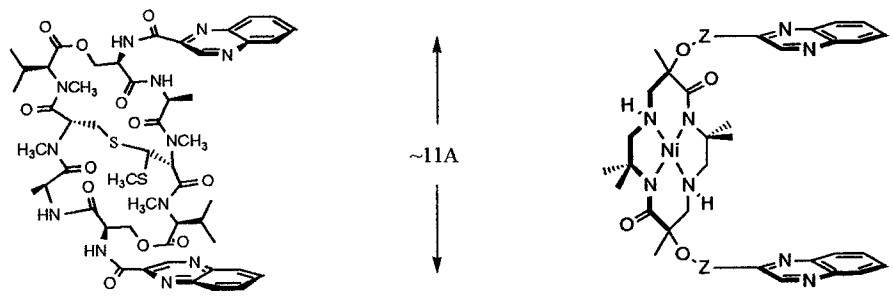

Figure 20. Schematic diagram of echinomycin and a quinoxaline nickel cyclam complex.

IV. Hypothesis and Goals

The structural similarities between the proposed quinoxaline ester dioxocyclam nickel complex and echinomycin, along with the well-established ability of nickel(II) square planar complexes to oxidize DNA in the presence of oxidants, suggested that 5,12-dioxocyclams with appended quinoxaline groups might give rise to novel DNA cleaving/binding agents. The initial goal of this project was to synthesize these types of compounds, then immediately subjected them to the circular DNA unwinding test to determine if they are capable of acting as functional analogs of the bisintercalating antibiotics discussed above. The final goal of this project was to assess the DNA cleaving ability of these complexes. A square planar nickel(II) complex designed to act as a *bisintercalator* might be useful in structure probing experiments. Additionally, these complexes might have antitumor/antibiotic properties if their mode of binding is similar to the bisintercalating antibiotics discussed above.

Results and Discussion

V. Synthesis of Dioxocyclams/Project Background

The photolysis of alkoxycarbene complexes in the presence of an imine results in a cycloaddition reaction to form β-lactams with high diastereoselectivity. One example that nicely illustrates the selectivity of this photoreaction is the photolysis of an alkoxycarbene complex in the presence of a protected imidazoline producing a protected azapenam (Scheme 7).[5]

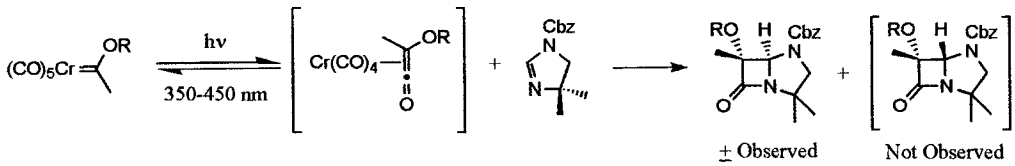

Scheme 7. Observed diastereoselectivity in Hegedus's photoreaction.

Since a stereocenter is set in this reaction, the resulting azapenams are racemic. Dimerization of a racemic mixture of azapenams results in production of two diastereomeric cyclams, the C-2 symmetric (cis) diastereomer, and the centrosymmetric (trans) diastereomer (Scheme 8).[6,7] Use of a chiral imidazoline in the photoreaction produces a single enantiomer of the azapenam. Dimerization of the chiral azapenam produces exclusively the C-2 symmetric cyclam as a single enantiomer.[8]

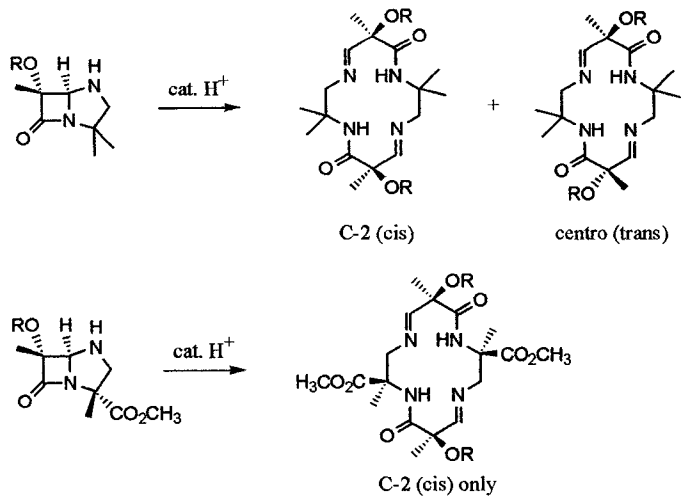

Scheme 8. Products from acid-catalyzed dimerization of deprotected azapenams.

Retrosynthetic analysis of the desired cis-cyclam revealed several possible routes (Figure 21). Since the methodology for making cyclams from chromium carbene complexes has been well refined by the Hegedus group, the simplest route would be to make the cyclam first, then attach quinoxaline to the tertiary alcohols. Other more obvious possibilities include attachment of quinoxaline at the azapenam stage, or even attachment at the carbene stage.

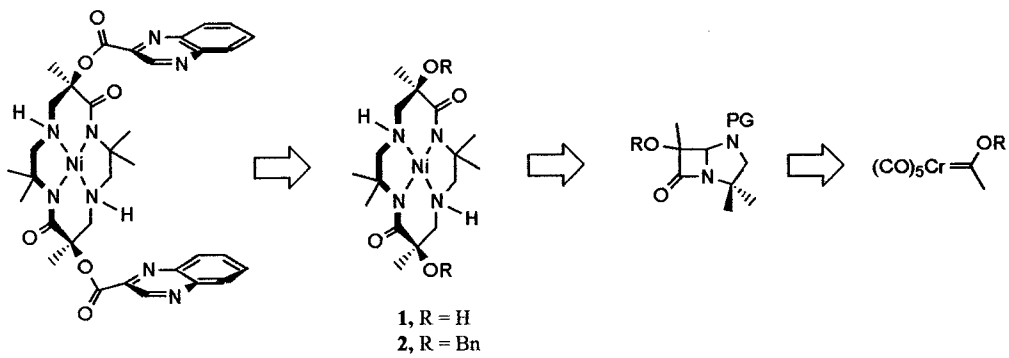

Figure 21. Quinoxaline ester cyclam retrosynthesis.

Joe Bullock's work while in the Hegedus group (1993-1999) showed that attachment of quinoxaline to an already-made cyclam was problematic (Scheme 9).[93]

Because the secondary amines within the cyclam ring would likely be more reactive towards acylation than the tertiary alcohol sites, the nickel complex was used for acylation attempts. Unfortunately, analysis of the crude reaction mixtures revealed mixtures of polyacylated products, none of which contained nickel. The tertiary alcohols were apparently less reactive than the secondary ring nitrogens, even though the nitrogens were coordinated to nickel prior to acylation attempts. Perhaps the secondary amines, once acylated, are no longer capable of complexation to nickel(II).

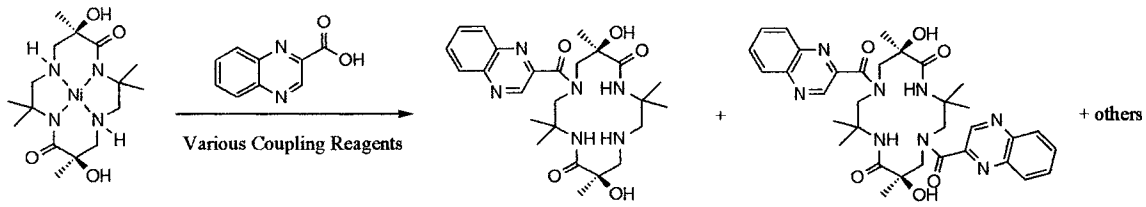

Scheme 9. Joe Bullock's attempt at acylating the C-2 symmetric nickel cyclam.

My approach was to go one step back in the synthesis and try to acylate at the azapenam stage (Scheme 10). The hydroxyazapenam **6** was coupled with quinoxaline-2-carboxylic acid using a reagent initially developed for hindered peptide coupling, bis(2-oxo-3-oxazolidinyl)phosphinic chloride (BOP-Cl),[94] to give the quinoxaline ester **7** in a modest 45% yield. Initial attempts to remove the carbamate protecting group were carried out using standard hydrogenolysis conditions with methanol and 40 psi H_2. Unfortunately, this resulted in formation of a significant amount of reduced quinoxaline, as well as the quinoxaline methyl ester resulting from methanolysis of the quinoxaline azapenam ester **7**. The analogous side reactions occurred with isopropanol as the solvent; no reaction occurred with *t*-butanol as the solvent. This was the first indication of the lability of the quinoxaline ester bond and also the ease with which quinoxaline could be reduced.

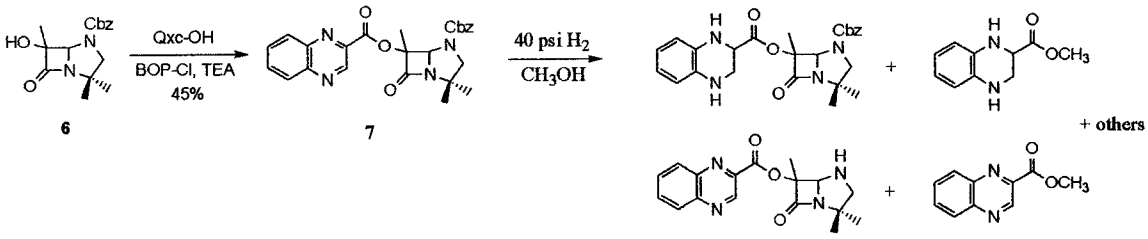

Scheme 10. Acylation at the azapenam stage followed by failed Cbz deprotection.

These problems were eventually overcome by switching to a non-nucleophilic solvent (CH_2Cl_2), eliminating the solvolysis reaction, and by reducing the H_2 pressure to 1 atm (Scheme 11), minimizing the formation of reduced quinoxaline. Fortunately, the deprotected azapenam **8** underwent clean dimerization in the presence of a catalytic amount of CSA to give an 80% yield of quinoxaline imine cyclam **9** (1:1 diastereomers by ^{1}H NMR). Although this seemed promising, subsequent reduction of the ring imines followed by separation of the cis and trans diastereomers was not accomplished due to the extreme labilility of the quinoxaline ester linkage. The first example of this lability came when the crude dimerization reaction mixture was washed with saturated $NaHCO_3$ to remove the CSA, resulting in *quantitative* hydrolysis of the quinoxaline ester bonds! Purification of the bis-imine quinoxaline ester cyclams **9** was eventually accomplished by adsorbing the crude material directly on to triethylamine-treated silica gel followed by flash chromatography on triethylamine-treated silica gel.

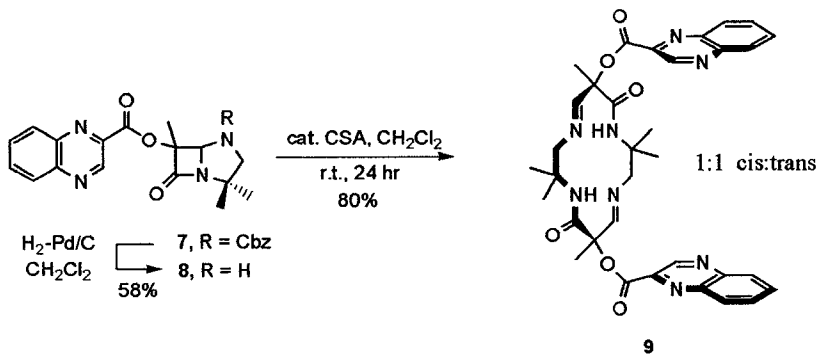

Scheme 11. Deprotection and dimerization of the quinoxaline ester azapenam.

Later examples of this lability came during attempts to reduce the ring imines. Hydrogenation with 10% palladium on carbon in various organic solvents with a range of H_2 pressures resulted exclusively in reduction of the quinoxaline heterocycle. Reduction attempts with sodium borohydride ($NaBH_4$) or sodium cyanoborohydride ($Na(CN)BH_3$) in either methanol or ethanol as the solvent resulted in complete solvolysis of the quinoxaline ester, and no reaction occurred with *t*-butanol as the solvent. Because this extraordinary lability would prevent meaningful DNA binding and cleaving studies, similar, but less labile, groups were examined--a quinoxaline ether **10**, and two versions of an extended quinoxaline amide; racemic **11** and chiral **12** (Figure 22).

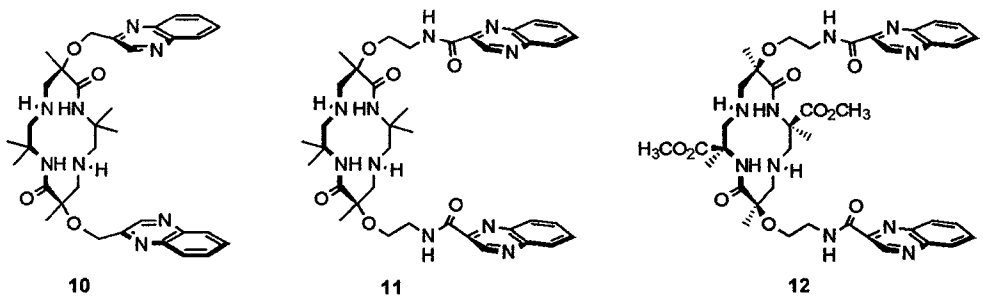

Figure 22. Quinoxaline cyclams with more robust quinoxaline attachments.

A. Quinoxaline ether cyclam synthesis

Although these problems concerning the labile quinoxaline ester bond were resulted in abandoning this strategy, two promising features about this strategy were revealed: 1) that it was possible to attach quinoxaline to the tertiary alcohol of the azapenam and 2) that the deprotected azapenam is capable of undergoing clean dimerization while carrying the bulky quinoxaline substituent. Therefore, the same strategy (quinoxaline attachment before dimerization) should work if the azapenam were connected to quinoxaline with a more robust linkage.

The key hydroxy azapenam intermediate **6** was made in 3 steps from the tetramethylammonium "ate" complex **13**. Treatment of the tetramethylammonium "ate" complex with pivaloyl chloride followed by *p*-methoxybenzyl (PMB) alcohol, afforded the carbene complex **14** in good yield as a red solid. Paramethoxybenzyl alcohol was chosen because it can be oxidatively removed with 2,3-dichloro-5,6-dicyano-1,4-benzoquinone (DDQ),[95-97] which normally does not cleave carbamate protecting groups (Cbz in **16**), unless forcing conditions are applied.[98] Photolysis of chromium carbene complex **14** with imidazoline **15** resulted formation of the differentially protected azapenam **16**. Selective deprotection of the para-methoxybenzyl protecting group with DDQ proceeded smoothly to provide the key hydroxyazapenam intermediate **6**.

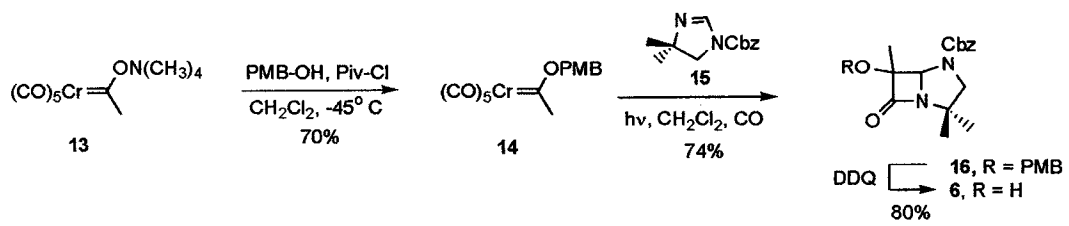

Scheme 12. Synthesis of hydroxyazapenam **6**.

The key steps of the synthesis were attachment of the quinoxaline chromophore and dimerization of the azapenam to form an imine cyclam. Standard benzylic bromination conditions were employed to brominate 2-methyl quinoxaline **17** giving a moderate yield of quinoxaline bromide **18** (Scheme 13). This reaction suffered from the formation of multibrominated products; however, some starting material was always recovered, making the 55% yield more tolerable. Coupling of the quinoxaline bromide to the hindered tertiary alcohol of the hydroxyazapenam required a catalytic amount of iodide to increase the reactivity of the electrophile by *in situ* generation of an iodomethylquinoxaline.[99,100] This method resulted in an excellent yield of the protected quinoxaline azapenam **19**. Deprotection of the carbamate protecting group with H_2, Pd/C provided the quinoxaline ether azapenam **20** in good yield, typically with only a very small amount of reduced quinoxaline.[101] Apparently, the ether linked quinoxaline chromophore of **19**, which lacks the nearby electron withdrawing group of the ester linked quinoxaline chromophore of **8**, is more difficult to reduce.

The quinoxaline ether azapenam **20** was surprisingly stable, surviving treatment with a catalytic amount of camphor sulphonic acid (CSA) for 9 days at room temperature. This is much more stable than the deprotected ester azapenam **8**, which dimerized completely in 24 hours under the same conditions, and also more stable than typical deprotected azapenams, with a methyl or benzyl substituent in place of quinoxaline, which dimerize in 2-3 days at room temperature. Fortunately, heating in a pressure tube for 15 hours produced the imine cyclams in a 2:1 ratio of diastereomers, favoring formation of the desired cis diastereomer! Furthermore, purification by flash

chromatography with triethylamine treated silica gel yielded the cis diastereomer exclusively in 50% yield. The trans isomer was never isolated.

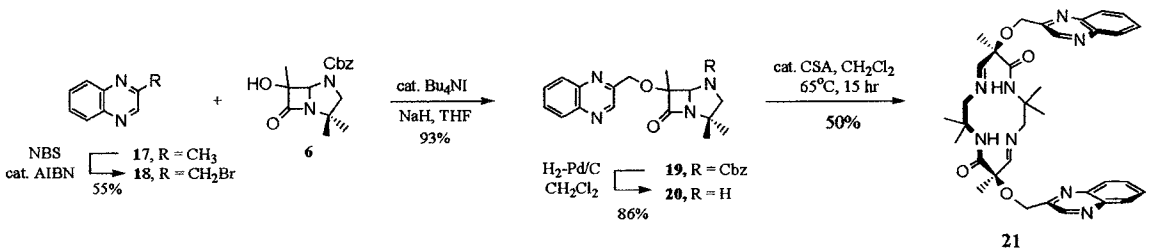

Scheme 13. Attachment of quinoxaline and azapenam dimerization.

Reduction of the imine cyclam to the amine cyclam was once again quite challenging due to the ease with which the aromatic quinoxaline rings were reduced. The first attempts involved the use of $NaBH_4$ in CH_3OH/H_2O, resulting in a significant amount of reduced quinoxaline (Scheme 14). Hydrogenation with Pd/C using a variety of solvents and a range of H_2 pressures reduced the aromatic quinoxaline faster than the ring imines, probably because of steric hindrance within the macrocyclic ring.

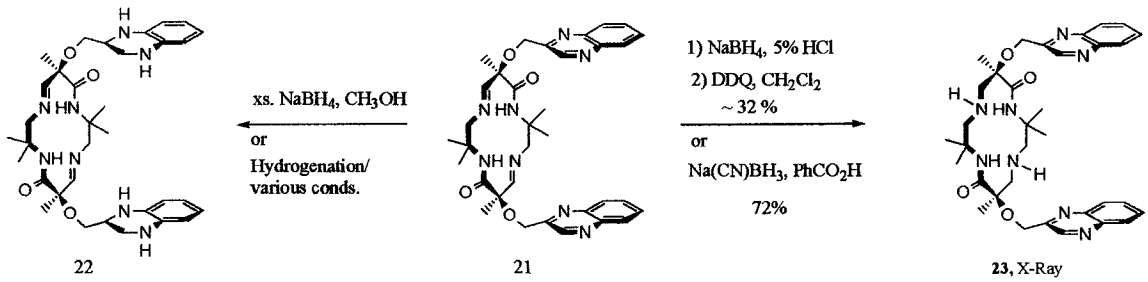

Scheme 14. Reduction of the ring imines.

In an attempt to take advantage of the large difference in basicity between a standard imine and quinoxaline ($C=NH^+$, pKa ~6 while $quinC=NH^+$, pKa ~ 0.6) acidic conditions were employed. This technique was originally developed by Meyers to reduce the C=N link in pyrrolines; it involves simultaneous dropwise addition of a 5 % HCl

solution and a $NaBH_4$/ethanol solution to the imine cyclam, while maintaining the solution's pH at ~3.[102] This approach also produced reduced quinoxaline, but only as the minor product. Separation of reduced quinoxaline cyclams from the mixture proved to be difficult, probably because of the presence of many different isomeric reduced quinoxaline products, and was never accomplished. Reoxidation of the reduced quinoxaline with DDQ, although low yielding, allowed for the first isolation and characterization of the cis quinoxaline ether cyclam **23** by X-ray crystallography (Figure 23).[103] This confirmed that the quinoxaline chromophores were indeed on the same side of the macrocycle. Interestingly, the rings aren't held parallel to each other in the crystal lattice, but are at an oblique angle to each other. The C8 – C27 distance is ~8.20 Å, which is slightly closer than expected. It is worth noting that the quinoxaline antibiotics, when crystallized, have significantly different geometries than when in the bound state.

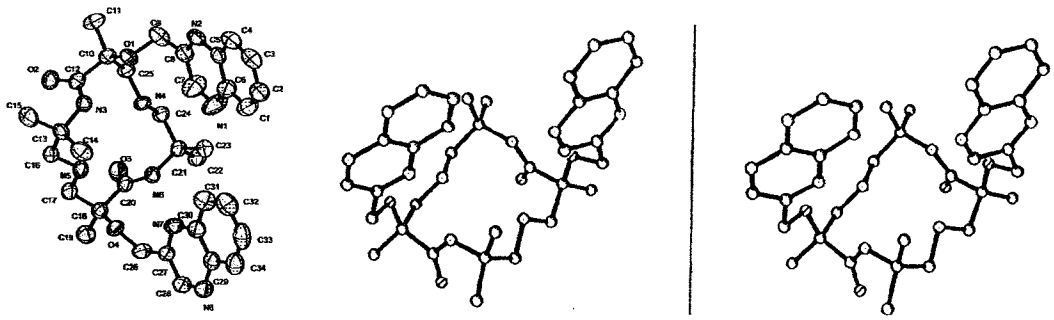

Figure 23. Ortep drawing and stereo view of the cis quinoxaline ether cyclam **23**.

Significant improvement in the reduction of the ring imines came with the use of benzoic acid in the reaction mixture. Benzoic acid (pKa ~ 4.2) should be a strong enough acid to protonate an imine but not quinoxaline. The benzoate anion is a stronger base than quinoxaline so it therefore should act as a buffer for the reaction. This method resulted in a 72% yield with no need for DDQ reoxidation.

Complexation of nickel(II) into the tetraazamacrocycle was also challenging. The first attempts involved the use of four equivalents of nickel tetrafluoroborate $Ni(BF_4)_2$ with potassium carbonate as the base. Since the resulting crude reaction material was pink/red in color and not soluble in organic solvents, it was postulated as being a $^-BF_4$ salt of the nickel cyclam. Apparently, the insoluble potassium carbonate was not a strong enough base to deprotonate the amide nitrogens after nickel complexation. Modest yields (35-45%) of the nickel complex **24** were obtained using 1.2 equivalents of $Ni(BF_4)_2$ and triethylamine as the base. Fortunately, a much improved method for nickel complexation came with the use of $Ni(OAc)_2{\cdot}4H_2O$. In this reaction, the cyclam is mixed with $Ni(OAc)_2{\cdot}4H_2O$ in methanol then heated for several minutes with a heat gun. This resulted in a better yield (72%) and a much more convenient procedure. Disappointingly, an X-ray-quality single crystal could not be obtained of **24** using a range of techniques and solvents. All attempt either resulted in oiling-out or the growth of very fine sand-like particles.

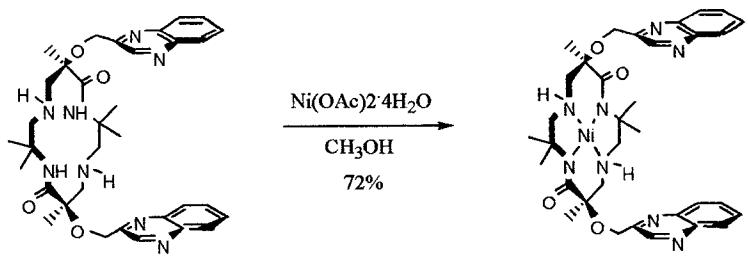

23 24

Scheme 15. Nickel complexation.

With the first quinoxaline cyclams in hand, **23** and **24** were subjected to the plasmid DNA circular-unwinding test discussed above. Unfortunately, no evidence for intercalation of any sort was found using agarose gel electrophoresis (more details from these tests will be discussed later). Before initializing cleaving studies on nickel complex **24**, new analogs were synthesized in an attempt to find one capable of bisintercalation. It was thought that increasing the water-solubility of the cyclam might help in an aqueous DNA reaction. It was also thought that extending the quinoxaline chromophores out from the cyclam ring might give the system increased flexibility and also the possibility for deeper intercalation. Particularly appealing would be the incorporation of quinoxaline amide bond analogous to those found in the quinoxaline antibiotics.

B. Attempted Synthesis of a 2-Hydroxyquinoxaline Analog

With the knowledge that dimerization of the azapenam followed by reduction of the ring imines is possible with the bulky, easily reduced quinoxaline moiety attached, work began on the synthesis of various quinoxaline cyclam analogs. The first envisioned route to analogs of **23** and **24** was to use the same procedure as above except with a slightly different quinoxaline chromophore, one possessing a hydroxyl group at the 2 position (Scheme 16). It was postulated that this extra functionality would increase

water-solubility and possibly provide additional opportunity for hydrogen-bonding to DNA.

TBS-protection of the 2-hydroxyquinoxaline **25** proceeded in moderate yield to give the TBS-protected quinoxaline **26**. Benzylic bromination using the conditions from above yielded the protected bromomethylquinoxaline **27** in low to moderate yields. Unfortunately, even when Finkelstein conditions were attempted with the hydroxyazapenam, silyl transfer to the hydroxyazapenam **6** took place in nearly quantitative yield, giving **29** and **30**. None of the desired product was detected.

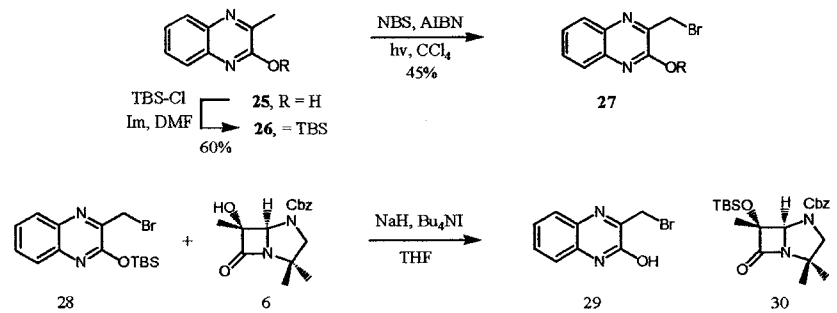

Scheme 16. Protected 2-hdroxyquinoxaline as a silyl transfer reagent.

C. Extended Quinoxaline Amide Cyclam Synthesis

Lacking a simple solution to the silyl-transfer problem just discussed, attention was shifted to making an extended quinoxaline amide bond. Initially, the inexpensive and readily available peptide coupling reagent dicyclohexylcarbodiimide (DCC) was used in the coupling of quinoxaline-2-carboxylic acid to ethanolamine. Unfortunately, these reactions were plagued by low to moderate yields. Furthermore, the dicyclohexylurea (DHU) was very difficult to remove from the product. Filtration of the DHU is the standard protocol for these reactions due to the limited solubility of it in most

organic solvents. This was not successful, however, because alcohol **16** was equally insoluble in a range of solvents. Column chromatography resulted in partial removal of the urea, but was not effective enough to move forward in the synthesis. To circumvent these problems the coupling reagent 1-[3-(dimethylamino)propyl]-3-ethylcarbodiimidehydorchloride (EDCI) was used. Although significantly more expensive, EDCI was easily removed from its corresponding urea by aqueous extraction. The coupling reaction with EDCI/hydroxybenzotriazole (HOBT) produced the extended alcohol **32** in 93% yield (scheme 17).

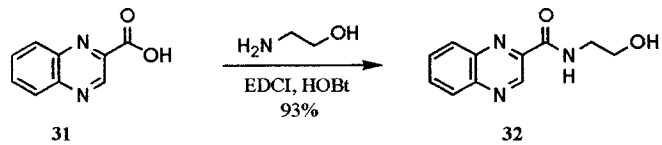

Scheme 17. Quinoxaline amide bond formation.

With multi-gram quantities of the hydroxyazapenam in hand, a direct coupling to the extended quinoxaline amide was attempted (Scheme 18). Tosylation of the primary alcohol **32** proceeded smoothly producing the tosylated quinoxaline amide **33** in 73% yield.[104] Unfortunately, all attempts to couple the tosylated amide **33** to the hydroxyazapenam **6** resulted in a complex mixture of products, one of which was thought to be from E2 elimination product of **33**.

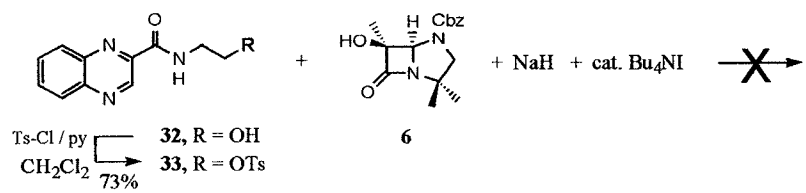

Scheme 18. Attempted S_N2 coupling reaction.

In order to avoid the necessity of an S_N2 reaction with the hindered tertiary alkoxide of **6**, the quinoxaline alcohol **32** was attached directly to the carbene complex (scheme 19). The reaction is slightly lower yielding (64%) than the corresponding reaction with paramethoxybenzyl alcohol to make carbene complex **14**, but this route eliminated two steps from the previous synthesis--attachment of the paramethoxybenzyl protecting group to the carbene, and removal of it from the protected azapenam.

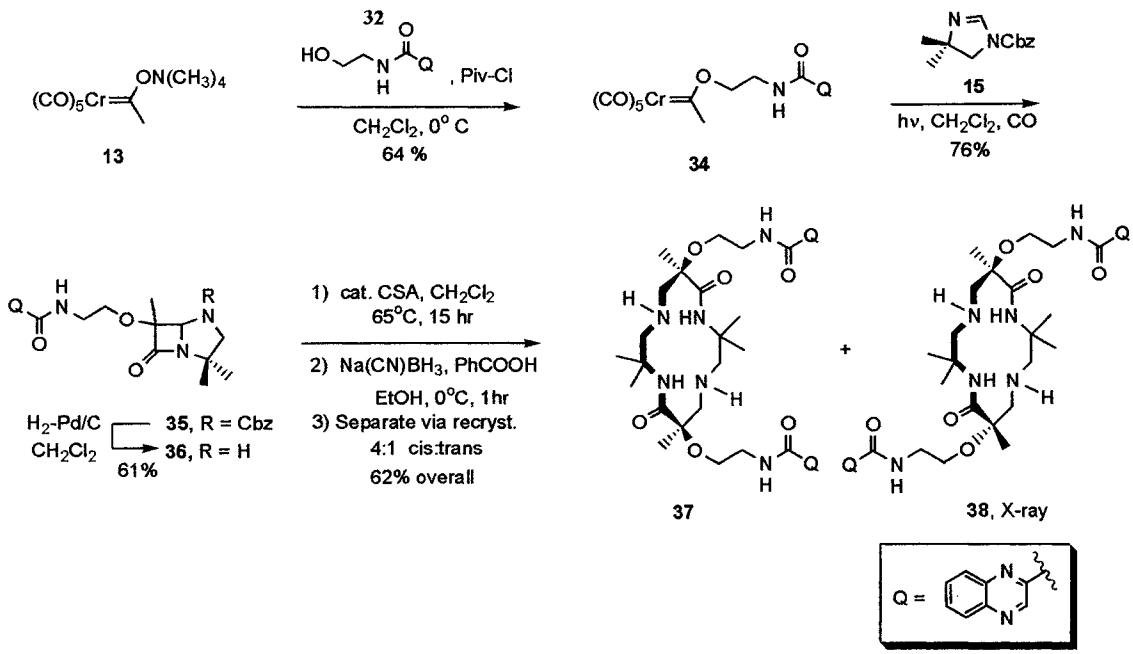

Scheme 19. Synthesis of extended quinoxaline amide cyclams **37** & **38**.

Photolysis of the quinoxaline carbene **34** with imidazoline **15** furnished the protected azapenam **35** which was then deprotected using the same hydrogenolysis conditions developed for the quinoxaline ether azapenam **19** (Scheme 19). The deprotection reaction is significantly lower yielding possibly because the electron withdrawing ability of the amide carbonyl makes the quinoxaline moieties more easily reduced. Dimerization of the deprotected azapenam **36** followed by $NaBH_3CN$ reduction

of the crude material provided a 4:1 mixture of diastereomers favoring the cis isomer. Many attempts to separate the two diastereomers by flash chromatography were unsuccessful; however, the trans isomer was much more crystalline than the cis which allowed for separation by recrystallization, and characterization by X-ray crystallography (Figure 24).

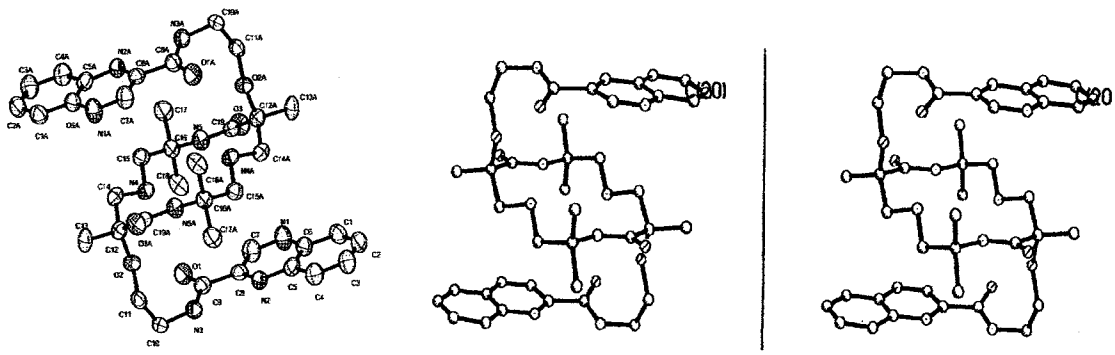

Figure 24. Ortep drawing and stereoview of trans quinoxaline cyclam **38**.

The nickel complexes were obtained in good yields using $Ni(OAc)_2 \cdot 4H_2O$ (Scheme 20). Again, the trans compound **40** was quite crystalline, providing good quality single crystals suitable for X-ray diffraction (Figure 25) while the cis isomer **39** either oiled-out of solution or precipitated as a fine powder. As can be seen by comparing the crystal structure of nickel complex **40** with the crystal structures of the ether **23** and the trans ligand **38**, nickel(II) complexation does indeed flatten the macrocyclic ring.

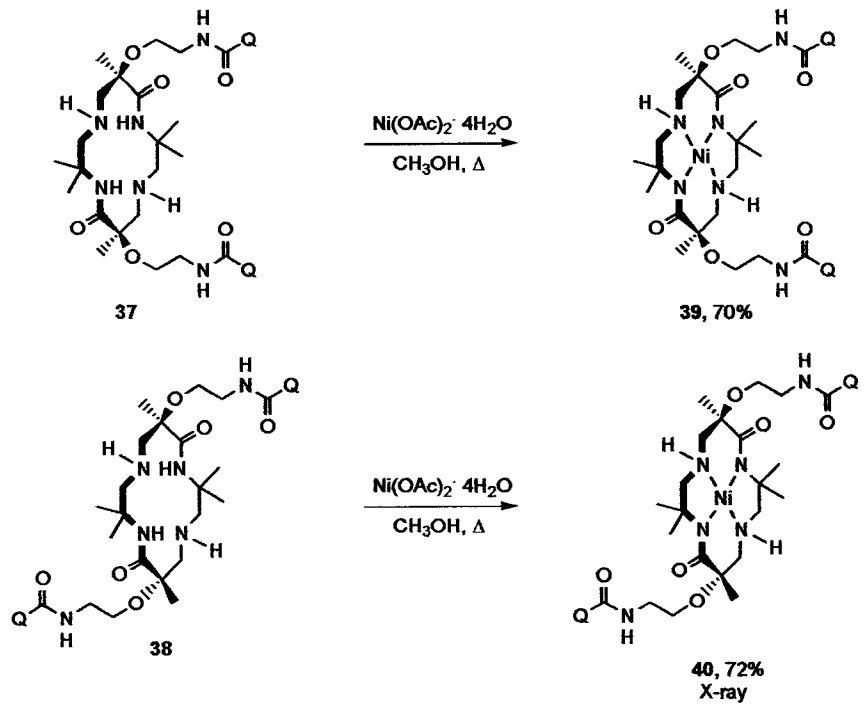

Scheme 20. Nickel complexation reactions of the extended amide cyclams.

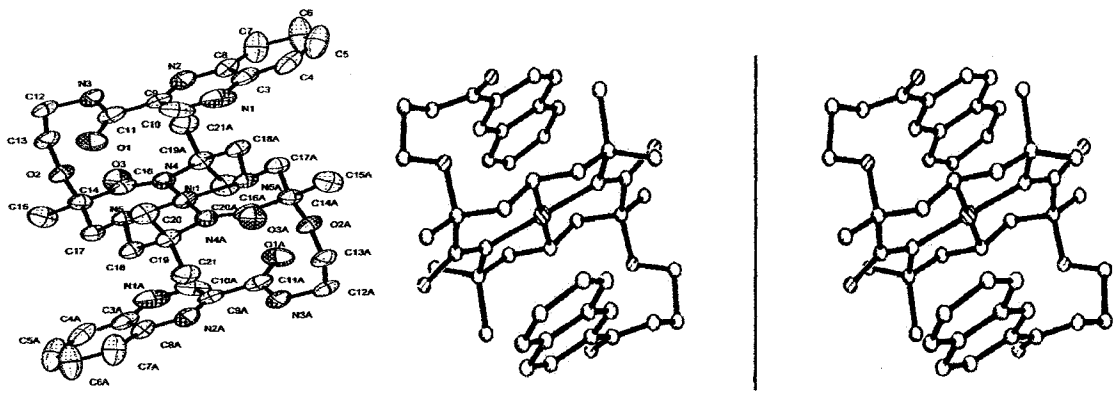

Figure 25. Ortep drawing and stereoview of trans quinoxaline nickel(II) complex **40**.

D. Extended Chiral Amide Quinoxaline Synthesis

The quinoxaline carbene complex **34** provided access to a chiral version of the extended quinoxaline cyclam (Scheme 21). It was hoped that since a chiral azapenams dimerize into the desired cis orientation of the apical alkoxy groups, the unwanted trans diastereomer could be avoided altogether. Photolysis of the quinoxaline chromium carbene complex **34** with chiral imidazoline **35** furnished the chiral protected azapenam **41** which was then deprotected with H_2, Pd/C. Unfortunately, dimerization of the deprotected azapenam **42** followed by reduction of the ring imines produced a complex mixture of products. All attempts to isolate cyclam **44** by column chromatography or recrystallization failed. However, nickel complex **43** was easy to isolate chromatographically and provided indirect access to cyclam **44**. Various recrystallization techniques, including solvent diffusion, vapor diffusion, and slow evaporation failed to yield an X-ray quality crystal of either the nickel complex **43** or the ligand **44**.

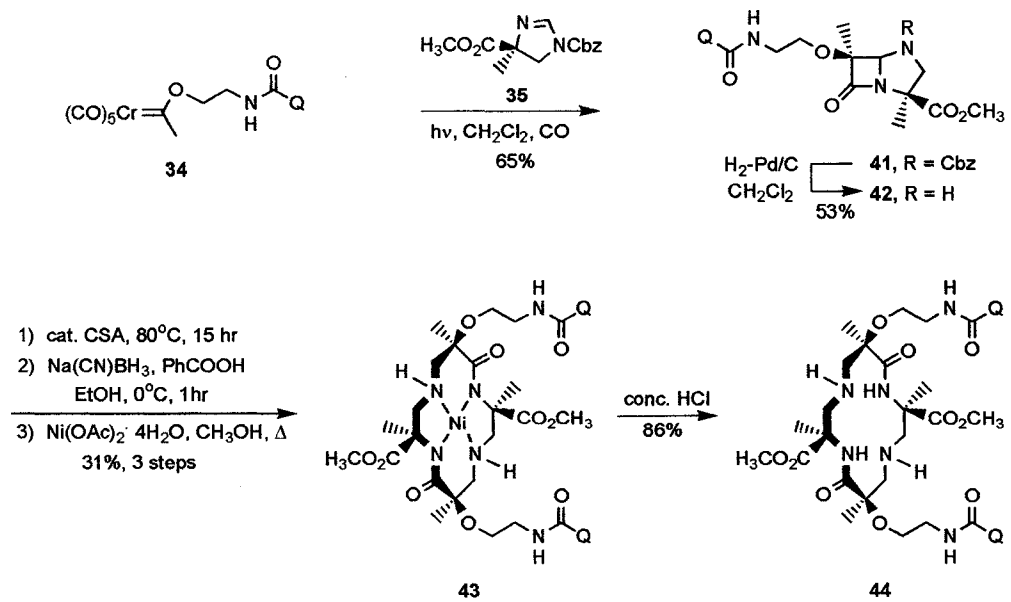

Scheme 21. Chiral extended amide cyclam synthesis.

E. DNA Bisintercalation Studies

After obtaining suitable quantities of quinoxaline cyclams **23, 37, 38, 44**, and their nickel complexes **24, 29, 40, 43**, DNA binding studies using supercoiled ΦX174 RFI DNA were carried out.[73] The [agent] / $[DNA]_{bp}$ ratios are shown above the gel (Figure 26). All of the above agents were added to ΦX174 RFI DNA (0.25 μg in 9 μL of 50 mM Tris-HCl pH 8) in 1 μL of DMSO due to the limited water solubility of the cyclams (the control DNA was also treated with 1 μL DMSO). The [agent] to [DNA] base pair ratios were varied from 0.02 up to 20 as in figure 2. Unfortunately, under a variety of conditions (3 hr incubation, 23° C & 37° C; and 15 hr incubation, 23° C & 37° C), none of the agents demonstrated the ability to change the mobility of supercoiled ΦX174 RFI DNA. In contrast, echinomycin converted all of the form I DNA into Form II DNA, even at the lowest [agent] to [DNA] base pair ratio tested of 0.02 (right side of figure 26). Boger demonstrated that sandramycin is also capable of completely uncoiling ΦX174 RFI DNA under very similar conditions at an [agent] to [DNA] base pair ratio of 0.02. Without further experimentation, it is impossible to say whether these cyclams fail to bind completely, or if they only associate transiently to DNA with a high off-rate. What is clear is however, is that they don't act as functional analogs of the quinoxaline antibiotics.

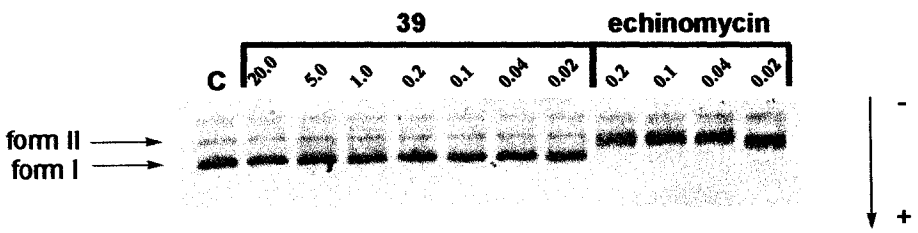

Figure 26. Agarose gel of **39** and echinomycin.

F. DNA Cleavage Studies

Since it is well-known that nickel(II) macrocycles can cleave DNA in the presence of oxidants, the DNA cleavage ability of quinoxaline nickel(II) complexes **24, 39, 40, 43**, as well as the hydroxy **1** and -Obenzyl **2** (Scheme 2) nickel(II) complexes were analyzed for their ability to oxidatively convert intact supercoiled pBR 322 plasmid DNA (form I) to the nicked open circular molecule (form II).[92] The pBR 322 supercoiled DNA (20 μM bp) was incubated with varying concentrations of each nickel (II) complex (e.g. 10 μM - 1000 μM) and with a constant amount of Oxone (1 mM) for 1 hr at room temperature (Figure 27).

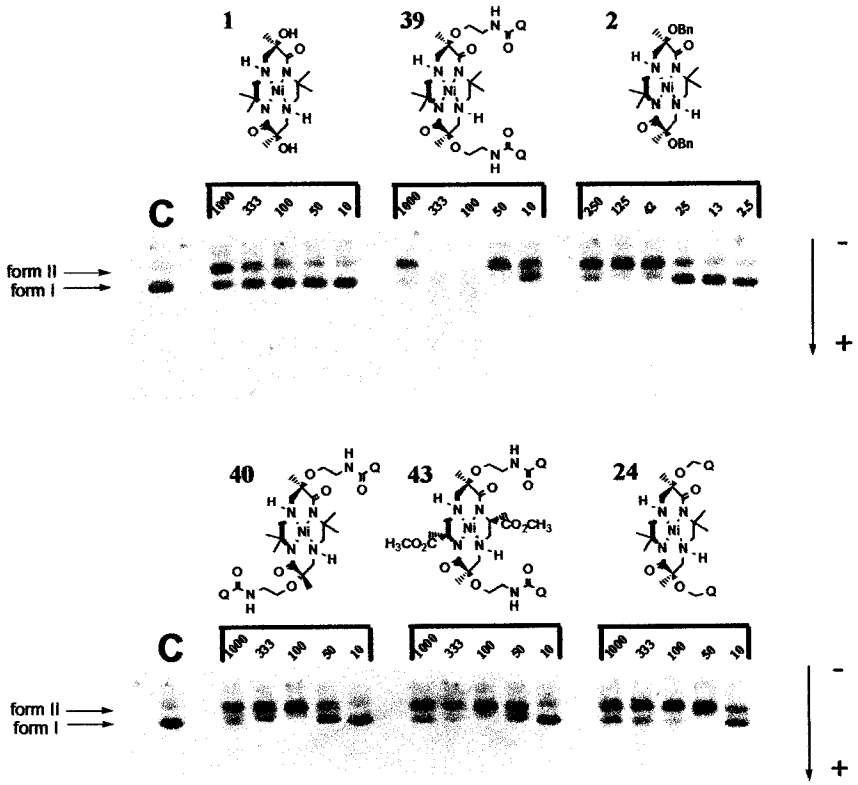

Figure 27. Nicking study with oxone, pBR 322 plasmid DNA, and various nickel(II) complexes.

Subjecting the 10 μL reactions to agarose gel electrophoresis (1%) showed that the DNA cleaving ability of these nickel(II) complexes varied as a function of the nature and orientation of the appended side-chains. Surprisingly, the simple hydroxy cyclam **1**, which was by-far the most water-soluble complex and the only complex lacking an appended pi-aromatic system, showed the least amount of cleavage activity, causing approximately 50% conversion to form II at 1000 μM. The trans extended amide **40** and the chiral cis extended amide **43** showed similar cleavage activity--100 % form II at 100 μM. The cis quinoxaline ether **24** and the cis benzyl ether **2**, which have the shortest link to their extended aromatic systems, showed similar reactivity by completely converting form I to form II at 50 μM. The best example of the effect of the orientation of the quinoxaline groups is in comparing the cis and trans quinoxaline-amide complexes **39** and **40**. These complexes are identical except for the orientation of the quinoxaline amide groups, but the cis complex **39** was much more reactive, causing multiple strand breaks at 100 and 333 μM. In contrast, the trans complex was able to convert all of form I to forms II and III at 100 μM, but was unable to induce multiple strand breaks at any of the concentrations tested. It is worth noting that in all cases except for the hydroxy nickel(II) complex **1**, DNA cleavage reached a maximum at a certain cyclam concentration then decreased as the ratio of nickel(II) complex to oxone approached 1. The reason for this is unclear at this point; it might be that the nickel(II) complex is sequestering or decomposing the oxone, reducing its ability to assist in the DNA oxidation reaction. Although these results don't reveal any direct evidence for DNA binding, they imply that there is some, at least transient, association of these complexes with DNA that depends on the nature and spacial orientation of the appended side chains.

VI. Conclusion

Several different quinoxaline cyclam analogs containing various quinoxaline moieties, including their nickel(II) complexes were synthesized and tested for their ability to bind and oxidatively cleave plasmid DNA. Although no direct evidence for bisintercalation was found, the ability to cleave plasmid DNA varied significantly depending on the nature and orientation of the ligand field. The nature of the association of these dioxocyclam nickel(II) complexes with DNA is not known; however, these results imply at least some sort of association between these nickel complexes and DNA since the macrocyclic core, and hence the redox properties of the bound nickel(II) ion, are identical in these complexes.

Further studies (i.e. microtitration calorimetry) would allow for better assessment of the binding ability of these complexes. In addition, a DNA cleaving study on a restriction fragment would determine if these complexes are oxidizing the DNA at the lowest ionization potential (i.e. 3'G-G5') similar to the nickel(II) complexes studied by Burrow's, or if their appended quinoxaline substituents cause the DNA oxidation to occur at other sites.

VII. Experimental Section

General Procedures. THF was distilled from sodium-benzophenone ketyl, DMF was distilled from $MgSO_4$ and stored over 4Å molecular sieves, CCl_4 was distilled from P_2O_5 and stored over 4Å molecular sieves, CH_2Cl_2 and Et_3N were distilled from CaH_2, Et_3N was stored over KOH pellets. Commercially available reagents were used as received except where indicated. Unless otherwise stated, all NMR spectra (300 MHz for ^1H NMR and 75 MHz for ^{13}C NMR) were recorded in $CDCl_3$. Chemical shifts are given in δ ppm relative to $CHCl_3$ (δ 7.27, ^1H) or $CDCl_3$ (δ 77.23, ^{13}C). Column chromatography was performed with ICN 32-66 nm, 60 Å silica gel using flash column techniques. IR spectra were recorded on an Avator 320 FT-IR. The masses (LSIMS) were obtained using a Fisons VG AutoSpec mass spectrometer with a cesium ion gun, *m* - nitrobenzylalcohol was used for the matrix and the resolution was set to 10000. The following chemicals were prepared according to literature procedures: Pentacarbonyl [(methyl)-{(tetramethyl-ammonio)oxy}carbene}chromium (0) **13**,[18] 1-(benzyloxycarbonyl)-4,4-dimethyl-Δ^2-imidazoline **15**,[19] (S)-N-(Benzyloxycarbonyl)-4-carbomethoxy-Δ^2-imidazoline **35**,[20] (6S*, 13S*) 3,3,6,10,10,13-hexamethyl-6,13-bis(phenylmethoxy)-1,4,8,11-tetraazacyclotetradecane-5,12-dione **2**.[20]

Hydroxycyclam 1. Benzyl ether cyclam **2** (175 mg, 0.33 mmol), 10% Pd/C (200 mg, excess), $Pd(OAc)_2$ (200 mg, excess), and ammonium formate (600 mg, excess) were combined in a 50 mL round bottom flask that had been purged with argon. Approximately 25 mL of methanol was slowly added under a steady stream of argon. The flask was then lowered into a 0°C ice bath before it was allowed to stir

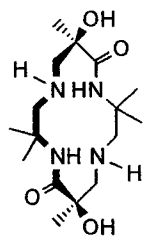

1

and slowly come to room temperature. After 2-3 days at room temperature, the crude reaction mixture was filtered through Celite and the solvent was removed *in vacuo*. The contents of the flask were taken up in 25 mL of dichloromethane then washed with 2 X 8 mL of saturated $NaHCO_3$. The aqueous layer was back extracted with 5 X 10 mL of dichloromethane. The combined organic fractions were dried over Na_2SO_4 before the solvent was removed *in vacuo*, producing hydroxycyclam **2** (114 mg, 99%) as a white solid: MP 194-196° C; ^{1}H NMR (300 MHz) δ 6.78 (bs, 2H), 3.57 (d, J = 11.4 Hz, 2H), 3.18 (d, J = 11.1 Hz, 2H), 2.38 (d, J = 11.4 Hz, 2H), 2.19 (d, J = 11.1 Hz, 2H), 1.37 (s, 6H), 1.36 (s, 6H), 1.28 (s, 6H); ^{13}C NMR δ174.4, 75.1, 58.6, 56.1, 53.3, 27.7, 25.5, 24.2; IR (neat) ν 3400, 3261, 1655, 1533 cm^{-1}; FABHRMS *m/z* 345.2502 ($M + H^+$, $C_{16}H_{33}N_4O_4$ requires 345.2502).

Quinoxaline Amide 32. Quinoxaline-2-carboxylic acid (2.2 g, 12.64 mmol) and ethanolamine (726 μL, 12.04 mmol) were stirred at 0° C in 100 mL of dry DMF. Under a stream of argon, 1-[3-(dimethylamino)propyl]-3-ethylcarbodiimide hydrochloride (6.5 g, 33.8 mmol) and 1-Hydroxybenzotriazole (6.5 g, 48.2 mmol) were added in portions over 30 minutes. The reaction was allowed to slowly warm to room temperature overnight before 250 mL of ethyl acetate was stirred in and used to transfer the crude reaction mixture to a separatory funnel. The organic layer was then washed with 3 X 75 mL of saturated NH_4Cl, followed by 3 X 75 mL of saturated $NaHCO_3$. Each aqueous layer was back-extracted with 5 X 35 mL of CH_2Cl_2. The combined organic fractions were dried with $MgSO_4$ before the solvent was removed *in vacuo*. Purification via flash chromatography (SiO_2, 3.5 X 15 cm, 6% *i*-PrOH:CH_2Cl_2), produced Q-C(O)NHCH$_2$CH$_2$OH (2.43 g, 93%) as an off-white solid. Alternatively, the alcohol could be

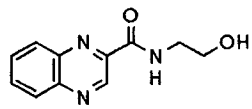

32

recrystallized from ethyl acetate / hexane (75-81%) producing off-white crystals: MP 127-130° C; ^{1}H NMR δ 9.69 (s, 1H), 8.39 (bs, 1H), 8.12-8.23 (m, 2H), 7.88 (m, 2H), 3.94 (m, 2H), 3.76 (m, 2H), 2.37 (bs, 1H); ^{13}C NMR δ 164.1, 143.9, 143.8, 143.2, 140.2, 131.8, 131.0, 129.7, 129.5, 62.2, 42.6; IR (neat) ν 3388, 1663 cm^{-1}; MS *m/z* 218.1 (MH^+). Anal. Calcd for $C_{11}H_{11}N_3O_2$: C, 60.82; H, 5.10; N, 19.34. Found: C, 61.02; H, 5.20; N, 19.50.

General Procedure for Preparation of Chromium Alkoxycarbene Complexes (14), (34). The tetramethyl ammonium carbene complex **13** (1 equiv) and the corresponding alcohol, *p*-methoxybenxyl alcohol or Q-C(O)NHCH$_2$CH$_2$OH (1.1 equiv), were dissolved in CH_2Cl_2 (25-30 mL/mmol **4**), placed under argon, then cooled to 0° C with an ice bath. Pivaloyl chloride (1.1 equiv) was then added slowly over several minutes and the reaction was allowed to come to room temperature overnight (~12-15 hours). The crude reaction mixture was filtered through Celite before washing twice with saturated $NaHCO_3$. The aqueous layer was back-extracted with CH_2Cl_2 until no color remained in the aqueous phase (1-3 times). The organic layers were combined, dried with $MgSO_4$ then filtered before addition of silica gel (1-1.5X wt. crude material) followed by rotary evaporation. The adsorbed crude mixture was purified by flash chromatography (SiO_2, 5% ethyl acetate / hexane for **14**, 60% ethyl acetate / hexane for **34**). Collection of the orange band followed by solvent evaporation provided the carbene complexes as orange-red solids.

***p*-Methoxybenzyl Chromium Carbene Complex 14.** Tetramethylammonium carbene complex **13** (3.07 g, 9.9 mmol), *p*-methoxybenzylalcohol (1.36 mL, 10.9 mmol), and pivaloyl chloride(1.34 mL, 10.9 mmol) were allowed to react according to the general procedure to give carbene complex **14** (2.87 g, 81%): MP 49°C D; ^{1}H

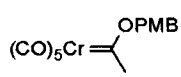

14

NMR δ 7.43 (d, J = 8.4 Hz, 2H), 7.01 (d, J = 8.7 Hz, 2H), 5.89 (bs, 2H), 3.86 (s, 3H), 2.99 (s, 3H); ^{13}C NMR δ 357.8, 223.5, 216.7, 160.6, 130.5, 126.2, 114.5, 83.4, 55.6, 26.7; IR (neat) υ 2063, 1920 cm^{-1}; MS *m/z* 357.0 (MH^+).

Quinoxaline Amide Carbene Complex 34. Tetramethyl ammonium carbene complex **13** (1.87 g, 6.05 mmol), Q-C(O)NHCH$_2$CH$_2$OH (1.45 g, 6.66 mmol), and pivaloyl chloride (0.82 mL, 6.66 mmol) were allowed to react according to the general procedure to give carbene complex **34** (1.68 g, 64%): MP 55°C D; ^1H NMR δ 9.68 (s, 1H), 8.44 (bs, 1H), 8.10-8.22 (m, 2H), 7.87 (m, 2H), 5.06 (bs, 2H), 4.19 (m, 2H), 3.02 (s, 3H); ^{13}C NMR δ 361.1, 223.7, 216.7, 164.1, 144.4, 144.0, 143.1, 140.5, 132.1, 132.0, 131.3, 130.0, 129.8, 49.3, 39.0; IR (neat) ν 2063, 1921, 1678 cm^{-1}; MS *m/z* 436.1 (MH^+).

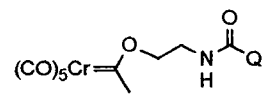

34

General Procedure for the Photoreaction of Chromium Alkoxycarbene Complex (14) with 1-(benzyloxycarbonyl)-4,4-dimethyl-Δ^2-imidazoline and Quinoxaline Chromium Alkoxycarbene Complex (34) with 1-(benzyloxycarbonyl)-4,4-dimethyl-Δ^2-imidazoline and (S)-N-(Benzyloxycarbonyl)-4-carbomethoxy-Δ^2-imidazoline (16) to Form Azapenams (35), (41),(6). The carbene complex (1 equiv), protected imidazoline (1 equiv), and CH_2Cl_2 (25-30 mL/mmol carbene complex, freshly distilled under argon, CaH_2) were combined into a dry Pyrex pressure tube. The solution was purged with argon by bubbling through a long needle for 1-2 hr. The reactions were either irradiated with a 450W Conrad-Hanovia 7825 medium-pressure mercury lamp at 35° C (**6** and **16**) or with 2 X 500W halogen lamps at 70° C (**23**) under 80 psi CO pressure. The reactions were monitored by the fading of color. After 1-3 days, the CH_2Cl_2 was removed from the crude reaction mixture by rotary evaporation. Methanol was used to dissolve

the crude material and the insoluble $Cr(CO)_6$ was then filtered and reused. After adsorbing onto silica gel (2-3X wt. crude carbene complex), the resulting crude mixtures were chromatographed (SiO_2, 35% EtOAc/hexane for **16**, 60% EtOAc/1% triethylamine/hexane for **35** and **41**).

Paramethoxybenzyl Azapenam 16. The paramethoxybenzyl carbene complex **5** (4.96 g, 13.9 mmol) and 1-(benzyloxycarbonyl)-4,4-dimethyl-Δ^2-imidazoline (3.23 g, 13.9 mmol) were allowed to react according to the general procedure at 35° C to provide **16** (4.35 g, 74 %) as an off-white solid: MP 67-70° C; ^{1}H NMR (Cbz rotamers) δ 7.38 (m, 5H), 7.19 (d, J = 8.7 Hz, 2H), 6.86 (m, 2H), 5.13-5.28 (m, 3H), 4.52-4.73 (m, 2H), 3.81 (s, 3H), 3.72-3.80 (m, 1H), 3.18 (d, J = 10.2 Hz, 1H), 1.65 (bs, 3H), 1.40s, 1.32s, 1.20s (6H); ^{13}C NMR δ 173.5, 159.3, 154.1, 153.5, 135.8, 129.8, 129.4, 129.2, 128.8, 128.5, 128.2, 127.7, 113.9, 90.6, 77.7, 75.2, 74.7, 68.2, 67.8, 61.0, 60.6, 55.5, 26.2, 22.3, 15.0, 14.6; IR (neat) υ 1774, 1709 cm^{-1}; MS *m/z* 425.2 (MH^+). Anal. Calcd for $C_{24}H_{28}N_2O_5$: C, 67.91; H, 6.65; N, 6.60. Found: C, 67.78; H, 6.73; N, 6.39.

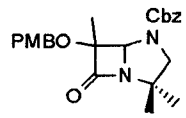

16

Extended Quinoxaline Azapenam 35. The quinoxaline amide carbene complex **34** (703 mg, 1.61 mmol) and 1-(benzyloxycarbonyl)-4,4-dimethyl-Δ^2-imidazoline (375 mg, 1.61 mmol) were allowed to react according to the general procedure at 35° C to provide **35** (621 mg, 77%) as a light-yellow viscous liquid: ^{1}H NMR (Cbz rotamers) δ 9.68 (s, 1H), 8.09-8.38 (m, 3H), 7.87 (m, 2H), 7.34 (m, 5H), 5.06-5.31 (m, 3H), 3.67-3.97m, 3.44s, (5H), 3.16 (d, J = 10.5, 1H), 1.63s, 1.38s, 1.31s, 1.26s, 1.28s (9H); ^{13}C NMR δ 173.4, 172.9, 171.0, 163.4, 154.0, 153.3, 143.9, 143.4, 143.2, 140.3, 136.0, 135.7, 131.7, 131.6, 130.9, 130.8, 130.0, 129.7, 129.6, 128.7, 128.5, 128.4, 128.2, 128.0, 90.3, 90.2, 74.9, 74.3, 67.7, 67.6, 64.9, 64.6, 63.2, 61.4, 60.9, 60.5, 55.7, 53.6, 39.6, 38.7,

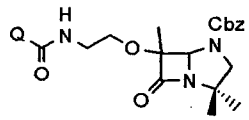

35

29.0, 25.9, 22.0, 21.0, 14.0, 13.9; IR (neat) υ 3400, 1774, 1712, 1678 cm^{-1}; MS *m/z* 504.2 (MH^+). Anal. Calcd for $C_{27}H_{29}N_5O_5$: C, 64.40; H, 5.80; N, 13.91. Found: C, 64.62; H, 5.90; N, 14.12.

Extended Chiral Quinoxaline Azapenam 41. The quinoxaline amide carbene complex **34** (1.67 g, 3.85 mmol) and chiral imidazoline **35** (1.07g, 3.85 mmol) were allowed to react according to the general procedure at 70° C providing **41** (1.15 g, 65%) as a light-yellow viscous liquid: $[\alpha]^{23}_D$ +21.1 (c 1.31, $CHCl_3$); ^1H NMR (Cbz rotamers) δ 9.61 (s, 1H), 8.03-8.38 (m, 3H), 7.79 (m, 2H), 7.53 (bs, 1H), 7.30 (m, 5H), 5.04-5.25 (m, 3H), 4.32m, 4.13d, J = 10.5 Hz (1H), 3.65-3.80 (m, 7H), 3.47d, J = 10.8 Hz, 3.23d, J = 11.4 Hz (1H), 1.75s, 1.49s, 1.39s, 1.35s, 1.24s (6H); ^{13}C NMR δ 172.8, 170.7, 163.2, 152.8, 143.7, 143.2, 140.1, 135.4, 135.0, 131.5, 130.7, 129.6, 129.3, 128.6, 128.5, 128.3, 128.1, 127.9, 90.5, 77.7, 76.6, 76.1, 68.2, 67.8, 66.1, 65.5, 64.9, 64.7, 58.6, 58.3, 53.2, 52.9, 52.6, 39.5, 25.7, 18.1, 14.0; IR (neat) υ 3400, 1781, 1735, 1678 cm^{-1}; FABHRMS *m/z* 548.2124 ($M + H^+$, $C_{28}H_{30}N_5O_7$ requires 548.2145).

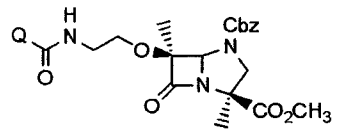

41

Hydroxyazapenam 6. *p*-Methoxybenzyl protected azapenam **16** (3.07 g, 7.23 mmol) was dissolved in CH_2Cl_2 (70 mL). Water was added (3.5 mL) and the flask was cooled to 0° C with an ice bath before 2,3 Dichloro-5,6-dicyano-1,4-benzoquinone (DDQ) (1.97 g, 8.68 mmol) was added in portions over 30 min. After stirring for 4 hours (monitored by analytical silica gel TLC using 50% EtOAc/hexane), the crude mixture was diluted with approximately 200 mL of CH_2Cl_2 then washed with 3 X 75 mL of saturated $NaHCO_3$. The combined aqueous layers were back-extracted with 3 X 75 mL of CH_2Cl_2. The combined organic fractions were dried over $MgSO_4$,

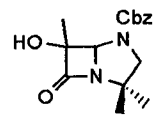

6

filtered and the solvent was removed by rotary evaporation. The crude mixture was purified by flash chromatography (SiO_2, 3.5 x 14 cm, 500 ml 30 % EtOAc/hexane, 500 ml 40 % EtOAc/hexane), yielding **6** (1.85 g, 84%) as an off white solid: MP 96-98° C; ^{1}H NMR (Cbz rotamers) δ 7.37 (m, 5H), 5.04-5.29 (m, 3H), 3.78d, J = 10.2 Hz, 3.70d, J = 10.5 Hz (1H), 3.54 (bs, 1H), 3.16 (d, J = 10.5 Hz, 1H), 1.61s, 1.36s, 1.26s, 1.19s (9H); ^{13}C NMR δ 175.3, 175.0, 154.3, 153.7, 136.0, 128.7, 128.5, 128.4, 128.0, 85.3, 85.2, 77.9, 67.9, 67.7, 61.3, 60.9, 60.7, 60.6, 26.1, 26.0, 22.2, 16.8; IR (neat) ν 3450, 1771, 1707 cm^{-1}; MS *m/z* 305.2 (MH^+). Anal. Calcd for $C_{16}H_{20}N_2O_4$: C, 63.14; H, 6.62; N, 9.20. Found: C, 62.92; H, 6.49; N, 9.03.

Carbamate Protected Quinoxaline Ester Azapenam 7. Hydroxyazapenam **6** (844 mg, 2.77 mmol), 2-quinoxalinecarboxylic acid (531 mg, 3.05 mmol), bis(2-oxo-3-oxazolidinyl)phosphinic chloride (848 mg, 3.33 mmol), and 50 mL of freshly distilled CH_2Cl_2 (CaH_2) were combined into a flame dried 100 mL round bottom flask and brought to 0°C under argon before triethylamine (1.39 mL, 9.98 mmol) was added dropwise. The reaction was allowed to come to room temperature slowly overnight before the crude reaction mixture was transferred to a separatory funnel then washed with 2 X 15 mL of 5% $NaHCO_3$. The combined aqueous fractions were back-extracted with 3 X 15 mL of CH_2Cl_2. The combined organic fractions were dried with $MgSO_4$ and the solvent was removed *in vacuo*. The crude reaction mixture was purified by flash chromatography (SiO_2, 3.5 X 15 cm, 40% EtOAc, hexane) providing 7 (574 mg, 45%) as a light yellow amorphous solid. Due to the extremely labile quinoxaline ester linkage, only ^{1}H NMR data was obtained: ^{1}H NMR (Cbz rotamers) δ 9.64 (m, 1H), 8.30 (d, J = 7.8 Hz, 1H), 8.22 (d, J = 7.2

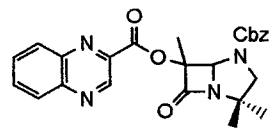

7

Hz, 1H), 7.93 (m, 2H), 7.37 (m, 5H), 5.61bs, 5.57bs, 5.04-5.29m (3H), 3.89bs, 3.86bs, 3.79d, J = 10.5 Hz, 3.70 d, J = 10.5 Hz (1H), 3.41s, 3.25d, J = 10.8 Hz, 3.16d, J = 10.2 Hz (1H), 1.69s, 1.62s, 1.37s, 1.28s, 1.27s, 1.19s (9H).

2-bromomethylquinoxaline 18. 2-Methylquinoxaline (2.25 mL, 17.5 mmol), N-bromosuccinimide (3.1 g, 17.5 mmol) that had been recrystallized from H_2O then dried (P_2O_5) just before use, 2,2'-azobisisobutyronitrile (57 mg, 0.35 mmol), and 50 mL of CCl_4 were combined in a 100 mL round bottom. The reaction was allowed to stir in front of two 500-W halogen lamps at 60° C for 1 hour. The succinimide floating in the crude reaction mixture was removed by filtration using 10 mL of CCl_4 to rinse the flask. The remaining solvent was removed *in vacuo*. Flash chromatography (SiO_2, 3.5 x 16 cm, 30 % EtOAc/hexane), yielded 2-bromomethylquinoxaline (2.22 g, 57%) as a light pink solid: MP 65-67°C; ^{1}H NMR δ 9.01 (s, 1H), 8.07-8.15 (m, 2H), 7.81 (m, 2H), 4.72 (s, 2H); ^{13}C NMR δ 151.9, 145.5, 141.8, 141.6, 130.7, 130.5, 129.4, 31.2, 25.5; MS *m/z* 223.0 (MH^+), 225.0 (MH^+). Anal. Calcd for $C_9H_7N_2Br$: C, 48.46; H, 3.16; N, 12.56. Found: C, 48.58; H, 3.32; N, 12.50.

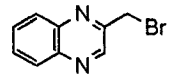

18

Carbamate Protected Quinoxaline Ether Azapenam 19. Hydroxyazapenam **6** (1.38 g, 4.54 mmol), 2-bromomethylquinoxaline (1.06 g, 4.76 mmol), tetrabutylammonium iodide (17 mg, 0.045 mmol), and 60% NaH in mineral oil (200 mg, 4.99 mmol) were combined in a 50 mL round bottom flask. This was cooled to 0° C under argon with an ice bath before 16 mL of THF was quickly added with a syringe. The ice bath was removed after 30 min. and the reaction was allowed to stir for 24 hr at room temperature at which time it was quenched with dropwise addition of 2 mL of H_2O. The crude mixture was diluted to ~75 mL with diethyl ether then

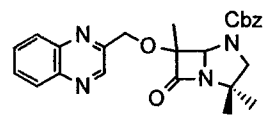

19

washed with 3 x 15 mL of H_2O; the aqueous layer was back-extracted with 2 x 15 mL of diethyl ether. The organics were dried over $MgSO_4$, and the solvent was removed by rotary evaporation. Purification was done with flash chromatography (SiO_2, 3.5 x 13 cm, 50 % EtOAc/hexane), giving the protected quinoxaline azapenam **19** (1.91 g, 94%) as an off-white solid: MP 78-80^0 C; ^{1}H NMR (Cbz rotamers) δ 9.06 (s, 0.33H), 8.95 (s, 0.66H), 7.98-8.11 (m, 2H), 7.72 (m, 2H), 7.22-7.36 (m, 5H), 5.11-5.32 (m, 3H), 4.55 (dd, J = 4.5, 12.6 Hz, 2H), 3.79 (d, J = 10.8 Hz, 0.66H), 3.72 (d, J = 10.2 Hz, 0.33H), 3.17 (d, J = 10.8 Hz, 1 H), 1.61s, 1.46s, 1.34s, 1.18s (9H); ^{13}C NMR δ 172.8, 172.4, 153.9, 153.2, 152.3, 152.2, 144.2, 142.0, 141.4, 135.9, 135.6, 130.1, 130.0, 129.7, 129.6, 129.3, 129.0, 128.6, 128.4, 128.1, 128.0, 90.7, 74.9, 74.4, 68.1, 67.7, 61.4, 61.0, 60.4, 25.9, 22.0, 14.4, 14.1; IR (neat) ν 1774, 1713 cm^{-1}; MS *m/z* 447.1 (MH^+). Anal. Calcd for $C_{25}H_{26}N_4O_4$: C, 67.25; H, 5.87; N, 12.55. Found: C, 67.41; H, 6.01; N, 12.73.

General Procedure for Deprotection of the N-Cbz azapenams (35), (41), (7), (19). The carbamate protected azapenams were dissolved in a mixture of 5:1 CH_2Cl_2:triethylamine (10 mL/mmol Cbz-azapenam). The 10 % Pd/C (55% wt. Cbz-azapenam) was carefully added under a steady flow of argon. A balloon filled with H_2 was appended and the flask purged briefly with a needle. After the reaction stirred at room temperature for 4 hours, it was filtered and most of the solvent was removed *in vacuo*. The yellow solid was dissolved in CH_2Cl_2 and washed three times with saturated $NaHCO_3$ (washed two times with 5% $NaHCO_3$ for **35**). The aqueous layer was back extracted twice with CH_2Cl_2 before the organic layers were combined, dried over $MgSO_4$, and the solvent removed *in vacuo*. After adsorbing onto silica gel (2X wt. crude), the crude reaction mixtures were chromatographed (SiO_2, 75% EtOAc/ 1% triethylamine/hexane for **9**, 1% triethylamine/EtOAc for **12**, 8% i-PrOH/1%triethylamine/EtOAc for **17**, 2% i-PrOH/1%triethylamine/EtOAc for **24**) to give the deprotected azapenams as bright-yellow solids.

Quinoxaline Ester Azapenam 8. The protected quinoxaline ester azapenam 7 (380 mg, 0.83 mmol) was deprotected according to the general procedure to give the quinoxaline ester

azapenam **8** (156 mg, 58%). Due to the extremely labile quinoxaline ester linkage, only ^{1}H NMR data was obtained: ^{1}H NMR δ 9.52 (s, 1H), 8.28 (dd, J = 1.5, 8.4 Hz, 1H), 8.19 (d, J = 7.8 Hz, 1H), 7.89 (m, 2H), 5.14 (s, 1H), 3.18 (d, J = 11.1 Hz, 1H), 2.78 (d, J = 10.8 Hz, 1H), 2.50 (bs, 1H), 1.71 (s, 3H), 1.64 (s, 3H), 1.18 (s, 3H).

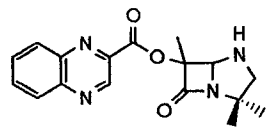

8

Quinoxaline Ether Azapenam 20. The protected quinoxaline ether azapenam **19** (1.13 g, 2.53 mmol) was deprotected according to the general procedure to give the quinoxaline ether azapenam **20** (678 mg, 86%): MP 131-133° C; ^{1}H NMR δ 9.06 (s, 1H), 8.11-8.15 (m, 1H), 8.05-8.08 (m, 1H), 7.78 (m, 2H), 5.10 (d, J = 12.9 Hz, 1H), 5.04 (d, J = 12.9 Hz, 1H), 4.89 (s, 1H), 3.12 (d, J = 10.8 Hz, 1 H), 2.69 (d, J = 11.4 Hz, 1H), 2.35 (bs, 1H), 1.61 (s, 3H), 1.48 (s, 3H), 1.15 (s, 3H); ^{13}C NMR δ 175.0, 152.8, 144.6, 142.2, 141.7, 130.3, 129.9, 129.5, 129.2, 90.4, 78.1, 68.2, 62.2, 61.3, 25.1, 22.0, 15.0; IR (neat) ν 3354, 1751 cm^{-1}; MS 313.2 (MH$^+$). Anal. Calcd for $C_{17}H_{20}N_4O_2$: C, 65.37; H, 6.45; N, 17.94. Found: C, 65.49; H, 6.51; N, 18.18.

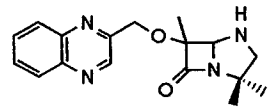

20

Extended Quinoxaline Azapenam 35. The protected extended quinoxaline azapenam **34** (371 mg, 0.74 mmol) was deprotected according to the general procedure to give the quinoxaline azapenam **35** (165 mg, 61%): MP 55-57° C; ^{1}H NMR δ 9.68 (s, 1H), 8.32 (bs, 1H), 8.18 (m, 2H), 7.88 (m, 2H), 4.77 (s, 1H), 3.95 (m,2H), 3.81 (m, 2H), 3.07 (d, J = 10.8 Hz, 1H), 2.64 (d, J = 10.2 Hz, 1H), 2.29 (bs, 1H), 1.57 (s, 3H), 1.38 (s, 3H), 1.10 (s, 3H); ^{13}C NMR δ174.9, 163.0, 143.5, 143.0, 139.9, 131.2, 130.4, 129.4, 129.1, 89.5, 77.0, 76.4, 64.3, 61.8, 60.8, 39.5, 24.7, 21.6, 14.6; IR (neat) ν 3345, 1752, 1671 cm^{-1}; FABHRMS *m/z* 370.1865 (M + H$^+$, $C_{19}H_{24}N_5O_3$ requires 370.1879).

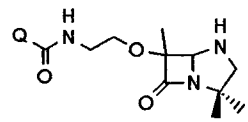

35

Extended Chiral Quinoxaline Azapenam 42. The protected chiral quinoxaline azapenam **41** (490 mg, 0.90 mmol) was deprotected according to the general procedure to give the chiral quinoxaline azapenam **42** (195 mg, 53%): MP 61-63° C; $[\alpha]^{23}_D$ +107.9 (c 0.61, $CHCl_3$); ^{1}H NMR δ 9.67 (s, 1H), 8.30 (bs, 1H), 8.17 (m, 2H), 7.86 (m, 2H); 4.90 (s, 1H), 3.73-3.99 (m, 4H), 3.72 (s, 3H), 3.67 (d, J = 12.0 Hz, 1H), 2.68 (d, J = 12.0 Hz, 1H), 2.33 (bs, 1H), 1.74

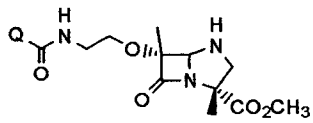

42

(s, 3H), 1.36 (s, 3H); ^{13}C NMR δ174.9, 172.0, 163.4, 143.8, 143.4, 140.3, 131.6, 130.8, 129.8, 129.5, 90.3, 80.1, 77.4, 66.4, 64.8, 60.8, 53.0, 39.8, 17.5, 14.9; IR (neat) ν 3349, 1761, 1738, 1673 cm^{-1}; FABHRMS *m/z* 414.1767 (M + H$^+$, $C_{20}H_{24}N_5O_5$ requires 414.1777).

General Procedure for Dimerization of quinoxaline azapenams (8), (20), (35), (42). The quinoxaline azapenams (1 equiv) and camphor sulphonic acid (0.12 equiv) were combined into a Pyrex pressure tube with CH_2Cl_2 (65 mL/mmol for **8** & **20**; 100 mL/mmol for **35,42**). The solution was heated (50° C for **8**, 65° C for **20, 35,** 80° C for **42**) for 15 hours then washed three times with saturated $NaHCO_3$ (except for **9**, in which the crude reaction mixture was concentrated *in vacuo* then loaded directly on a flash column; SiO_2, 1% triethylamine/EtOAc, producing a 1:1 mixture of **9** in 80% yield). The aqueous layer was back extracted twice with CH_2Cl_2 before the organic layers were combined, dried with Na_2SO_4, and the solvent removed *in vacuo*. The crude reaction mixture from the dimerization of **20** was dissolved in a minimum amount of ethyl acetate before being loaded on to a 1.5 x 10 cm silica gel column that had been slurry packed with 2% triethylamine/EtOAc, then eluted with 1% triethylamine/EtOAc for the first 100 mL followed by 500 mL of 10% iPrOH/1% triethylamine/EtOAc; 5 mL fractions were collected for the first ten, 20 mL fractions for the rest. Collection of the bright yellow band provided the cis imine cyclam in 50 % yield; the trans cyclam was never isolated. For azapenams **35** and **42**, the crude reaction mixtures were taken directly to the reduction step without further purification.

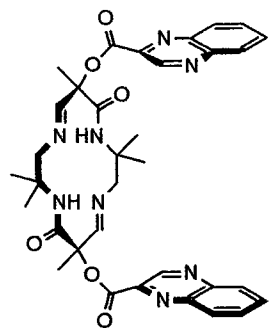

9

Cis and Trans Imine Ester cyclams 9: Due to the extremely labile quinoxaline ester linkage, only ^{1}H NMR and mass spec. data were obtained: ^{1}H NMR δ 9.61 (s, 2H), 9.59 (s, 2H), 9.35 (s, 2H), 8.70 (s, 2H), 8.32 (m, 4H), 8.21 (m, 4H), 8.03 (s, 2H), 7.99 (s, 2H), 7.90 (m,8H), 3.97 (d, J = 9.9 Hz, 2H), 3.72 (d, J = 12.9 Hz, 2H), 3.49 (d, J = 12.9 Hz, 2H), 3.11 (d, J = 11.7 Hz, 2H), 1.94 (s, 12H), 1.60 (s, 6H), 1.53 (s, 6H), 1.46 (s, 6H), 1.35 (s, 6H); MS 653.0 (MH$^+$).

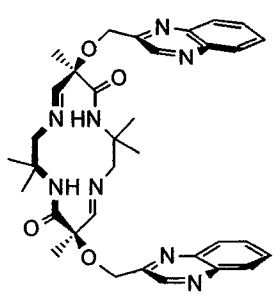

21

Cis Imine Ether Cyclam 21: MP 125°C D; ^{1}H NMR δ 9.11 (s, 2H), 7.97 (m, 4H), 7.80 (s, 2H), 7.72 (m, 4H), 7.61 (s, 2H), 5.14 (d, J = 12.6 Hz, 2H), 4.85 (d, J = 12.6 Hz, 2H), 4.07 (d, J = 11.7 Hz, 2H), 3.37

(d, J = 12.0 Hz, 2H), 1.68 (s, 6H), 1.48 (s, 6H), 1.36 (s, 6H); ^{13}C NMR δ 169.7, 166.5, 153.1, 145.0, 142.1, 141.6, 129.9, 129.8, 129.6, 129.3, 82.2, 67.8, 65.9, 54.3, 27.0, 25.3, 22.4; IR (neat) ν 3400, 1673 cm^{-1}; MS 625.3 (MH^+). Anal. Calcd for $C_{34}H_{40}N_8O_4$: C, 65.37; H, 6.45; N, 17.94. Found: C, 65.51; H, 6.31; N, 17.76.

General Procedure for Reduction of Imine cyclams to Form Cyclams (13), (18a), (18b), (26). The imine cyclams (1 equiv) and benzoic acid (2.2 equiv) were dissolved in EtOH (20 mL/mmol imine cyclam), placed under argon, then brought to -5° C with a salt water / ice bath. $NaBH_3CN$ (2.0 equiv) was dissolved in a minimum amount of EtOH (0.5-2 mL) at room temperature then added dropwise to the reaction mixture. The reaction was allowed to run for 1 hour before slow addition of 2-5 mL's of EtOAc followed by dropwise addition of 1-2 mL's of 5% NaOH. After stirring for several minutes at this temperature, the contents were transferred to a separatory funnel, diluted with ethyl acetate (enough to prevent an emulsion) and washed 3 times with 5% NaOH. The aqueous layers were combined and back-extracted twice with CH_2Cl_2. After drying the combined organic layers with Na_2SO_4 the solvent was removed *in vacuo*. The crude reaction mixtures were dissolved in a minimum amount of CH_2Cl_2 and loaded onto a flash column (SiO_2, 90% EtOAc/1% triethylamine/hexane for **13**, 10% *i*-PrOH/1%triethylamine/EtOAc for **18a/18b**, 1% i-PrOH/1%triethylamine/EtOAc for **26**).

Cis Quinoxaline Ether Cyclam 23. The imine cyclam (87 mg, 0.14 mmol) was allowed to react according to the general procedure to afford **23** (63 mg, 72%) as a light yellow solid. To obtain suitable crystals for X-ray diffraction, the purified cyclam **23** (~ 10-15 mg) was dissolved in a minimum amount of CH_2Cl_2 then filtered through a small piece of cotton into an NMR tube (~1 cm deep). Hexane (~3-4 cm) was then very slowly layered on top. After 2-3 days, several X-ray quality crystals were harvested from the tube and X-ray data was obtained: MP 185 - 188°C; ^{1}H NMR δ 9.02 (s, 2H), 8.03 (m, 4H), 7.72 (m, 4H), 7.25 (bs, 2H), 4.95 (d, J = 12.6 Hz, 2H), 4.81 (d, J = 12.3 Hz, 2H), 3.55 (d, J = 11.1 Hz, 2H), 3.00 (d, J = 12.6 Hz, 2H), 2.82 (d, J = 12.6 Hz, 2H), 2.18 (d, J = 11.1 Hz, 2H), 1.46 (s, 6H), 1.37 (s, 6H), 1.17 (s, 6H); ^{13}C NMR δ 171.5, 153.2, 144.5, 142.2, 141.8, 130.5, 129.9, 129.4, 129.1, 81.6, 65.5, 56.8, 56.6, 53.3, 27.3, 25.5,

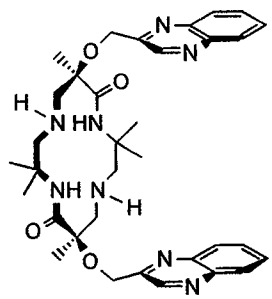

23

20.0; IR (neat) ν 3400, 1672 cm^{-1}; MS 629.3 (MH^+). Anal. Calcd for $C_{34}H_{44}N_8O_4$: C, 64.95; H, 7.05; N, 17.82. Found: C, 65.04; H, 6.99; N, 17.54.

Cis and Trans Extended Amides (37), (38). The crude material (60 mg, 0.081 mmol) from the dimerization of **17** was allowed to react according to the general procedure to produce a 1:4 (**38:39**) mixture of extended amide cyclams (37 mg, 62%). After flash chromatography (necessary to separate **38,38** from other unidentified impurities) the two diastereomers were separated by recrystallization (solvent diffusion): **38,39** were dissolved in a minimum amount of CH_2Cl_2 (3-5 mL) then filtered through cotton into a small vial. Diethyl ether (3-5X volume CH_2Cl_2) was gently layered on top of the CH_2Cl_2 layer which immediately formed a turbid interface that became clear after ~10 minutes. After 2-3 days, crystals had formed at the interface and on the bottom of the vial; the mother liquor was pipetted off and a second recrystallization was set up. After two recrystallizations, the diastereomers were completely separated (7 mg **18a**, 30 mg **18b**). X-ray diffraction showed the crystals to be the trans diastereomer.

Trans amide 38: MP 166-168° C; ^1H NMR δ 9.66 (s, 2H), 8.42 (bs, 2H), 8.19 (m, 2H), 8.05 (m, 2H), 7.85 (m, 4H), 3.68 (m, 6H), 3.46 (m, 2H), 2.58 (d, J = 12.0 Hz, 2H), 2.50 (d, J = 11.7 Hz, 2H), 1.98 (d, J = 12.0 Hz, 2H), 1.93 (d, J = 12.3 Hz, 2H), 1.59 (bs, 2H), 1.37 (s, 6H), 1.33 (s, 6H), 1.15 (s, 6H); ^{13}C NMR δ 171.6, 163.5, 144.2, 143.6, 140.4, 131.9, 131.3, 131.1, 129.8, 79.1, 77.4, 62.8, 60.9, 57.2, 52.8, 40.0, 25.8, 23.4, 19.5; IR (neat) ν 3308, 1666, 1531 cm^{-1}; MS 743.8 (MH^+).

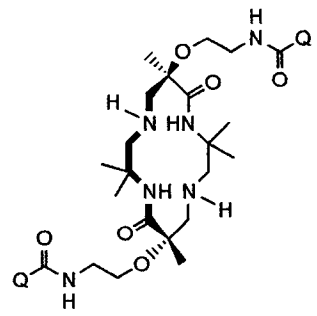

38

Cis amide 37: MP 99-102° C; ^1H NMR δ 9.64 (s, 2H), 8.36 (bs, 2H), 8.16 (m, 2H), 8.09 (m, 2H), 7.83 (m, 4H), 7.13 (bs, 2H), 3.60-3.74 (m, 8H), 3.40 (d, J = 11.4 Hz, 2H), 2.83 (d, J = 12.3 Hz, 2H), 2.63 (d, J = 12.3 Hz, 2H), 2.11 (d, J = 11.4 Hz, 2H), 1.37 (s, 6H), 1.31 (s, 6H), 1.22 (s, 6H); ^{13}C NMR δ 172.1, 163.9, 144.1, 144.0, 131.8, 131.1, 129.8, 129.7, 80.4, 62.2, 57.1, 56.1, 53.0, 40.2, 26.9, 25.3, 19.7; IR (neat) ν 3360, 1667, 1532 cm^{-1}; FABHRMS *m/z* 743.3964 ($M + H^+$, $C_{20}H_{24}N_5O_5$ requires 743.3993).

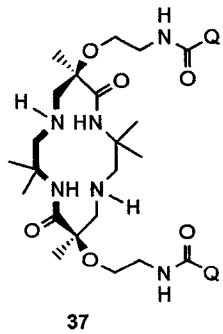

37

Chiral Extended Amide (44). The chiral amide imine cyclam (156 mg, 0.19 mmol) was allowed to react according to the general procedure to produce a complex mixture of products

that could be partially purified by flash chromatography (95 mg, 61%). The resulting solid was subjected to the next reaction without further purification.

General Procedure for Synthesis of Nickel Complexes (1), (24), (40), (39). In a small round bottom flask (10-25 mL), $Ni(OAc)_2 \cdot 4H_2O$ (1.20 equiv) was mixed with 2-4 mL of methanol and gently warmed over a heat gun for several minutes to generate a slurry. The quinoxaline cyclam (1 equiv) was dissolved in 2-4 mL of methanol and then pipetted into the slurry. A reflux condenser was attached for a handle and the flask was continually warmed to boiling over a heat gun for 5-10 minutes (monitored by the color change from light yellow to bright pink). After the remainder of the solvent was removed *in vacuo*, the crude reaction mixture was dissolved in CH_2Cl_2 and washed three times with saturated $NaHCO_3$. The aqueous layer was back extracted until no more color remained in the water (3-5 times). The resulting crude mixtures were dissolved in a minimum amount of CH_2Cl_2 and loaded onto a flash column (SiO_2, 10% *i*-PrOH/1% triethylamine/EtOAc).

Hydroxycyclam Nickel Complex 1. The hydroxycyclam (40 mg, 0.12 mmol) and $Ni(OAc)_2 \cdot 4H_2O$ (36 mg, 0.15 mmol) were allowed to react according to the general conditions providing nickel complex **1** (28 mg, 60%) as a bright pink solid: MP 112-115°C; ^1H NMR and ^{13}C NMR were isolated as a complex mixture of N-H isomers; spectra are included in the supplemental material; IR (neat) ν 3184, 1574 cm^{-1}; FABHRMS *m/z* 401.1685 ($M + H^+$, $C_{16}H_{31}N_4NiO_4$ requires 401.1699).

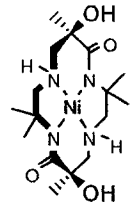

1

Cis Ether Nickel Complex 24. The cis ether cyclam **23** (38 mg, 0.060 mmol) and $Ni(OAc)_2 \cdot 4H_2O$ (18 mg, 0.072 mmol) were allowed to react according to the general conditions providing nickel complex **24** (29.5 mg, 72%, all N-H isomers) as a pink solid. Flash chromatography allowed for separation of the clean N-H isomers: MP 72-75° C; ^1H NMR δ 9.03 (s, 2H), 8.03 (d, J = 8.1 Hz, 2H), 7.83 (d, J = 7.8 Hz, 2H), 7.63 (m, 2H), 7.54 (m, 2H), 5.24 (d, J = 13.5 Hz, 2H), 5.03 (d, J = 13.8 Hz, 2H), 3.34 (bt, J = 12.9, 2H), 2.82 (m, 4H), 2.35 (dd, J = 2.1, 11.4 Hz, 2H), 1.95 (dd, J = 3.0, 7.2 Hz, 2H), 1.43 (s, 6H), 1.38 (s, 6H), 1.33 (s, 6H); ^{13}C NMR δ 172.9, 153.8, 144.5, 142.0, 130.2, 129.5, 129.4, 129.0, 78.0, 77.4, 66.1, 66.0, 59.1, 57.5, 24.9, 23.2, 21.0; IR (neat) ν 3400, 1567 cm^{-1};

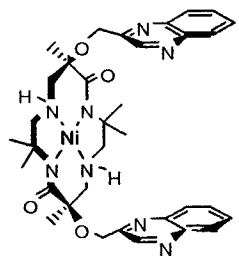

24

FABHRMS *m/z* 685.2756 ($M + H^+$, $C_{34}H_{43}N_8NiO_4$ requires 685.2761).

Trans Extended Amide Nickel Complex 40. The trans extended amide cyclam **38** (10.5 mg, 0.014 mmol) and $Ni(OAc)_2 \cdot 4H_2O$ (4.5 mg, 0.017 mmol) were allowed to react according to the general conditions providing nickel complex **40** (8.0 mg, 71%) as a pink solid: MP 135-138° C; ^1H and ^{13}C NMR are included in the supplemental (N-H isomers); IR (neat) ν 3400, 1665, 1570, 1532 cm^{-1}; MS 799.8 (MH^+).

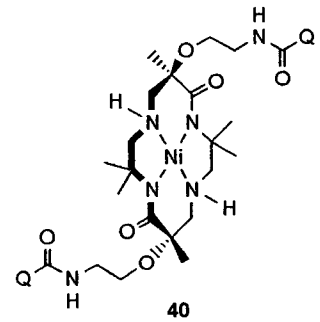

40

Cis Extended Amide Nickel Complex 39. The cis extended amide cyclam **37** (44 mg, 0.059 mmol) and $Ni(OAc)_2 \cdot 4H_2O$ (18 mg, 0.071 mmol) were allowed to react according to the general conditions providing nickel complex **39** (34 mg, 72%, all N-H isomers) as a pink solid. Flash chromatography allowed for separation of the clean N-H isomers: MP 96-99° C; ^1H NMR δ 9.62 (s, 2H), 8.27 (bt, J = 5.6 Hz, 2H), 8.08 (d, J = 8.0, 2H), 7.97 (d, J = 8.0 Hz, 2H), 7.78 (m, 4H), 4.08 (m, 4H), 3.78-3.90 (m, 4H), 3.12 (bt, J = 12.8 Hz, 2H), 2.80 (t, J = 10.8 Hz, 2H), 2.61 (t, J = 11.6 Hz, 2H), 2.19 (d, J = 9.2 Hz, 2H), 1.90 (dd, J = 3.2, 10.8 Hz, 2H), 1.41 (s, 6H), 1.35 (s, 6H), 1.25 (s, 6H); ^{13}C NMR δ 173.1, 163.8, 144.1, 143.9, 143.6, 140.3, 131.7, 131.0, 129.7, 129.6, 77.43, 66.1, 63.3, 59.0, 57.4, 40.7, 25.2, 23.1, 20.8; IR (neat) ν 3251, 1672, 1576, 1530 cm^{-1}; FABHRMS *m/z* 799.3159 ($M + H^+$, $C_{34}H_{49}N_{10}NiO_6$ requires 799.3190).

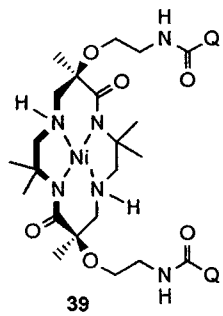

39

Cis Extended Amide Chiral Nickel Complex 43. The partially purified extended chiral cyclam **44** (58 mg, 0.070 mmol) and $Ni(OAc)_2 \cdot 4H_2O$ (22 mg, 0.087 mmol) were allowed to react according to the general conditions providing clean nickel complex **43** (34 mg, 55%, all N-H isomers) as a pink solid. Flash chromatography allowed for the separation of the clean N-H isomers: MP 128° C D; $[\alpha]^{23}_D$ -362.8 (c 0.43, $CHCl_3$); ^1H NMR δ 9.63 (s, 2H), 8.48 (bs,2H), 8.08 (d, J = 6.9 Hz, 2H), 7.98 (d, J = 7.2 Hz, 2H), 7.77 (m, 4H), 3.98-4.22 (m, 8H), 3.59 (s, 6H), 2.95 (t, J = 12.0 Hz, 2H), 2.26-2.42 (m, 6H), 1.49 (s, 6H), 1.26 (s, 6H); ^{13}C NMR δ176.3, 174.6, 164.0, 144.3, 144.0, 143.9, 140.4, 131.5, 130.8, 129.8, 129.6, 77.1, 64.0, 63.3, 60.4, 56.2, 52.4, 41.0, 20.8, 20.5; IR (neat) ν

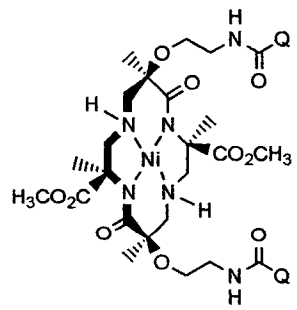

43

1740, 1670, 1582 cm^{-1}; FABHRMS *m/z* 885.2824 (M - H^+, $C_{40}H_{47}N_{10}NiO_{10}$ requires 885.2830).

Extended Amide Chiral cyclam 44. The chiral amide nickel complex **43** (15 mg, 0.017 mmol) was dissolved in 2 mL of CH_2Cl_2 and brought to 0° C with an ice bath. Concentrated HCl (~37%) was dripped in with a pipet (~3-5 drops) until the solution turned from pink to light yellow. At this time, 5% NaOH (2 mL) was very slowly dripped into the reaction and the contents were transferred to a separatory funnel. The organic layer was diluted with 20 mL of CH_2Cl_2 before washing with 3 X 5 mL of 5% NaOH. The aqueous layer was back extracted with 2 X 8 mL of CH_2Cl_2. The combined organic layers were dried with Na_2SO_4 and the solvent removed *in vacuo* to provide, after purification by flash chromatography (SiO_2, 4% i-PrOH/1%TEA, EA), the chiral amide cyclam (12 mg, 14 mg theoretical, 86%) as a light yellow solid: MP 144-146° C; $[\alpha]^{23}_D$ +20.7 (c 0.15, $CHCl_3$); ^1H NMR δ 9.68 (s, 2H), 8.30 (bs, 2H), 8.17 (m, 4H), 8.00 (bs, 2H), 7.85 (m, 4H), 3.60-3.80 (m, 10H), 3.69 (s, 6H), 2.80 (t, J = 12.0 Hz, 3H), 2.68 (t, J = 12.0 Hz, 3H), 1.61 (s, 6H), 1.32 (s, 6H); ^{13}C NMR δ 174.8, 171.9, 163.9, 144.2, 144.1, 143.8, 140.6, 131.8, 130.9, 129.9, 129.7, 80.5, 61.9, 61.4, 55.9, 53.3, 53.1, 40.1, 21.4, 19.5; IR (neat) ν 3394, 1737, 1677 cm^{-1}; FABHRMS *m/z* 831.3778 (M + H^+, $C_{40}H_{51}N_{10}O_{10}$ requires 831.3790).

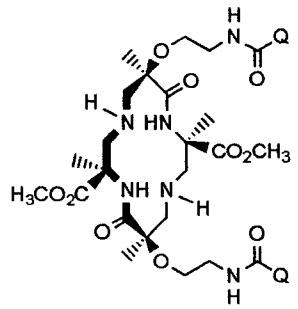

44

General Procedure for Agarose Gel Electrophoresis Bisintercalation Studies with cyclams (23), (37), (38), (44), and their nickel complexes (24), (29), (40), (43). Because of the limited solubility of some of the cyclams in water, all agents were dissolved in DMSO as either 100X or 1000X stock solutions and diluted with DMSO to the working concentrations just prior to addition of the DNA solution. The DNA solution containing 0.25 μg of supercoiled ΦX174 RFI DNA (purchased from New England Biolabs and used without further purification) in 9 μL of 50 mM Tris-HCl buffer solution (pH 8) was treated with 1 μL of agent in DMSO. The control DNA was also treated with 1 μL DMSO. The [agent] to [DNA] base pair ratios tested were 0.02, 0.04, 0.1, 0.2, 1, 5, 20. Each agent was tested under a variety of conditions: 25° C for 3 hours, 25° C for 15 hours; 37° C for 3 hours, and 37° C for 15 hours. After incubation for the given time and temperature, the reactions were quenched with 5 μL of Keller loading buffer

formed by mixing Keller buffer (0.4 M Tris-HCl, 0.05 M NaOAc, 0.0125 M EDTA, pH 7.9) with glycerol (40%), sodium dodecyl sulfate (0.4%), and bromophenol blue (0.3 %). The agarose gels (1%) were run at 90V for 3 hours. The gel was stained with 0.1 μg/mL ethidium bromide for 30 minutes, then destained by soaking in water for 15-20 minutes. The gel was then photographed under UV transillumination at 302 nm with a Polaroid 667 ISO 3000/36° using black and white film.

General Procedure for DNA nicking studies using nickel complexes (24), (29), (40), (43), (1), (2). Stock solutions of the compounds to be tested were prepared in water (the nickel complexes were much more soluble in water than the free ligand cyclams) as 2.5 mM stock solutions (except **1** which was prepared as a 625 μM stock solution because of its limited solubility in water). A stock solution of supercoiled pBR322 plasmid DNA (purchased from New England Biolabs and used without further purification) was prepared by diluting 12.5 μL of 1000 μg/mL solution with 372 μL of Tris-EDTA (10 mM Tris-HCl and 1 mM EDTA at pH 8). This solution was stored in the -20°C freezer until just before use. A nicking reaction cocktail was prepared with 84 μL of 50 μM bp pBR 322, 10.5 μL of 200 mM phosphate buffer, pH 7.4, 5.25 μL of 200 mM NaCl, and 5.25 μL of water which provided 105 μL of 40 μM base pair pBR 322. A solution of 10 mM oxone was prepared with 5.0 mg oxone and 813 μL of water. Nicking reactions were prepared with 5 μL of DNA cocktail and 4 μL of the agent in water (the control DNA was also treated with 4 μL water. After centrifugation, the reactions were allowed to equilibrate for 15 minutes before addition of 1 μL of 10mM oxone, providing a solution of 20 μM base pair supercoiled pBR 322 DNA, 10 mM phosphate, 5 mM NaCl, and 1 mM oxone. After 1 hour the reactions were quenched with 1 μL of 10X Ficoll loading buffer (25% Ficoll 400, 0.25% bromophenol blue, and 0.25% xylene cyanol) then loaded onto a 1% agarose gel. The gel was run at 115V for 1 hour before staining with Sybr Gold ® nucleic acid stain (purchased from Molecular Probes) for 2 hours and scanning on a Storm Scanner 840 (Molecular Dynamics) . The data was analyzed by comparing the density of the remaining form I DNA of the reactions to the control lane's form I DNA using Image Quant version 5.0 (Molecular Dynamics).

References:

1. Curtis, N.F. *Coord. Chem. Rev.* **1968**, 3,3,3-47.
2. Kimura, E. *J. Coord. Chem.* **1986**, 15,1.
3. Kimura, E. *Tetrahedron* **1992**, 48, 6175.
4. Busch, D.H.; Alcock, N.W. *Chem. Rev.* **1994**, 94, 585.
5. Betshart, C.; Hegedus, L.S. *J. Am. Chem. Soc.* **1991**, 113, 5884-5886.
6. Hegedus, L.S,; Moser, W.H. *J. Org. Chem.*, **1994**, 55, 7779-7784.
7. Dumas, S.; Lastra, E.; Hegedus, L.S. *J. Am. Chem. Soc.*, **1995**, 117, 3368-3379.
8. Hsiao, Y.; Hegedus, L.S.; *J. Org. Chem.*, **1997**, 62, 3586-3591.
9. Capelle, N.; Barbet, J.; Dessen, P.; Blanquet, S.; Roques, P.B; Le Pecq, J., *Biochemistry,* **1979**, 18,3354-3362.
10. Atwell, G.J.; Leupin, W.; Twigden, S.J.; Denny, D. A., *J. Am. Chem. Soc.*, **1983**, 105, 2913-2914.
11. Chaires, J. B.; Leng, F.; Przewloka, T.; Fokt, I.; Ling, Y.H. *J. Med. Chem.*, **1997**, 40-261-266.
12. Onfelt, B.; Lincoln, P.; Norden, B, *J. Am. Chem. Soc.*, **1999**, 121, 10846-10847.
13. Butler, J.A.V.; Smith, K.A., *J. Chem. Soc.*, **1950,** 3411-3418.
14. Conway, B.E.; Gilbert, L.; Butler, J.A.V. *J. Chem. Soc.*, **1950**, 3421-3425.
15. Press, E.M.; Butler, J.A.V., *J. Chem. Soc.*, **1952,** 626-631.
16. Lawley, P.D.; Brookes, P., *Biochem. J.* **1963**, 89, 127-138.
17. Tamm, C.; Shapiro, H. S.; Lipshitz, R.; Chargaff, E.*J. Biol. Chem.*, **1953**, 203, 678-688.
18. Lawley, P.D. Prog. *Nucleic Acid Res. Mol. Biol.* **1966**, 5, 89-131.
19. Maxam, A.M.; Gilbert, W., Proc. *Natl. Acad. Sci. U.S.A.*, **1977**, 74, 560-564.
20. Maxam, A.M.; Gilbert, W., *Methods, Enzymol.* **1980**, 65, 499-560.
21. Grosch, D.S.; Hopwood, L.E. In *Biological Effects of Radiations*; Academic Press: London, **1979**.
22. Muller, H.J. *Proc. Natl. Acad. Sci. U.S.A.* **1928**, 14, 714-726.
23. Dustin, P., Jr. *Nature* **1947**, 159, 794-797.
24. Shapiro, R.; Danzig, M., *Biochemistry*, **1972**, 11, 23-29.
25. Klein, C.B.; Frenkel, K.; Costa, M. *Chem. Res. Toxicol.* **1991**, 4, 592-604.
26. Wetterhahn, K.E.; Dudek, E.J. *New J. Chem.* **1996**, 20, 199-203.
27. Kasprzak, K.S. *Chem. Res. Toxicol.* **1991**, 4, 604-615.
28. Costa, M.; Salnikov, K.; Cosentino, S.; Klein, C.B.; Huang, Z.; Zhuang, Z. Environ. Health Perspect. **1994**, 102, suppl 3, 127-130.
29. Nieboer, E.; rossetto, F.E.; Menon, C.R. *Met. Ions Biol. Systems*, **1988**,23, 359-403.
30. Lloyd, D.R.; Phillips, D.H.; Carmichael, P.L. *Chem. Res. Toxicol.* **1997**, 10, 393-400.
31. Oller, A.R.; Costa, M.; Oberdorster, G., *Tox.Appl. Pharmacol.* **1997**, 143, 152-166.
32. Inoue, S.; Kawanishi, S. *Biochem. Biophys. Res. Comun.* **1989**, 159, 445-451.
33. Datta, A.K.; North, S.L.; Kasprzak, K. S. *Sci. Total Environ.* **1994**, 148, 207-216.
34. Bal, W.; Lukszo, J.; Kasprzak, k. s. *Chem Res. Toxicol.* **1996**, 9, 535-540.
35. Chen, X.; Rokita, S.E.; Burrows, C.J.; *J. Am. Chem. Soc.*, **1991**, 113, 5884-5886.

36. Muller, J.G.; Chen, X.; Dadiz, A.C.; Rokita, S.E.; Burrows, C.J.; *J. Am. Chem. Soc.*, **1992**, 114, 6407-6411.
37. Chen, X.; Woodson, S.; Burrows, C.; Rokita, S. *Biochemistry* **1993,** 32, 7610.
38. Burrows, C.J.; Rokita, S.E. *Acc. Chem. Res.* **1994**, 27,295-301
39. Muller, J.G.; Hickerson, R.J.P.; Burrows, C.J. *J. Am. Chem. Soc.*, **1997**, 119, 1501-1506.
40. Shih, H-C; Tang, N.; Burrows, C.J.; Rokita, S.E.; *J. Am. Chem. Soc.*, **1998**, 120, 3284-3288.
41. Lepentsiotis, V.; Domagala, J.; Grgic, I.; van Eldik, R.; Muller, J.G.; Burrows, C.J.; *Inorg. Chem*, **1999**, 38, 3500-3505.
42. Burrows, C.J.; Muller, J.G. *Chem. Rev*, **1998**, 98, 1109-1151.
43. Holmlin, R.E.; Dandliker, P.J.; Barton, J.K. *Angew. Chem.* **1997**, 109,2830
44. Holmlin, R.E.; Dandliker, P.J.; Barton, J.K. *Angew. Chem. Int. Ed. Engl.*, **1997**, 36, 2714.
45. Arkin, M.R.; Stemp, E.D.A.; Coates-Pulver, S.; Barton, J.K. *Chem Biol.* **1997**, 4, 389.
46. Hall, D.B.; Holmlin, R.E.; Barton, J.K. *Nature* **1996**, 382, 731.
47. Hall, D.B.; Barton, J.K. *J. Am. Chem. Soc.*, **1997**, 119, 5045
48. Nunez, M.J.E.; Hall, D.B.; Barton, J.K. *Chem Biol.* **1999**, 6, 85.
49. Saito, I.; Takayama, M.; Sugiyama, H.; Nakatani, K.; Tsuchida, A.; Yamamoto, M. *J. Am. Chem. Soc.*, **1995**, 117,6406.
50. Prat, F.; Houk, K.N.; Foote, C.S. *J. Am. Chem. Soc.*, **1998**, 120, 845.
51. Dervan, P.B. *Science* **1986**, 232, 464.
52. Price, M.A. Tillius, T.D. *Methods Enzymol*, **1992**, 212, 194.
53. Latham, J.A. Chech, T.R. *Science*, **1989**, 245, 276.
54. Kasai, h.; Yamaizumi, Z.; Berger, M.; Cadet, J. *J. Am. Chem. Soc.*, **1992**, 114, 9692-9694.
55. Shigenaga, M.K.; Park, J.W.; Cundy, K.C.; Gimeno, C.J.; Ames, B.N. *Methods Enzymol., 1990, 186, 521-530.*
56. Albert, A. '*Selective Toxicity*,' Wiley, New York 1979.
57. Gale, E.F.; Cundliffe, E.; Reynolds, P.E.; Richmond, M.H. Waring, M.J.; '*The Molecular Basis of Antibiotic Action*,' 2nd edn., Wiley, London, 1981, p.258.
58. Waring, M.J. Pathol. Biol. 1992, 40, 1022
59. Waring, M.J. in *Molecular Aspects of Anticancer Drug-GNA Interactions*; Neidle, S., Waring, M., Eds.; CRC: Boca Raton, Fl, 1993; Vol.1 Chapter 7.
60. Wakelin, L.P.G. *Med. Res. Rev.* **1986**, 6, 275
61. Gale, E.F.; Cundliffe, E.; Reynolds, P.E.; Richmond, M.H.; Waring, M.J. *The Molecular Basis of Antibiotic Action*, 2nd ed.; Wiley; London, 1981; pp333-337.
62. Lerman, L.S. *J. Mol. Biol.* **1961**, 3, 18.
63. Waring, M.J. *J. Mol. Biol.* **1970**, 54, 247-279.
64. Gale, E.F.; Cundliffe, E.; Reynolds, P.E.; Richmond, M.H. Waring, M.J.; '*The Molecular Basis of Antibiotic Action*,' 2nd edn., Wiley, London, 1981, p.258.
65. Waring, M.J. *Recognition of DNA by quinoxaline antibiotics. Molecular Mechanisms of Carcinogenic and Antitumoror Activity, Scripta Varia*, Vol. 70. Pontifical Academy of Sciences, Vatican City, PP. 317-337.

66. Mollegaard, N.E.; Bailly, C.; Waring,M.J.' Nielsen, P.E. *Biochemistry*, **2000**, 39, 9502-9507.
67. Alfredson, T.V.; Maki, A.H.; Waring, M.J. *Biopolymers*, **1991**, 31, 1689-1708.
68. Low, C.M.L.; Drew, H.R.; Waring, M.J. *Nucleic Acids Res.*, **1984**, 4865-4879.
69. Low, C.M.L.; Fox, K.R.; Olsen, R.K. Waring M.J. *Nucleic Acids res.*, **1986**, 2015-2033.
70. Waring, M.J.; Wakelin, L.P.G., *Nature*, **1974**, 252, 653
71. Wakelin, *Med. Res. Rev.*, **1986**, 6, 275.
72. Neidle, S.; Pearl, L.H.; Skelly, J.V. *Biochemical Journal*, **1987**, 243,1
73. Boger, D.L.; Chen, J-H.; Saionz, K.W. *J. Am. Chem. Soc.*, **1996**, 118, 1629-1644.
74. Jennette, K.W.; Lippard, S.J.; Vassiliades, G.A.; Bauer, W.R. *Proc. Natl. Acad. Sci. U.S.A.* **1974**, 71, 3839.
75. Barton, J.K.; Dannenberg, J.J.; Raphael, A.L. *J. Am. Chem. Soc.*, **1982**, 104, 4967.
76. Barton, J.K.; Danishefsky, A.T.; Goldberg, J.M. *J. Am. Chem. Soc.*, **1984**, 106, 2172.
77. Kumar, C.V.; Barton, J.K.; Turro, N.J. *J. Am. Chem. Soc.*, **1985**, 107, 5518.
78. Barton, J.K.; Goldberg, J.M.; Kumar, C.V.; Turro, N.J. *J. Am. Chem. Soc.*, **1988**, 106, 2081.
79. Barton, J.K.; Raphael, A.L. *Proc. Natl. Acad. Sci.* U.S.A., **1985**, 82, 6460.
80. Rehmann, J.P.; Barton, J.K. *Biochemistry*, **1990**, 29, 1701.
81. Barton, J.K. *Science* **1986**, 233,272
82. Yamagishi, A. *J. Chem. Soc., Chem. Commun.* **1983**, 572.
83. Pyle A. M; Barton, J.K. In *Progress in Inorganic Chemistry: Bioinorganic Chemistry*; Lippard, S.J., Ed.; John Wiley & Sons: New York, 1990; Vol 38 pp413-475.
84. Johann, T.W.; Barton, J.K. *Philos. Trans. R. Soc.*, **1996**, 354, 299.
85. Chow, C.S. Barton, J.K. *Methods Enzymol.* **1992**, 212, 219.
86. Murphy, C.J.; Barton, J.K. *Methods Enzymol.* **1993**, 226, 576.
87. Chow, C.S.; Behlen, L.S.; Uhlenbeck, O.C.; Barton, J.K. *Biochemistry*, **1992**, 31, 972.
88. Lim, A.C.; Barton, J.K. *Biochemistry* **1993**, 32, 11029.
89. Lincoln, P.; Norden, B. *Chem. Commun.*, **1996**, 2145
90. Onfelt, B.; Lincoln, P. Norden, B., *J. Am. Chem. Soc.*, **1999**, 121, 10846-10847.
91. Onfelt, B.; Lincoln, P. Norden, B., *J. Am. Chem. Soc.*, **2001**, 123, 3630-3637.
92. Drexler, C.; Hosseini, M.W.; Pratviel, G.; Meunier, B., *Chem. Commun.*, **1998**, 1343.
93. Hegedus, L.S.; Bullock, J.P. Unpublished studies.
94. Tung, R.D.; Rich, D.H.; *J. Am. Chem. Soc.*, **1985**, 107, 4342-4343.
95. Horita, K.; Yoshioka, T.; Tanaka, Y.; Oikawa, Y., *Tetrahedron*, **1986**, 42, 3021.
96. Oikawa, Y.; Tanaka, T.; Horita, K.; Yonemitsu, O., *Tetrahedron Lett.*, **1984**, 25, 5397.
97. Oikawa, Y.; Tanaka, T.; Horita, K.; Yonemitsu, O., *Tetrahedron Lett.*, **1982**, 23, 885.
98. Ikemoto, N.; Schreiber, S.L., *J. Am. Chem. Soc.*, **1992**, 114, 2524.
99. Czernecki, S.; Georgoulis, C.; Provelenghiou, C., *Tetrahedron Lett.*, **1976**, 35, 3535.

100. Kanai, K.; Sakamoto, I.; Ogawa, S.; Suami, T., *Bull. Chem. Soc. Jpn.*, **1987**, 60, 1529.
101. Bergmann, M.; Zervas, L., *Ber.* **1932**, 65, 1192.
102. Meyers, A.I.; Libano, W.Y., *J. Org. Chem.*, **1961**, 26, 4399.
103. See supporting information for full X-ray data sets.
104. Cunico, R.F.; Bedell, L., *J. Org. Chem.*, **1980**,45,4797.

CHAPTER 2

Introduction:

Recently in the Hegedus labs, a short, efficient, high-yielding synthesis of mono- and bis-dioxocyclams has been developed. The secondary amines of these tetraazamacrocycles are nucleophilic and readily alkylated with reactive carbon electrophiles. The appropriate bis-electrophiles can "cap" the cyclam, either blocking one face or providing a fifth coordination site or both. The first example of this was accomplished by Tom Wynn who "capped" the (methyl) (methoxy) cyclam **1** with 2,6-bis-bromomethyl pyridine **2** providing the "capped" (methyl) (methoxy) cyclam **3** in good yield (Scheme 1).[1]

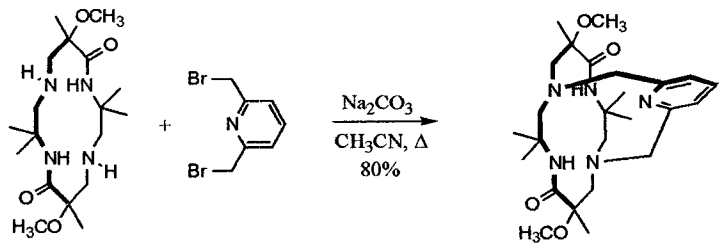

1 2 3

Scheme 1. Capping of the (methyl) (methoxy) cyclam with 2,6-bis-bromomethyl pyridine.

More recently, mono- and bis- dioxocyclams have been capped with 2,6-bis-bromomethyl pyrazine **5** (Scheme 2). Pyrazine is interesting because it provides the opportunity to coordinate to other metals through the donor site on its 4 position (see below). In the capping of bis-cyclams such as **4**, the first ring caps considerably faster than the second, perhaps because of unfavorable conformation changes in the second ring upon rigidification of the first. This phenomenon makes *unsymmetrical* capping of bis-cyclams possible.[2,3]

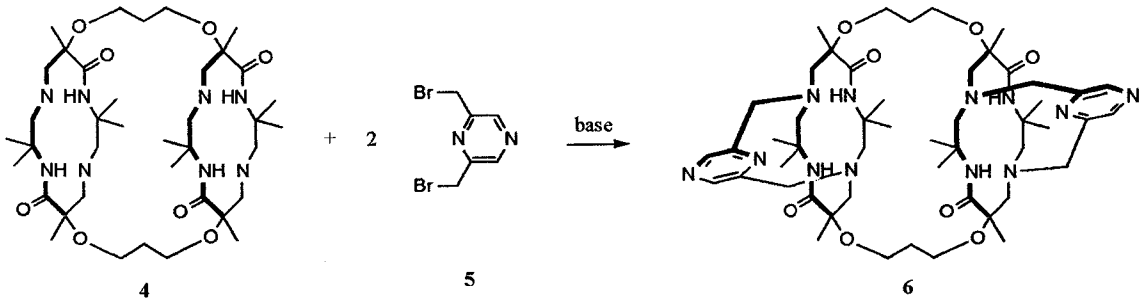

Scheme 2. Capping of bis-cyclam **4** with 2,6-bis-bromomethyl pyrazine **5**.

Since these examples, a range of mono- and bis- cyclam-metal complexes containing a variety of different "caps" have been made.[2,3] A significant development was the synthesis of the 4-bromopyridyl capping reagents (**2a, 2b,** Scheme 3). The capping reaction with these reagents goes in good yield (up to 85%), and provides the opportunity to further develop these systems with a variety of different functionalities. The 4-bromopyridyl tosylate capping reagent[2] **2b** has the advantage over the 4-bromopyridyl bisbromomethyl capping reagent **2a** because it does not require a benzylic bromination reaction in its synthesis. Benzylic brominations of these compounds tend to be low yielding due to over-bromination; in addition, separation of the desired di-bromo compound **2a** from the over-brominated products is extremely difficult.[4]

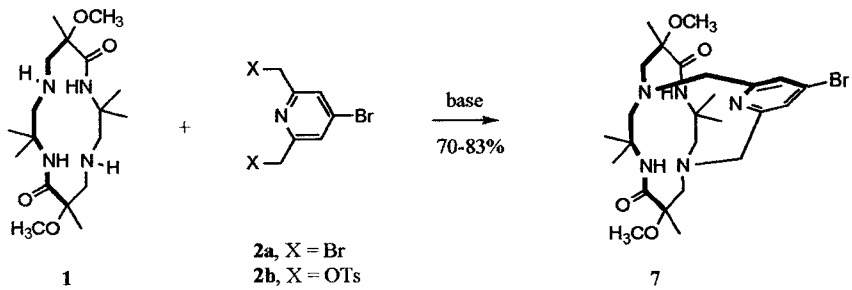

Scheme 3. Capping with the 4-bromopyridyl capping reagents.

A key feature of these systems is the ability of capped cyclam complexes such as **8** and its analogs (Scheme 4) to coordinate to other metals through the donor site on the 4-position of the capping agent, producing oligomeric, polymetallic complexes in which the metals are in electronic communication. In a recent example, Mike Sundermann showed that treatment of the pyrazine-capped dioxocyclam copper complex **8** with $Rh_2(OAc)_4$ produced tetrametallic complex **9** which was characterized by X-ray crystallography (Scheme 4).[5] Although copper is redox active in the uncapped dioxocyclams, it was found to be completely redox inactive in this "capped" system. Further characterization of complex **9** showed that these coppers are antiferromagnetically coupled, proving these pyrazine complexes can both coordinate additional metals and exhibit electronic coupling across extended metal-ligand arrays.

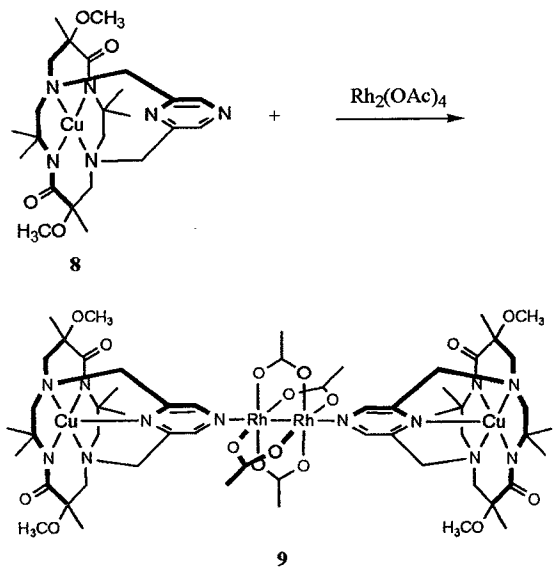

Scheme 4. Formation of tetrametallic complex **9** from pyrazine-capped copper complex **8**.

Rational:

Self-assembly of supramolecular constructs via transition metal coordination is has become the subject of much current study. Transition metal macrocyclic compounds with extended pi-chromophores are particularly interesting because of their ability to communicate electronically and magnetically across the ligand array. When the metals are in different oxidation states (mixed-valence complexes) the complexes may be conductive, exhibit nonlinear optical and magnetic properties, and have potential application in molecular electronics.[6-16]

The dioxocyclams made in the Hegedus labs are sufficiently unique that the effect of bridging ligands on electronic coupling of metals in these systems is unknown. The research presented below is based upon the idea that incorporation of a ruthenium (II) terpyridine (tpy) photosensitizer to the 4-bromo capped dioxocyclam 7 could give rise to novel complexes such as **10** and **11** (Scheme 5), and that eventual testing of these complexes for their electronic, magnetic, and photochemical properties, could help to determine this fundamental information. Although $Ru(tpy)^{2+}$ itself has limited luminescent and photosensitization properties at room temperature, these properties improve dramatically when incorporated into an extended delocalized system like the proposed examples in Scheme 5.[15,16] Hence, these complexes will eventually be studied extensively for their photochemical properties. For now however, the focus is on their synthesis and characterization.

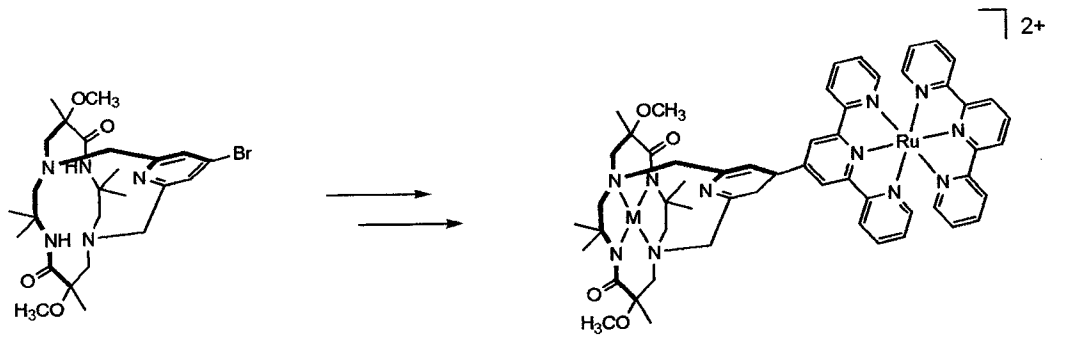

7

10

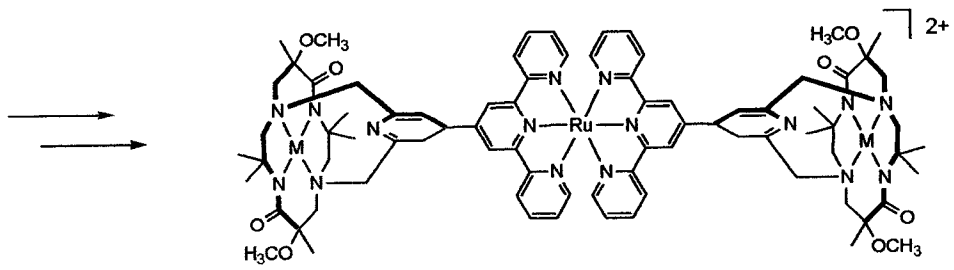

11

Scheme 5. Potential synthesis of terpy complexes **10** and **11**.

Results and Discussion:

Retrosynthetic analysis of compound **12** revealed several possible approaches (Scheme 6). The key terpyridine capped cyclam **12** could come from the 4-bromoterpyridine-capped dioxocyclam which, in turn, could come from either a Stille or Suzuki coupling reaction with the newly-developed 4-bromopyridine-capped cyclam (approach a). It was envisioned that incorporation of either the stannane or the borate to the terpyridine moiety (approach a) would be better than approach (b) since the synthesis of the 4-bromopyridine capped dioxocyclam is more demanding than the synthesis of 4-bromoterpyridine, and successful incorporation of a tin reagent was anticipated to take several attempts. Approach (c) was attractive because the Stille or Suzuki reaction could be developed before introduction of the dioxocyclam. Route (a) was chosen mainly because the chemistry to make the main cyclam building block was already in place. Additionally, synthesis of terpyradines functionalized with a halogen at the 4' position is known in the literature.[17]

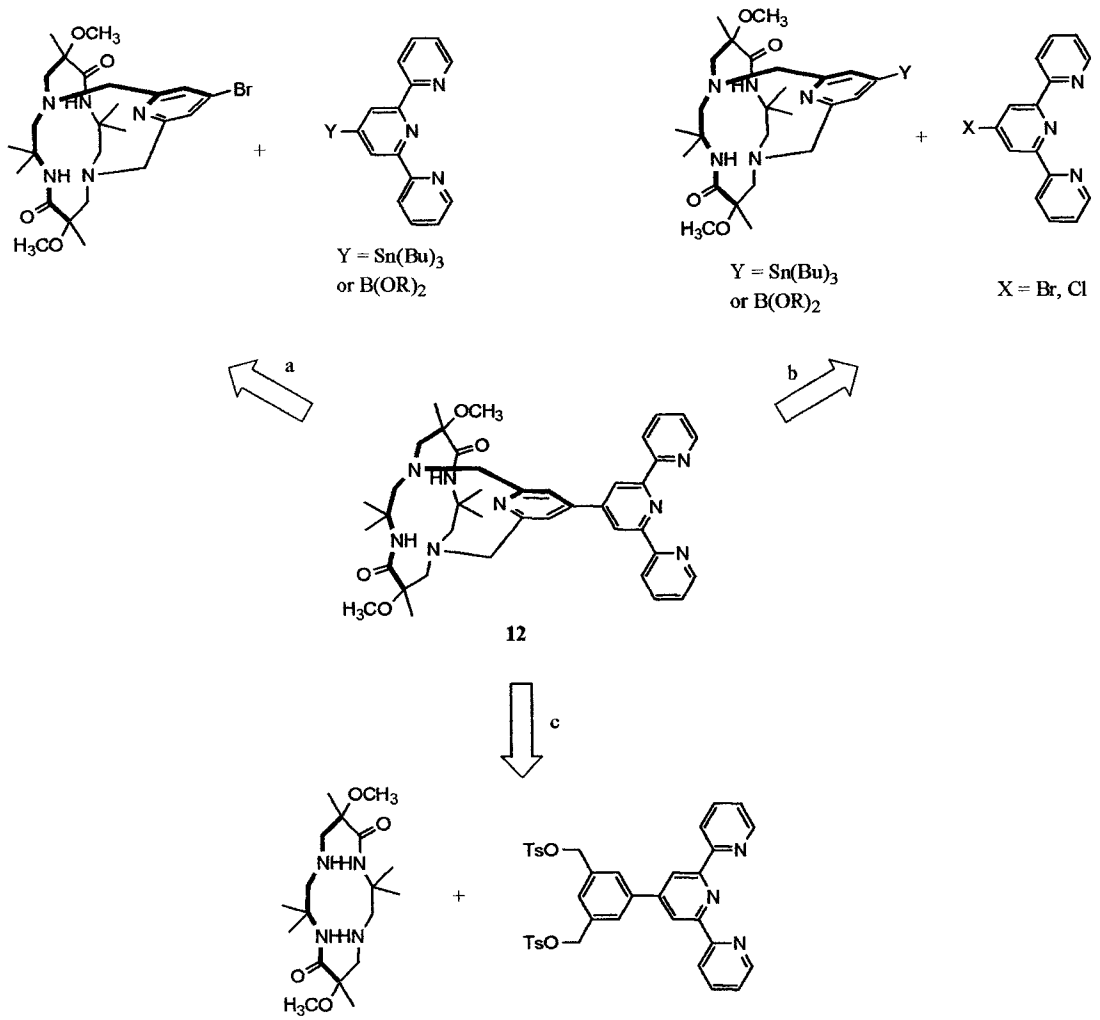

Scheme 6. Retrosynthesis of a terpyridine-capped cyclam **12**.

The requisite 4'halo-2,2':6',2"-terpyridines were synthesized by base-catalyzed condensation of acetone with ethylpicolinate **12** forming trione **13** in good yield (Scheme 7). Ring closure with ammonium acetate produced 2,6-bis(2'-pyridyl)-4-pyridone **14**. Since $POCl_3$ was already on-hand, and is significantly less-expensive than $POBr_3$, the 4'chloro-2,2':6',2"-terpyridine **15** was synthesized first.[17]

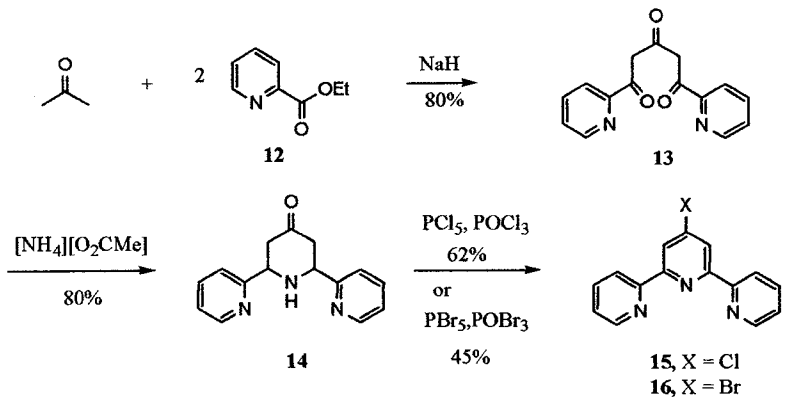

Scheme 7. Synthesis of 4'-halo-2,2':6',2"-terpyridine.

The typical method for making either alkyl-stannanes or alkyl borates is to generate the lithiate of **15** followed by a nucleophilic attack on a halo-stannane or a halo-borate. However, this is problematic in these types of poly-pyridyl systems probably because the nitrogens from the pyridines not bearing the halide can guide the lithiation to the positions alpha to the halide, creating multiple strong base sites. In the presence of an electrophile such as a tin- or a boron-halide, this leads to a complex mixture of products.[18] Therefore, other methods have been developed that don't involve a halogen-exchange reaction with lithium.[18,19] One of the methods is a palladium-mediated halogen-metal exchange reaction with hexamethyl- or hexabutylditin. Unfortunately, all attempts to stannylate **15** with either Me_6Sn_2 or Bu_6Sn_2 using $PdCl_2(PPh_3)_2$ either resulted in no reaction or only a trace of product (Scheme 8).

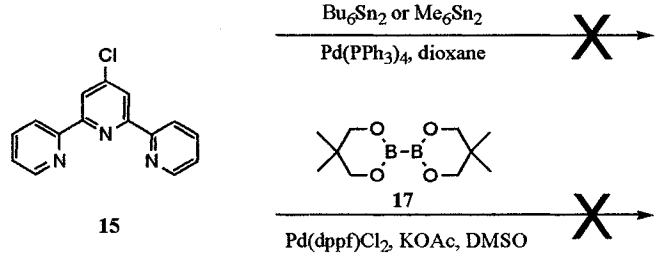

Scheme 8. Failed attempts to activate chloroterpyridine **15**.

An elegant method for making boron esters from a palladium-catalyzed coupling of aryl halides appeared in 1995 from Miyaura.[20] This method involves the use of bis(neopentylglycolato)diboron **17** with potassium acetate and $Pd(dppf)Cl_2$ (dppf = diphenylphosphinoferrocine). Unfortunately, this also resulted in no reaction even with scrupulously dried and degassed DMSO. Apparently, chloroterpyridine **15** is not reactive enough for these kinds of palladium-catalyzed coupling reactions.

At this point, attention was shifted to making the 4'bromo-2,2':6',2"-terpyridine **16**. Fortunately, bromoterpyridine **16** was much more reactive than chloroterpyridine **15**. With the high toxicity of tin reagents in mind, attention was focused on making the boron ester **18**. After conquering a few initial problems, namely that the bromoterpyridine **15** needed to be absolutely clean and the DMSO *completely* dried and *thoroughly* degassed, this reaction proved to be quite reliable, consistently producing yields around 80%.

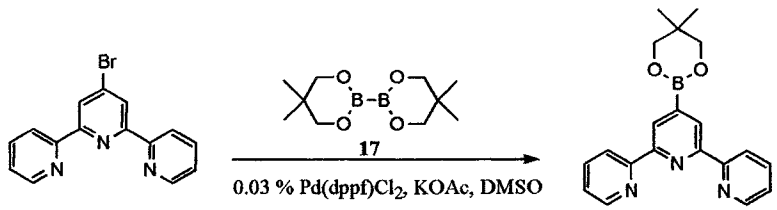

16 80% 18

Scheme 9. Synthesis of the terpyridine boron ester 9.

With the Suzuki precursor boron ester **18** in hand, synthesis of the 4-bromopyridine capped (methyl) (methoxy) cyclam commenced (Scheme 10). Nucleophilic attack on chromium hexacarbonyl by methyllithium followed by trapping with dimethyl sulfate produced the (methyl) (methoxy) carbene complex **19** in good yields. Photolysis of carbene complex **19** in the presence of dimethyl imidazoline resulted in an excellent yield of protected azapenam **20** which was deprotected via

hydrogenation to produce the deprotected azapenam **21**. Dimerization was accomplished by allowing **21** to react with a catalytic amount of camphor sulphonic acid (CSA) for several days. Because the cis and trans imine cyclams are in equilibrium with each other and the trans is much more crystalline, layering hexane on to the reaction mixture resulted in the slow (1-2 days) formation of trans (methyl) (methoxy) crystals. After collecting two crops of crystals in this manner, then reducing the cyclam's ring imines, the trans (methyl) (methoxy) cyclam **1** was obtained in reasonable yield. Capping with the previously mentioned ditosylate provided the 4-bromopyridine capped trans (methyl) (methoxy) cyclam **7** in very good yield.

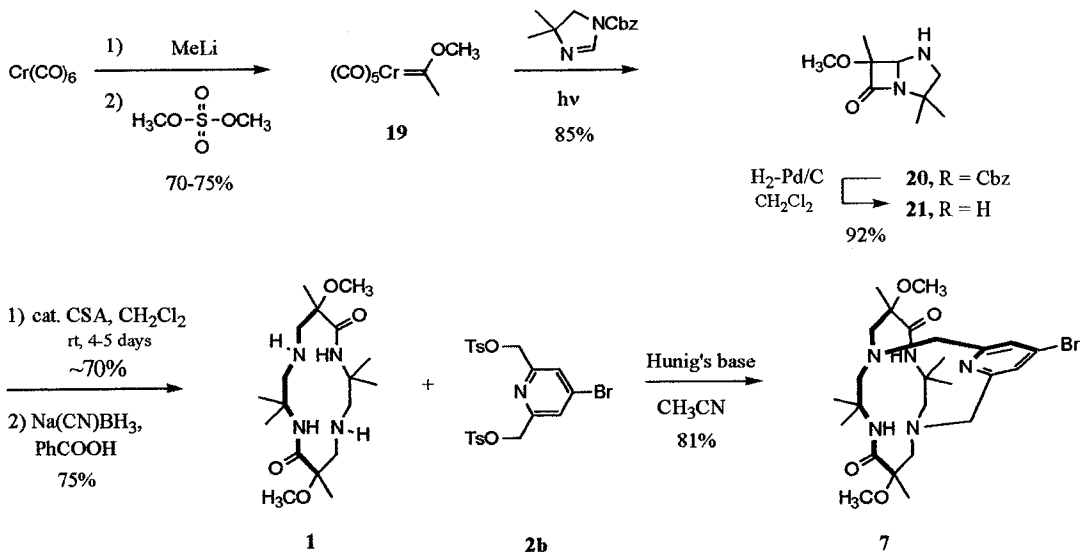

Scheme 10. Synthesis of 4-bromopyridine capped dioxocyclam 7.

The Suzuki coupling reaction of the 4-bromocapped cyclam **7** and the terpyridine boron ester **18**[19] proceeded smoothly, provided that the solvent was completely dried and thoroughly degassed, to produce the key terpyridine-capped dioxocyclam **22** in ~65% yield. The reaction is believed to go in significantly higher yield than 65%; however, separation of **22** from the triphenylphosphine (PPh_3) that is generated in this reaction was extremely difficult, requiring multiple flash columns. Recrystallization was also only marginally successful.

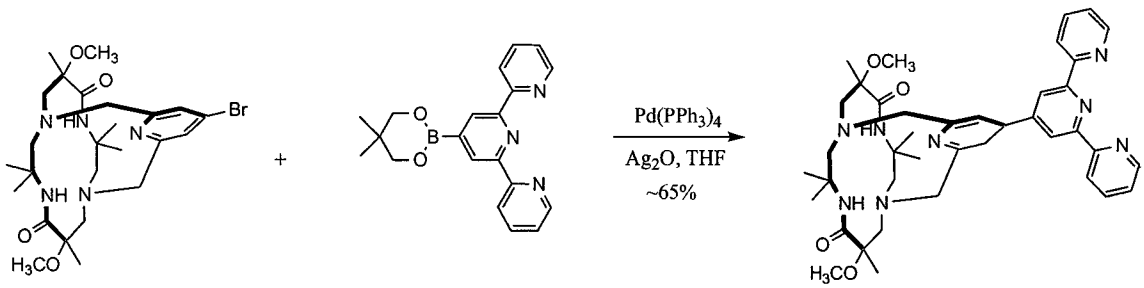

7 **18** **22**

Scheme 11. Suzuki coupling reaction to form terpyridine cyclam **22**.

Future Plans:

With the synthesis of the key terpyridine capped dioxocyclam **22** accomplished, ruthenium complexation might give rise to structures such as **10** (Scheme 11). Ruthenium should complex to the terpyridines first since complexation of metals into the pyridine capped cyclams requires somewhat forcing conditions. This would allow the possibility of incorporating a different metal into the cyclam. Osmium will probably be tried first since Ru / Os are the classic acceptor / donor groups for photoinduced intervalence electron transfer.[16,21]

Metal pthalocyanines have long been studied for their physical properties.[22,23] They form bridged oligomers with bis-donors, including pyrazine, bipyridine, and cyanide ion (and many others) that have useful electrical conductivity properties. Pyrazine / metal octaethylporphyrin oligomers also show interesting electrical conductivity properties.[22-24] Incorporation of either a pthalocyanine or porphyrin to the terpyridine capped cyclam **22** could lead to novel structures such as **23**. Many other new and interesting dioxocyclam complexes featuring multiple metals connected through a pi-ligand array are possible. Once synthesized, these novel compounds will be tested for their electronic, magnetic, and photochemical properties in order to determine fundamental information on the effect of the nature of the substitution on the cyclam's cap on the physical properties of these various complexes.

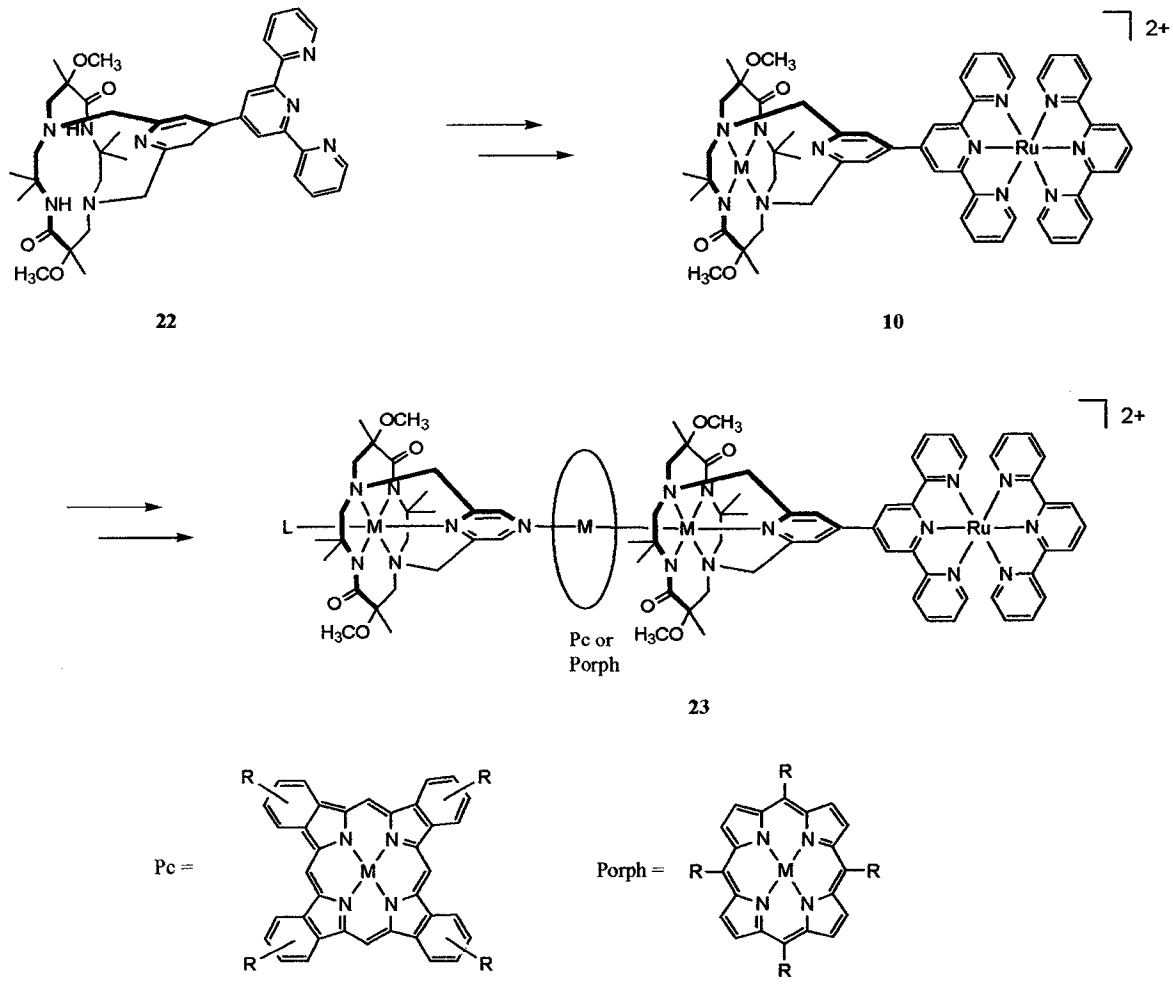

Scheme 12. Possible future plans for terpyridine capped cyclam **22**.

Conclusions:

By taking advantage of the recent development of the 4-bromopyridine capping reagent **2b**, a capped cyclam was functionalized with a terpyridine moiety. It is hoped that complexation of metals, in particular Ru(II) and Os(II), to the terpyridine moiety as well as the dioxocyclam will give rise to new structures with interesting electronic, magnetic, and photochemical properties from potential building blocks such as **22**.

Experimental Section:

General Procedures. The general methods described for chapter 1 were followed exactly. The following compounds were compared according to literature procedure, *p*-bromocapped dioxocyclam **7**,[2] chloroterpyridine **15**,[17] bromoterpyridine **16**,[19] and terpyridine boron ester **18**.[19]

Terpyridine Capped Dioxocyclam (22). Under a steady stream of argon, the terpyridine boron ester **18** (45 mg, 0.13 mmol), 4 –bromocapped dioxocyclam **7** (58 mg, 0.10 mmol), palladium tetrakistriphenyphosphine (30 mg, 0.026 mmol), and silver oxide (Ag_2O) (67 mg, 0.29 mmol) were combined into a flame-dried pressure tube. Tetrahydrofuran (8 mL) that had been freshly distilled from sodium benzophenone ketyl and freeze-pump-thaw degassed three times was then added via syringe. After heating the reaction mixture for 15 hours, it was cooled then filtered. The solvent was removed *in vacuo* before the crude reaction material was loaded on to a 1 X 12 cm silica gel column and eluted with 80% of ethyl acetate:20% hexane. This resulted in partial removal of the residual triphenylphosphine. A second column (same size) was run using a gradient elution of 100 mL of 60% ethyl acetate: 40% hexane followed by 100 mL of 80% ethyl acetate: 20% hexane. This resulted in removal of all but a trace of the PPh_3, producing **22** (55 mg, 74%) as a white solid. ^{1}H NMR δ 9.11 (s, 1H), 8.75 (s, 2H), 8.24 (m, 4H), 8.09 (s, 1H), 7.92 (m, 2H), 7.43 (m, 4H), 4.14 (m, 5H), 3.44 (s, 3H), 3.25 (d, J = 13.8 Hz, 1H), 2.91 (m, 3H), 2.63 (d, J = 14.4 Hz, 1H), 2.54 (s, 3H), 2.38 (m, 2H), 1.31 (m, 18H); ^{13}C NMR δ 173.3, 172.7, 163.9, 159.4, 156.4, 155.7, 149.3, 147.7, 147.3, 137.2, 124.4, 121.6, 118.6, 117.2, 117.0, 82.6, 79.7, 76.8, 74.6, 72.8, 69.4, 67.4, 65.8, 64.8, 56.0, 54.9, 51.9, 50.5, 26.4, 25.7, 23.7, 23.6, 19.4.; MS *m/z* 709.9 (MH^+).

References:

1. Wynn, T.; Hegedus, L.S., *J. Am. Chem. Soc.,* 122, 5034, **2000**.
2. Achmatowicz, M.; Hegedus, L.S. *J. Org. Chem.*, **2003**, 68, submitted.
3. Brugel, T.A.; Hegedus, L.S. *J. Org. Chem.*, **2003**, 68, submitted.
4. Bullert, A.L.; Hegedus, L.S. unpublished results.
5. Hegedus, L.S.; Sundermann, M.J.; Dorhout, P.K. *Inorg. Chem.*, **2003**, submitted.
6. Lehn, J. M. Angew. *Chem. Int. Ed. Engl.* **1988**, 27, 89
7. Ringsdorf, H.; Schlarb, B.; Venzmer, J. *Angew. Chem. Int. Ed. Engl.* **1990**, 29, 1304.
8. Vogtle, F. *Supramolecular Chemitry*; Wiley: Chichester, U.K., **1991**.
9. Balzani, V., De Cola, L., Eds *Supramolecular Chemistry*; Kluwer: Dordrecht, Holland, **1992**.
10. Balzini, V. *Tetrahedron*, **1992**, 48, 10443.
11. Balzini, V.; Moggi, L.; Scandola, F. In *Supramolecular Photochemistry*; Balzani, V., The Netherlands, **1987**; p1.
12. Fox, M.A.; Jones, W.E., Watkins, S.M. *Chem Eng News* **1993**, 71 (March 15), 38.
13. Nowakowska, M.; Foyle, V.P.; Guillet, J.E. *J. Am. Chem. Soc.*, **1993,** 115, 5975.
14. Gust, D.; Moore, T.A.; Moore, A.L. *Acc. Chem. Res.* **1993**, 26, 198.
15. Walielewski, M.R. *Chem Rev.* **1992**, 92, 435.
16. Sauvage, J.P.; Collin, J.P.; Chambron, J.C.; Guillerez, S.G.; Coudret, C. *Chem. Rev.* **1994**, 94, 993-1019.
17. Constable, E.C.; Ward, M.D. *J. Chem. Soc. Dalton Trans.* **1990**, 1405.
18. Grosshenny, V.; Romero, F.M.; Ziessel, R. *J. Org. Chem.*, **1997**, 1491-1500.
19. Aspley, C.J.; Williams, J.A. *New J. Chem.* **2001**, 25, 1136-1147.
20. Ishiyama, T.; Murata, M.; Miyaura, N. *J. Org. Chem.*, **1995**, 60, 7508.
21. Baragelletti, F.; Flamingni, L., *Chem. Soc. Rev.* **2000**, 29, 1-12.

Appendix: Tables of X-Ray Structure Data

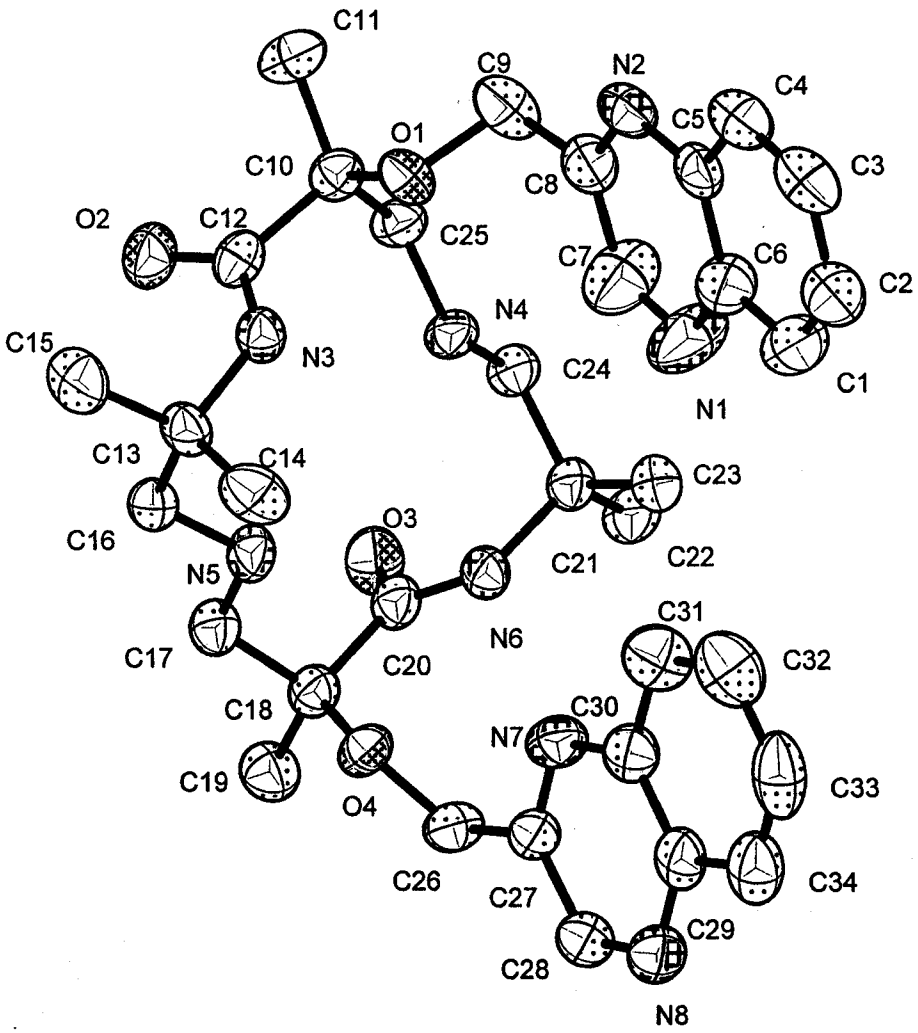

Table 1. Crystal data and structure refinement for lsh39z.

Identification code	lsh39z
Empirical formula	$C_{34}H_{44}N_8O_4$
Formula weight	628.77
Temperature	173(2) K
Wavelength	0.71073 Å
Crystal system	Monoclinic
Space group	$P2_1/c$
Unit cell dimensions	a = 10.542(7) Å alpha = 90° b = 13.601(9) Å beta = 90.000(15)° c = 23.271(16) Å gamma = 90°
Volume, Z	3337(4) $Å^3$, 4
Density (calculated)	1.252 Mg/m^3
Absorption coefficient	0.085 mm^{-1}
F(000)	1344
Crystal size	0.40 x 0.40 x 0.80 mm
θ range for data collection	1.73 to 23.48°
Limiting indices	$-11 \le h \le 11$, $-15 \le k \le 15$, $-17 \le l \le 25$
Reflections collected	15354
Independent reflections	4823 (R_{int} = 0.0723)
Completeness to θ = 23.48°	97.9 %
Absorption correction	None
Refinement method	Full-matrix least-squares on F^2
Data / restraints / parameters	4823 / 0 / 433
Goodness-of-fit on F^2	0.829
Final R indices [$I>2\sigma(I)$]	R1 = 0.0401, wR2 = 0.0719
R indices (all data)	R1 = 0.0893, wR2 = 0.0801
Largest diff. peak and hole	0.160 and -0.150 $eÅ^{-3}$

Table 2. Atomic coordinates [x 10^4] and equivalent isotropic displacement parameters [$Å^2$ x 10^3] for lsh39z. U(eq) is defined as one third of the trace of the orthogonalized U_{ij} tensor.

	x	y	z	U(eq)
C(1)	12799(3)	3717(2)	1240(1)	66(1)
C(2)	13839(3)	3716(2)	899(1)	56(1)
C(3)	15019(3)	3924(2)	1125(1)	52(1)
C(4)	15140(2)	4124(2)	1701(1)	46(1)
C(5)	14079(2)	4107(2)	2063(1)	37(1)
C(6)	12894(2)	3911(2)	1829(1)	50(1)
C(7)	12004(3)	4046(2)	2718(1)	73(1)
C(8)	13197(2)	4215(2)	2960(1)	43(1)
C(9)	13267(2)	4318(2)	3602(1)	52(1)
C(10)	12186(2)	3481(2)	4398(1)	33(1)
C(11)	13112(2)	3819(2)	4849(1)	46(1)
C(12)	11725(2)	2424(2)	4520(1)	34(1)
C(13)	11068(2)	863(2)	4033(1)	34(1)
C(14)	11003(2)	594(2)	3398(1)	51(1)
C(15)	11977(2)	176(2)	4342(1)	52(1)
C(16)	9770(2)	806(2)	4321(1)	36(1)
C(17)	7613(2)	1355(2)	4343(1)	36(1)
C(18)	6577(2)	1932(2)	4041(1)	33(1)
C(19)	5318(2)	1749(2)	4335(1)	45(1)
C(20)	6932(2)	3028(2)	4063(1)	34(1)
C(21)	8025(2)	4395(2)	3540(1)	34(1)
C(22)	6941(2)	5138(2)	3609(1)	48(1)
C(23)	8582(2)	4465(2)	2936(1)	49(1)
C(24)	9017(2)	4591(2)	3995(1)	36(1)
C(25)	11000(2)	4133(2)	4411(1)	34(1)
C(26)	5646(2)	1910(2)	3097(1)	42(1)
C(27)	6147(2)	1912(2)	2492(1)	36(1)
C(28)	5340(2)	1656(2)	2036(1)	44(1)
C(29)	6923(3)	1894(2)	1387(1)	43(1)
C(30)	7740(2)	2154(2)	1837(1)	40(1)
C(31)	9005(2)	2394(2)	1704(1)	55(1)
C(32)	9421(3)	2368(2)	1145(1)	62(1)
C(33)	8595(3)	2110(2)	701(1)	61(1)
C(34)	7371(3)	1878(2)	816(1)	54(1)
N(1)	11826(2)	3897(2)	2168(1)	82(1)
N(2)	14223(2)	4256(1)	2645(1)	42(1)
N(3)	11573(2)	1872(1)	4053(1)	33(1)
N(4)	10081(2)	3905(1)	3967(1)	35(1)
N(5)	8840(2)	1453(1)	4062(1)	37(1)
N(6)	7523(2)	3387(1)	3598(1)	32(1)
N(7)	7330(2)	2165(1)	2398(1)	41(1)
N(8)	5683(2)	1642(1)	1496(1)	49(1)
O(1)	12753(1)	3434(1)	3835(1)	38(1)
O(2)	11486(2)	2160(1)	5013(1)	47(1)
O(3)	6699(2)	3500(1)	4503(1)	46(1)
O(4)	6615(1)	1572(1)	3463(1)	36(1)

Table 3. Bond lengths [Å] and angles [°] for lsh39z.

C(1)-C(2)	1.354(3)	C(1)-C(6)	1.400(3)
C(2)-C(3)	1.381(3)	C(3)-C(4)	1.374(3)
C(4)-C(5)	1.400(3)	C(5)-N(2)	1.380(3)
C(5)-C(6)	1.388(3)	C(6)-N(1)	1.373(3)
C(7)-N(1)	1.310(3)	C(7)-C(8)	1.398(3)
C(8)-N(2)	1.308(3)	C(8)-C(9)	1.501(3)
C(9)-O(1)	1.426(3)	C(10)-O(1)	1.442(2)
C(10)-C(11)	1.505(3)	C(10)-C(25)	1.533(3)
C(10)-C(12)	1.543(3)	C(12)-O(2)	1.230(3)
C(12)-N(3)	1.330(3)	C(13)-N(3)	1.472(3)
C(13)-C(15)	1.520(3)	C(13)-C(14)	1.523(3)
C(13)-C(16)	1.526(3)	C(16)-N(5)	1.449(3)
C(17)-N(5)	1.455(3)	C(17)-C(18)	1.517(3)
C(18)-O(4)	1.431(3)	C(18)-C(19)	1.514(3)
C(18)-C(20)	1.539(3)	C(20)-O(3)	1.233(2)
C(20)-N(6)	1.340(3)	C(21)-N(6)	1.476(3)
C(21)-C(24)	1.513(3)	C(21)-C(23)	1.526(3)
C(21)-C(22)	1.535(3)	C(24)-N(4)	1.460(3)
C(25)-N(4)	1.449(3)	C(26)-O(4)	1.407(2)
C(26)-C(27)	1.505(3)	C(27)-N(7)	1.312(3)
C(27)-C(28)	1.403(3)	C(28)-N(8)	1.307(3)
C(29)-N(8)	1.374(3)	C(29)-C(30)	1.401(3)
C(29)-C(34)	1.412(3)	C(30)-N(7)	1.376(3)
C(30)-C(31)	1.407(3)	C(31)-C(32)	1.374(3)
C(32)-C(33)	1.396(4)	C(33)-C(34)	1.355(3)

C(2)-C(1)-C(6)	121.2(3)	C(1)-C(2)-C(3)	120.3(3)
C(4)-C(3)-C(2)	119.8(2)	C(3)-C(4)-C(5)	120.5(3)
N(2)-C(5)-C(6)	120.8(2)	N(2)-C(5)-C(4)	120.0(2)
C(6)-C(5)-C(4)	119.2(3)	N(1)-C(6)-C(5)	121.1(3)
N(1)-C(6)-C(1)	120.0(3)	C(5)-C(6)-C(1)	118.9(3)
N(1)-C(7)-C(8)	123.3(3)	N(2)-C(8)-C(7)	121.6(3)
N(2)-C(8)-C(9)	120.9(2)	C(7)-C(8)-C(9)	117.5(2)
O(1)-C(9)-C(8)	106.31(19)	O(1)-C(10)-C(11)	112.20(18)
O(1)-C(10)-C(25)	112.40(18)	C(11)-C(10)-C(25)	109.80(18)
O(1)-C(10)-C(12)	104.82(18)	C(11)-C(10)-C(12)	111.18(19)
C(25)-C(10)-C(12)	106.18(18)	O(2)-C(12)-N(3)	125.0(2)
O(2)-C(12)-C(10)	120.5(2)	N(3)-C(12)-C(10)	114.5(2)
N(3)-C(13)-C(15)	109.25(19)	N(3)-C(13)-C(14)	105.77(18)
C(15)-C(13)-C(14)	109.9(2)	N(3)-C(13)-C(16)	110.97(18)
C(15)-C(13)-C(16)	109.05(19)	C(14)-C(13)-C(16)	111.9(2)
N(5)-C(16)-C(13)	113.23(18)	N(5)-C(17)-C(18)	112.60(18)
O(4)-C(18)-C(19)	113.09(19)	O(4)-C(18)-C(17)	103.76(18)
C(19)-C(18)-C(17)	109.68(18)	O(4)-C(18)-C(20)	110.89(18)
C(19)-C(18)-C(20)	110.96(18)	C(17)-C(18)-C(20)	108.10(19)
O(3)-C(20)-N(6)	125.0(2)	O(3)-C(20)-C(18)	118.9(2)
N(6)-C(20)-C(18)	116.0(2)	N(6)-C(21)-C(24)	110.33(18)
N(6)-C(21)-C(23)	106.29(18)	C(24)-C(21)-C(23)	111.64(19)
N(6)-C(21)-C(22)	109.56(18)	C(24)-C(21)-C(22)	108.97(18)
C(23)-C(21)-C(22)	110.02(19)	N(4)-C(24)-C(21)	112.76(18)
N(4)-C(25)-C(10)	114.07(18)	O(4)-C(26)-C(27)	108.22(19)
N(7)-C(27)-C(28)	121.0(2)	N(7)-C(27)-C(26)	119.3(2)
C(28)-C(27)-C(26)	119.7(2)	N(8)-C(28)-C(27)	124.2(2)
N(8)-C(29)-C(30)	120.6(2)	N(8)-C(29)-C(34)	119.3(3)

C(30)-C(29)-C(34)	120.1(3)	N(7)-C(30)-C(29)	121.3(2)
N(7)-C(30)-C(31)	120.2(3)	C(29)-C(30)-C(31)	118.5(3)
C(32)-C(31)-C(30)	120.3(3)	C(31)-C(32)-C(33)	120.6(3)
C(34)-C(33)-C(32)	120.4(3)	C(33)-C(34)-C(29)	120.1(3)
C(7)-N(1)-C(6)	116.1(3)	C(8)-N(2)-C(5)	117.0(2)
C(12)-N(3)-C(13)	126.6(2)	C(25)-N(4)-C(24)	110.19(17)
C(16)-N(5)-C(17)	111.10(17)	C(20)-N(6)-C(21)	125.41(19)
C(27)-N(7)-C(30)	116.9(2)	C(28)-N(8)-C(29)	115.9(2)
C(9)-O(1)-C(10)	117.78(17)	C(26)-O(4)-C(18)	115.86(17)

Symmetry transformations used to generate equivalent atoms:

Table 4. Anisotropic displacement parameters [$Å^2$ x 10^3] for lsh39z.

The anisotropic displacement factor exponent takes the form:

$-2\pi^2 [(ha^*)^2 U_{11} + ... + 2hka^* b^* U_{12}]$

	U11	U22	U33	U23	U13	U12
C(1)	53(2)	93(3)	51(2)	15(2)	-11(2)	-19(2)
C(2)	64(2)	52(2)	51(2)	3(2)	-3(2)	-11(2)
C(3)	51(2)	40(2)	63(2)	1(2)	16(2)	-5(1)
C(4)	41(2)	37(2)	61(2)	1(2)	7(2)	-4(1)
C(5)	36(2)	26(2)	50(2)	8(1)	0(2)	0(1)
C(6)	35(2)	66(2)	50(2)	12(2)	1(2)	-5(1)
C(7)	38(2)	123(3)	58(2)	14(2)	6(2)	3(2)
C(8)	40(2)	39(2)	49(2)	6(1)	2(2)	-1(1)
C(9)	60(2)	40(2)	56(2)	-3(2)	11(2)	-12(1)
C(10)	35(1)	32(2)	32(2)	-5(1)	-3(1)	3(1)
C(11)	40(2)	45(2)	52(2)	-14(1)	-16(1)	8(1)
C(12)	31(2)	37(2)	33(2)	2(2)	-3(1)	8(1)
C(13)	38(2)	22(2)	43(2)	2(1)	-1(1)	0(1)
C(14)	62(2)	38(2)	53(2)	-14(1)	6(2)	-7(1)
C(15)	40(2)	34(2)	82(2)	9(2)	1(2)	10(1)
C(16)	36(2)	30(2)	42(2)	6(1)	-5(1)	0(1)
C(17)	39(2)	31(2)	38(2)	3(1)	-3(1)	2(1)
C(18)	36(2)	31(2)	31(2)	-1(1)	-3(1)	1(1)
C(19)	36(2)	44(2)	54(2)	5(1)	3(1)	1(1)
C(20)	36(2)	29(2)	36(2)	2(1)	-5(1)	5(1)
C(21)	38(2)	28(2)	36(2)	3(1)	-7(1)	2(1)
C(22)	50(2)	31(2)	63(2)	3(1)	-20(2)	6(1)
C(23)	57(2)	46(2)	44(2)	14(1)	-10(2)	-13(1)
C(24)	40(2)	25(2)	44(2)	-1(1)	-11(1)	4(1)
C(25)	32(1)	31(2)	41(2)	-3(1)	-7(1)	2(1)
C(26)	39(2)	42(2)	43(2)	-2(1)	-10(2)	-4(1)
C(27)	48(2)	23(2)	38(2)	-4(1)	-12(2)	-2(1)
C(28)	51(2)	33(2)	47(2)	-2(2)	-9(2)	-5(1)
C(29)	63(2)	25(2)	39(2)	-2(1)	-6(2)	2(1)
C(30)	51(2)	31(2)	37(2)	-4(1)	-3(2)	0(1)
C(31)	57(2)	55(2)	53(2)	-6(2)	5(2)	-4(2)
C(32)	70(2)	48(2)	67(2)	-3(2)	15(2)	1(2)
C(33)	102(3)	37(2)	44(2)	4(2)	9(2)	16(2)
C(34)	83(2)	37(2)	41(2)	-1(1)	-4(2)	5(2)
N(1)	41(2)	150(3)	55(2)	16(2)	-4(2)	-10(2)
N(2)	43(1)	31(1)	52(2)	1(1)	1(1)	-7(1)
N(3)	41(1)	27(1)	29(1)	0(1)	0(1)	1(1)
N(4)	36(1)	27(1)	42(1)	-3(1)	-12(1)	3(1)
N(5)	31(1)	38(1)	42(1)	11(1)	-1(1)	5(1)
N(6)	39(1)	25(1)	31(1)	-1(1)	-3(1)	1(1)
N(7)	41(1)	41(1)	41(2)	-6(1)	-7(1)	-3(1)
N(8)	64(2)	38(1)	44(2)	-3(1)	-15(1)	-4(1)
O(1)	42(1)	29(1)	43(1)	-1(1)	4(1)	-5(1)
O(2)	61(1)	48(1)	33(1)	4(1)	-5(1)	0(1)
O(3)	66(1)	38(1)	35(1)	-6(1)	2(1)	3(1)
O(4)	38(1)	34(1)	37(1)	-3(1)	-11(1)	5(1)

Table 5. Hydrogen coordinates (x 10^4) and isotropic displacement parameters ($Å^2$ x 10^3) for 1sh39z.

	x	y	z	U(eq)
H(1)	11991	3585	1077	79
H(2)	13757	3570	501	67
H(3)	15745	3929	884	62
H(4)	15952	4274	1856	56
H(7)	11286	4039	2964	88
H(9A)	14157	4406	3727	63
H(9B)	12767	4894	3731	63
H(11A)	13922	3477	4796	68
H(11B)	12773	3671	5231	68
H(11C)	13244	4530	4812	68
H(14A)	10483	1078	3194	76
H(14B)	10623	-60	3356	76
H(14C)	11861	590	3236	76
H(15A)	12817	218	4163	78
H(15B)	11662	-500	4315	78
H(15C)	12038	368	4747	78
H(16A)	9457	121	4298	43
H(16B)	9863	978	4732	43
H(17A)	7684	1587	4744	43
H(17B)	7373	651	4352	43
H(19A)	4652	2127	4141	67
H(19B)	5373	1954	4737	67
H(19C)	5113	1046	4316	67
H(22A)	6296	5018	3314	72
H(22B)	7275	5807	3567	72
H(22C)	6560	5065	3991	72
H(23A)	9230	3956	2886	73
H(23B)	8966	5114	2882	73
H(23C)	7906	4369	2652	73
H(24A)	9340	5270	3949	43
H(24B)	8617	4543	4379	43
H(25A)	10586	4063	4790	41
H(25B)	11264	4828	4369	41
H(26A)	5387	2583	3210	50
H(26B)	4897	1474	3125	50
H(28)	4490	1482	2125	52
H(31)	9573	2575	2002	66
H(32)	10278	2526	1060	74
H(33)	8893	2098	316	73
H(34)	6815	1704	511	65
H(1A)	8770(30)	1280(20)	3678(11)	98
H(2A)	7669(19)	2956(15)	3295(9)	50
H(3A)	11764(19)	2144(15)	3709(9)	39
H(4A)	9796(19)	3298(15)	4032(9)	42

Table 6. Hydrogen bonds for lsh39z [Å and °].

D-H...A	d(D-H)	d(H...A)	d(D...A)	<(DHA)

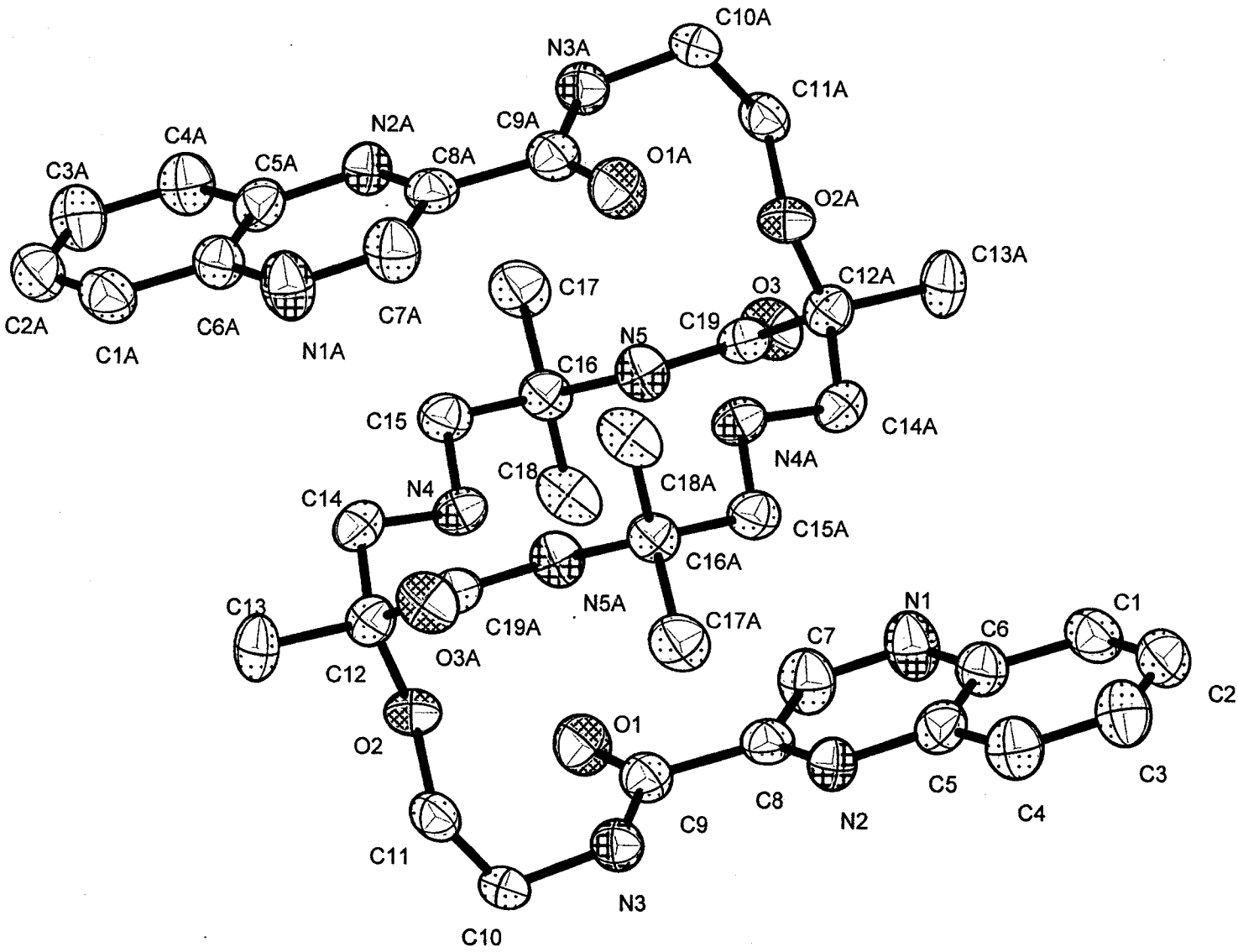

Table 1. Crystal data and structure refinement for lsh501m.

Identification code	lsh501m JL/321 f-1
Empirical formula	$C_{38}H_{50}N_{10}O_6$
Formula weight	742.88
Temperature	168(2) K
Wavelength	0.71073 Å
Crystal system	Triclinic
Space group	P-1
Unit cell dimensions	a = 10.6454(16) Å alpha = 99.598(3)° b = 12.2561(18) Å beta = 99.330(3)° c = 16.539(3) Å gamma = 112.471(3)°
Volume, Z	1904.7(5) Å^3, 2
Density (calculated)	1.295 Mg/m^3
Absorption coefficient	0.090 mm^{-1}
Absorption correction	None
F(000)	792
Crystal size	0.55 x 0.22 x 0.15 mm
θ range for data collection	1.86 to 26.40°
Limiting indices	$-13 \le h \le 11$, $-15 \le k \le 15$, $-14 \le l \le 20$
Reflections collected	11685
Independent reflections	7717 (R_{int} = 0.0610)
Completeness to θ = 26.40°	98.7 %
Refinement method	Full-matrix least-squares on F^2
Data / restraints / parameters	7717 / 0 / 517
Goodness-of-fit on F^2	0.710
Final R indices [I>2σ(I)]	R1 = 0.0481, wR2 = 0.0621
R indices (all data)	R1 = 0.1974, wR2 = 0.0836
Largest diff. peak and hole	0.188 and -0.161 eÅ^{-3}

Table 2. Atomic coordinates [x 10^4] and equivalent isotropic displacement parameters [$Å^2$ x 10^3] for lsh501m. U(eq) is defined as one third of the trace of the orthogonalized U_{ij} tensor.

	x	y	z	U(eq)
C(1)	1058(4)	1218(3)	6745(2)	43(1)
C(2)	-120(4)	1348(3)	6859(2)	49(1)
C(3)	-927(4)	1612(3)	6235(2)	50(1)
C(4)	-573(3)	1726(3)	5487(2)	46(1)
C(5)	625(3)	1584(3)	5343(2)	36(1)
C(6)	1444(3)	1346(3)	5986(2)	37(1)
C(7)	2939(3)	1314(3)	5142(2)	45(1)
C(8)	2084(3)	1541(3)	4492(2)	34(1)
C(9)	2550(4)	1651(3)	3681(2)	36(1)
C(10)	1887(3)	1817(3)	2230(2)	36(1)
C(11)	2497(3)	3117(2)	2165(2)	34(1)
C(12)	4583(3)	4992(3)	2881(2)	31(1)
C(13)	4772(3)	5456(3)	2091(2)	43(1)
C(14)	6013(3)	5295(2)	3448(2)	34(1)
C(15)	7319(3)	4997(3)	4671(2)	34(1)
C(16)	7329(3)	4390(3)	5405(2)	32(1)
C(17)	8840(3)	4929(3)	5933(2)	48(1)
C(18)	6747(3)	3005(2)	5080(2)	45(1)
C(19)	6273(3)	4447(3)	6658(2)	31(1)
C(20)	1810(3)	4355(3)	-1394(2)	48(1)
C(21)	607(4)	4327(3)	-1895(2)	51(1)
C(22)	-21(3)	5031(3)	-1612(2)	47(1)
C(23)	2392(3)	5100(3)	-598(2)	40(1)
C(24)	1770(3)	5851(3)	-298(2)	36(1)
C(25)	555(3)	5833(3)	-803(2)	38(1)
C(26)	1787(3)	7367(3)	735(2)	36(1)
C(27)	2456(3)	8324(3)	1571(2)	36(1)
C(28)	4228(3)	9072(3)	2920(2)	39(1)
C(29)	5658(3)	9896(3)	2872(2)	39(1)
C(30)	6736(3)	11373(3)	2092(2)	32(1)
C(31)	7828(3)	12311(2)	2859(2)	47(1)
C(32)	6206(3)	12028(2)	1511(2)	38(1)
C(33)	4441(3)	11904(2)	337(2)	34(1)
C(34)	7369(3)	10549(3)	1646(2)	32(1)
C(35)	6872(3)	8870(3)	374(2)	32(1)
C(36)	8138(3)	9515(3)	47(2)	46(1)
C(37)	7154(3)	8017(3)	880(2)	53(1)
C(38)	542(3)	7305(3)	217(2)	45(1)
N(1)	2636(3)	1212(2)	5878(2)	49(1)
N(2)	947(3)	1683(2)	4587(2)	35(1)
N(3)	1623(3)	1713(2)	3054(2)	36(1)
N(4)	5911(3)	4659(2)	4133(2)	32(1)
N(5)	6447(3)	4723(2)	5918(2)	34(1)
N(6)	2390(2)	6648(2)	496(2)	37(1)
N(7)	-78(3)	6557(2)	-533(2)	47(1)
N(8)	3404(3)	8182(2)	2121(2)	39(1)
N(9)	6542(3)	9771(2)	908(2)	34(1)

N(10)	4917(3)	11207(3)	853(2)	32(1)
O(1)	3699(2)	1667(2)	3630(1)	45(1)
O(2)	3902(2)	3690(2)	2688(1)	33(1)
O(3)	6801(2)	3836(2)	6984(1)	43(1)
O(4)	2086(2)	9160(2)	1691(2)	53(1)
O(5)	5498(2)	10620(2)	2310(1)	34(1)
O(6)	8518(2)	10608(2)	1987(1)	45(1)

Table 3. Bond lengths [Å] and angles [°] for lsh501m.

C(1)-C(2)	1.362(4)	C(1)-C(6)	1.396(4)
C(2)-C(3)	1.395(4)	C(3)-C(4)	1.364(4)
C(4)-C(5)	1.402(4)	C(5)-N(2)	1.362(4)
C(5)-C(6)	1.406(4)	C(6)-N(1)	1.375(4)
C(7)-N(1)	1.321(4)	C(7)-C(8)	1.428(4)
C(8)-N(2)	1.317(3)	C(8)-C(9)	1.512(4)
C(9)-O(1)	1.233(3)	C(9)-N(3)	1.344(4)
C(10)-N(3)	1.453(4)	C(10)-C(11)	1.503(3)
C(11)-O(2)	1.433(3)	C(12)-O(2)	1.430(3)
C(12)-C(13)	1.522(4)	C(12)-C(14)	1.524(4)
C(12)-C(19)#1	1.554(4)	C(14)-N(4)	1.475(4)
C(15)-N(4)	1.476(3)	C(15)-C(16)	1.527(4)
C(16)-N(5)	1.485(4)	C(16)-C(17)	1.525(3)
C(16)-C(18)	1.529(3)	C(19)-O(3)	1.235(3)
C(19)-N(5)	1.345(4)	C(19)-C(12)#1	1.554(4)
C(20)-C(23)	1.362(4)	C(20)-C(21)	1.393(4)
C(21)-C(22)	1.348(4)	C(22)-C(25)	1.402(4)
C(23)-C(24)	1.397(4)	C(24)-N(6)	1.382(3)
C(24)-C(25)	1.412(4)	C(25)-N(7)	1.366(4)
C(26)-N(6)	1.321(3)	C(26)-C(38)	1.425(4)
C(26)-C(27)	1.515(4)	C(27)-O(4)	1.229(3)
C(27)-N(8)	1.330(4)	C(28)-N(8)	1.455(3)
C(28)-C(29)	1.494(4)	C(29)-O(5)	1.421(3)
C(30)-O(5)	1.433(3)	C(30)-C(31)	1.515(3)
C(30)-C(32)	1.522(4)	C(30)-C(34)	1.566(4)
C(32)-N(10)	1.475(3)	C(33)-N(10)	1.466(4)
C(33)-C(35)#2	1.522(4)	C(34)-O(6)	1.230(3)
C(34)-N(9)	1.340(4)	C(35)-N(9)	1.481(3)
C(35)-C(36)	1.516(4)	C(35)-C(33)#2	1.522(4)
C(35)-C(37)	1.527(4)	C(38)-N(7)	1.306(3)

C(2)-C(1)-C(6)	118.9(4)	C(1)-C(2)-C(3)	120.8(4)
C(4)-C(3)-C(2)	121.0(4)	C(3)-C(4)-C(5)	119.7(4)
N(2)-C(5)-C(4)	118.7(3)	N(2)-C(5)-C(6)	122.7(3)
C(4)-C(5)-C(6)	118.6(4)	N(1)-C(6)-C(1)	118.4(3)
N(1)-C(6)-C(5)	120.7(3)	C(1)-C(6)-C(5)	121.0(3)
N(1)-C(7)-C(8)	122.5(3)	N(2)-C(8)-C(7)	122.4(3)
N(2)-C(8)-C(9)	120.1(3)	C(7)-C(8)-C(9)	117.5(3)
O(1)-C(9)-N(3)	124.9(3)	O(1)-C(9)-C(8)	120.1(3)
N(3)-C(9)-C(8)	114.9(3)	N(3)-C(10)-C(11)	112.7(2)
O(2)-C(11)-C(10)	107.0(2)	O(2)-C(12)-C(13)	112.0(3)
O(2)-C(12)-C(14)	103.5(2)	C(13)-C(12)-C(14)	109.7(3)
O(2)-C(12)-C(19)#1	110.1(2)	C(13)-C(12)-C(19)#1	109.3(3)
C(14)-C(12)-C(19)#1	112.1(2)	N(4)-C(14)-C(12)	112.6(2)
N(4)-C(15)-C(16)	114.7(3)	N(5)-C(16)-C(17)	109.5(3)
N(5)-C(16)-C(15)	106.7(2)	C(17)-C(16)-C(15)	107.4(3)
N(5)-C(16)-C(18)	110.6(3)	C(17)-C(16)-C(18)	111.5(3)
C(15)-C(16)-C(18)	110.9(3)	O(3)-C(19)-N(5)	123.5(3)
O(3)-C(19)-C(12)#1	120.7(3)	N(5)-C(19)-C(12)#1	115.7(3)
C(23)-C(20)-C(21)	120.7(3)	C(22)-C(21)-C(20)	121.6(3)
C(21)-C(22)-C(25)	119.9(3)	C(20)-C(23)-C(24)	118.6(3)
N(6)-C(24)-C(23)	118.9(3)	N(6)-C(24)-C(25)	120.1(3)
C(23)-C(24)-C(25)	121.0(3)	N(7)-C(25)-C(22)	119.2(3)
N(7)-C(25)-C(24)	122.6(3)	C(22)-C(25)-C(24)	118.2(3)

N(6)-C(26)-C(38)	122.1(3)	N(6)-C(26)-C(27)	119.6(3)
C(38)-C(26)-C(27)	118.3(3)	O(4)-C(27)-N(8)	125.2(3)
O(4)-C(27)-C(26)	118.3(3)	N(8)-C(27)-C(26)	116.5(3)
N(8)-C(28)-C(29)	112.6(3)	O(5)-C(29)-C(28)	108.0(3)
O(5)-C(30)-C(31)	112.2(3)	O(5)-C(30)-C(32)	103.5(2)
C(31)-C(30)-C(32)	108.9(3)	O(5)-C(30)-C(34)	109.4(2)
C(31)-C(30)-C(34)	109.8(3)	C(32)-C(30)-C(34)	113.0(3)
N(10)-C(32)-C(30)	113.3(2)	N(10)-C(33)-C(35)#2	114.3(2)
O(6)-C(34)-N(9)	124.6(3)	O(6)-C(34)-C(30)	120.5(3)
N(9)-C(34)-C(30)	114.8(3)	N(9)-C(35)-C(36)	110.4(3)
N(9)-C(35)-C(33)#2	106.6(2)	C(36)-C(35)-C(33)#2	112.5(3)
N(9)-C(35)-C(37)	110.3(3)	C(36)-C(35)-C(37)	109.9(3)
C(33)#2-C(35)-C(37)	107.2(3)	N(7)-C(38)-C(26)	123.2(3)
C(7)-N(1)-C(6)	116.1(3)	C(8)-N(2)-C(5)	115.7(3)
C(9)-N(3)-C(10)	122.7(3)	C(14)-N(4)-C(15)	110.6(2)
C(19)-N(5)-C(16)	125.4(3)	C(26)-N(6)-C(24)	116.3(3)
C(38)-N(7)-C(25)	115.6(3)	C(27)-N(8)-C(28)	123.3(3)
C(34)-N(9)-C(35)	125.6(3)	C(33)-N(10)-C(32)	110.3(2)
C(12)-O(2)-C(11)	116.9(2)	C(29)-O(5)-C(30)	117.1(2)

Symmetry transformations used to generate equivalent atoms:

#1 -x+1,-y+1,-z+1 #2 -x+1,-y+2,-z

Table 4. Anisotropic displacement parameters [$Å^2$ x 10^3] for lsh501m.

The anisotropic displacement factor exponent takes the form:

$-2\pi^2 [(ha^*)^2 U_{11} + ... + 2hka^* b^* U_{12}]$

	U11	U22	U33	U23	U13	U12
C(1)	53(3)	40(2)	32(3)	10(2)	6(2)	17(2)
C(2)	67(3)	35(2)	40(3)	9(2)	20(2)	13(2)
C(3)	53(3)	55(3)	48(3)	15(2)	21(2)	26(2)
C(4)	47(3)	50(2)	46(3)	14(2)	14(2)	23(2)
C(5)	35(2)	30(2)	40(3)	12(2)	10(2)	10(2)
C(6)	41(2)	34(2)	34(2)	11(2)	9(2)	14(2)
C(7)	47(3)	55(3)	43(3)	22(2)	12(2)	27(2)
C(8)	38(2)	25(2)	32(2)	4(2)	4(2)	8(2)
C(9)	41(3)	29(2)	33(3)	7(2)	8(2)	11(2)
C(10)	34(2)	36(2)	26(2)	-1(2)	4(2)	8(2)
C(11)	36(2)	41(2)	24(2)	7(2)	4(2)	16(2)
C(12)	30(2)	30(2)	33(2)	10(2)	8(2)	13(2)
C(13)	47(2)	50(2)	42(3)	28(2)	21(2)	22(2)
C(14)	31(2)	29(2)	40(2)	10(2)	10(2)	9(2)
C(15)	28(2)	38(2)	35(2)	3(2)	6(2)	14(2)
C(16)	27(2)	39(2)	31(2)	7(2)	5(2)	17(2)
C(17)	32(2)	69(2)	40(2)	8(2)	2(2)	23(2)
C(18)	59(2)	48(2)	35(2)	8(2)	6(2)	35(2)
C(19)	31(2)	26(2)	32(2)	10(2)	-1(2)	9(2)
C(20)	55(3)	36(2)	50(3)	6(2)	15(2)	18(2)
C(21)	61(3)	39(2)	38(3)	3(2)	2(2)	12(2)
C(22)	43(2)	45(2)	48(3)	16(2)	3(2)	14(2)
C(23)	39(2)	33(2)	46(3)	8(2)	8(2)	15(2)
C(24)	39(2)	28(2)	37(3)	12(2)	12(2)	9(2)
C(25)	36(2)	32(2)	38(3)	7(2)	5(2)	9(2)
C(26)	34(2)	32(2)	43(3)	16(2)	16(2)	11(2)
C(27)	38(2)	27(2)	40(3)	12(2)	15(2)	9(2)
C(28)	48(2)	42(2)	32(2)	20(2)	14(2)	18(2)
C(29)	45(2)	44(2)	31(2)	15(2)	9(2)	20(2)
C(30)	34(2)	36(2)	26(2)	12(2)	7(2)	12(2)
C(31)	49(2)	43(2)	25(2)	-6(2)	-3(2)	7(2)
C(32)	38(2)	34(2)	35(2)	9(2)	5(2)	10(2)
C(33)	37(2)	32(2)	32(2)	8(2)	11(2)	14(2)
C(34)	31(2)	34(2)	29(2)	15(2)	7(2)	8(2)
C(35)	34(2)	37(2)	32(2)	13(2)	10(2)	21(2)
C(36)	35(2)	65(2)	34(2)	8(2)	11(2)	19(2)
C(37)	72(3)	58(2)	46(3)	24(2)	14(2)	40(2)
C(38)	41(2)	40(2)	59(3)	13(2)	14(2)	21(2)
N(1)	55(2)	63(2)	42(2)	25(2)	16(2)	31(2)
N(2)	37(2)	35(2)	33(2)	10(2)	11(2)	13(2)
N(3)	32(2)	41(2)	32(2)	9(2)	6(2)	15(2)
N(4)	25(2)	32(2)	36(2)	8(2)	3(1)	11(1)
N(5)	36(2)	39(2)	34(2)	13(2)	8(2)	22(2)
N(6)	41(2)	33(2)	41(2)	12(2)	15(2)	17(2)
N(7)	44(2)	44(2)	53(2)	10(2)	3(2)	21(2)
N(8)	42(2)	36(2)	40(2)	8(2)	7(2)	20(2)
N(9)	25(2)	46(2)	30(2)	7(2)	0(2)	18(2)

N(10)	35(2)	31(2)	28(2)	12(2)	7(2)	12(2)
O(1)	38(2)	58(2)	44(2)	10(1)	11(1)	25(1)
O(2)	31(1)	31(1)	33(2)	4(1)	1(1)	13(1)
O(3)	52(2)	46(2)	41(2)	15(1)	7(1)	30(1)
O(4)	72(2)	47(2)	50(2)	9(1)	9(1)	39(1)
O(5)	36(1)	39(1)	31(2)	16(1)	11(1)	17(1)
O(6)	30(1)	65(2)	39(2)	11(1)	1(1)	21(1)

Table 5. Hydrogen coordinates (x 10^4) and isotropic displacement parameters ($Å^2$ x 10^3) for lsh501m.

	x	y	z	U(eq)
H(1)	1608	1044	7174	52
H(2)	-396	1258	7371	59
H(3)	-1736	1714	6332	60
H(4)	-1135	1901	5065	55
H(7)	3757	1233	5043	54
H(10A)	996	1350	1789	43
H(10B)	2544	1449	2118	43
H(11A)	2501	3145	1571	41
H(11B)	1935	3540	2364	41
H(13A)	5203	5023	1761	64
H(13B)	5379	6332	2256	64
H(13C)	3855	5310	1748	64
H(14A)	6589	5067	3099	41
H(14B)	6496	6186	3699	41
H(15A)	7774	5893	4904	41
H(15B)	7890	4782	4312	41
H(17A)	9188	5817	6123	72
H(17B)	9428	4730	5589	72
H(17C)	8876	4587	6427	72
H(18A)	6751	2635	5561	67
H(18B)	7333	2804	4735	67
H(18C)	5784	2690	4734	67
H(20)	2229	3848	-1611	57
H(21)	220	3800	-2448	61
H(22)	-852	4985	-1961	57
H(23)	3203	5109	-253	48
H(28A)	4322	8637	3364	47
H(28B)	3724	9570	3087	47
H(29A)	6220	10425	3440	47
H(29B)	6149	9408	2661	47
H(31A)	7400	12768	3168	70
H(31B)	8599	12874	2674	70
H(31C)	8194	11898	3229	70
H(32A)	6022	12666	1856	45
H(32B)	6950	12439	1233	45
H(33A)	5207	12353	88	40
H(33B)	4253	12514	710	40
H(36A)	7937	10035	-296	69
H(36B)	8349	8908	-300	69
H(36C)	8948	10018	527	69
H(37A)	8051	8467	1304	80
H(37B)	7192	7335	496	80
H(37C)	6399	7703	1163	80
H(38)	143	7833	426	54
H(4B)	5450(30)	3790(20)	3852(17)	40(10)
H(5B)	5930(30)	5060(30)	5690(20)	56(11)
H(3B)	820(30)	1710(30)	3120(20)	66(13)
H(8B)	3680(30)	7480(20)	1956(19)	67(11)

H(9B)	5840(30)	9860(20)	674(18)	37(10)
H(10C)	4380(30)	10880(30)	1160(20)	63(14)

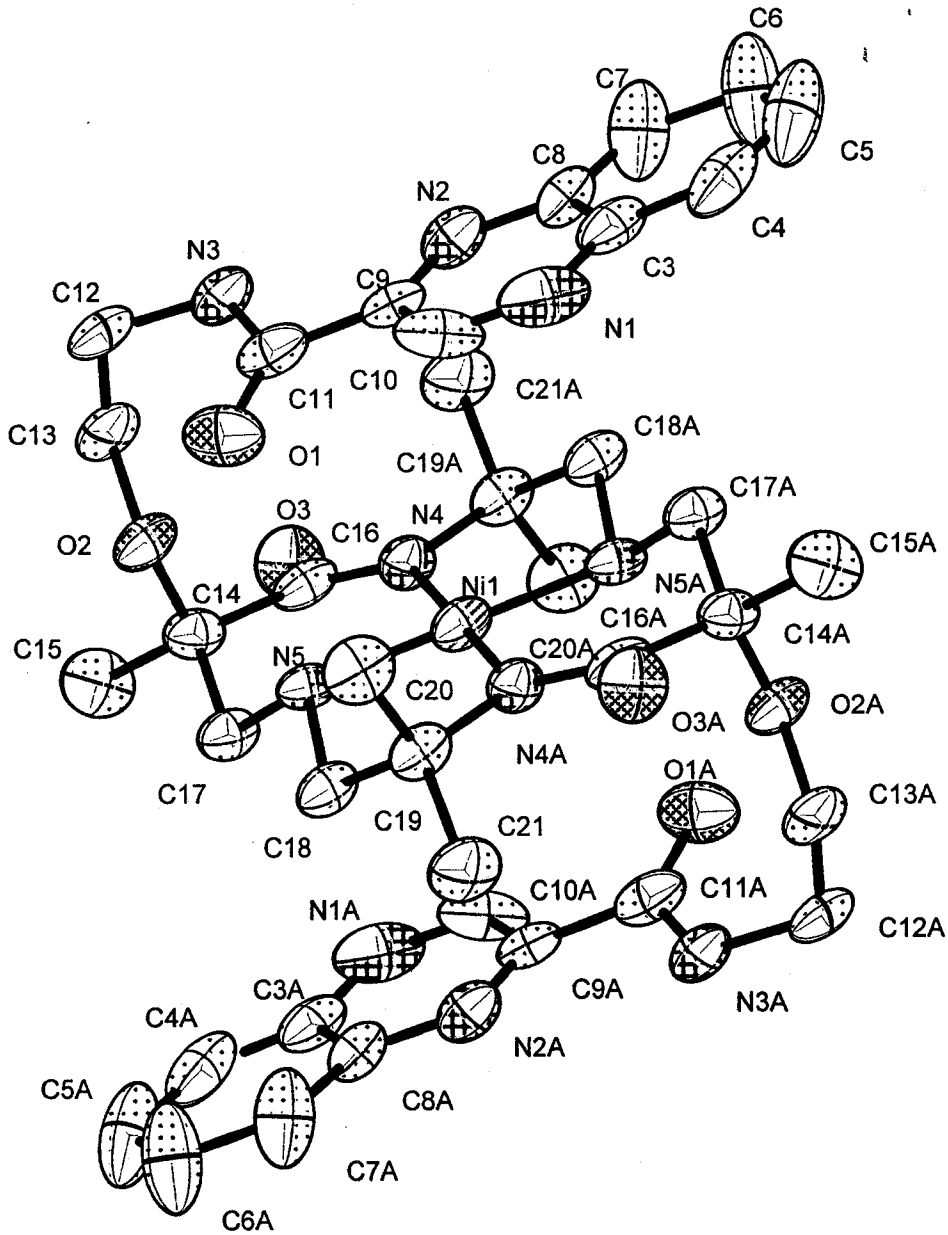

Table 1. Crystal data and structure refinement for sad.

Identification code	sad JW340fr2
Empirical formula	$C_{60}H_{46}Cl_6N_{10}NiO_6$
Formula weight	1274.48
Temperature	172(2) K
Wavelength	0.71073 Å
Crystal system	Monoclinic
Space group	P2(1)/c
Unit cell dimensions	a = 12.244(3) Å alpha = 90° b = 12.566(3) Å beta = 99.223(6)° c = 17.406(4) Å gamma = 90°
Volume, Z	2643.3(11) Å^3, 2
Density (calculated)	1.601 Mg/m^3
Absorption coefficient	0.738 mm^{-1}
Absorption correction	SADABS
Transmission factors	0.690 - 0.980
F(000)	1308
Crystal size	0.68 x 0.32 x 0.11mm
θ range for data collection	3.13 to 23.34°
Limiting indices	$-13 \le h \le 13$, $-13 \le k \le 13$, $-19 \le l \le 19$
Reflections collected	9948
Independent reflections	3789 (R_{int} = 0.0998)
Completeness to θ = 23.34°	98.7 %
Refinement method	Full-matrix least-squares on F^2
Data / restraints / parameters	3789 / 0 / 351
Goodness-of-fit on F^2	1.146
Final R indices [I>2σ(I)]	R1 = 0.0938, wR2 = 0.2146
R indices (all data)	R1 = 0.1778, wR2 = 0.2377
Largest diff. peak and hole	0.839 and -0.456 eÅ^{-3}

Table 2. Atomic coordinates [x 10^4] and equivalent isotropic displacement parameters [$Å^2$ x 10^3] for sad. U(eq) is defined as one third of the trace of the orthogonalized U_{ij} tensor.

	x	y	z	U(eq)
C(1)	187(15)	11030(20)	2159(11)	33(6)
C(2)	-598(17)	7616(19)	416(11)	42(6)
C(3)	4271(9)	9077(7)	-642(5)	46(3)
C(4)	3565(11)	9653(8)	-1208(6)	60(3)
C(5)	2536(11)	9903(10)	-1104(6)	78(4)
C(6)	2149(9)	9582(11)	-406(7)	88(4)
C(7)	2854(9)	9055(10)	167(6)	67(3)
C(8)	3930(8)	8801(7)	76(5)	39(2)
C(9)	5574(8)	8027(7)	489(5)	37(2)
C(10)	5906(9)	8277(8)	-221(6)	56(3)
C(11)	6363(8)	7447(8)	1086(6)	45(3)
C(12)	6801(8)	6929(8)	2449(5)	53(3)
C(13)	6464(8)	5788(8)	2559(4)	51(3)
C(14)	6179(8)	4187(7)	1773(4)	36(2)
C(15)	6523(8)	3407(8)	2425(5)	55(3)
C(16)	4911(8)	4358(7)	1629(5)	36(2)
C(17)	6613(7)	3774(7)	1057(4)	37(2)
C(18)	6975(7)	4143(7)	-230(4)	37(2)
C(19)	6725(7)	4869(7)	-933(4)	35(2)
C(20)	7491(8)	5845(7)	-822(5)	50(3)
C(21)	6965(8)	4219(8)	-1622(5)	52(3)
Cl(1)	196(6)	9381(6)	3238(4)	83(2)
Cl(2)	-83(11)	11401(13)	2492(6)	75(5)
Cl(3)	689(9)	9602(11)	1693(6)	60(4)
Cl(4)	203(5)	8456(6)	1115(3)	86(2)
Cl(5)	-821(7)	8366(8)	-593(5)	75(3)
Cl(6)	-40(40)	11420(40)	2280(30)	18(10)
Cl(7)	0(50)	6740(60)	680(60)	140(30)
Cl(8)	-14(19)	6210(20)	590(20)	30(5)
Cl(9)	-540(20)	7876(19)	-494(13)	30(6)
Cl(10)	0(20)	6400(30)	960(17)	38(7)
Cl(1A)	80(12)	8244(13)	3369(8)	42(4)
Cl(7A)	-252(10)	5933(11)	786(10)	31(4)
Cl(8A)	266(13)	6660(20)	306(10)	32(4)
Cl(9A)	-160(20)	7680(20)	-361(14)	24(8)
Cl(1C)	680(30)	10230(30)	2520(20)	47(10)
N(1)	5303(9)	8795(7)	-777(5)	61(3)
N(2)	4602(6)	8276(6)	643(4)	41(2)
N(3)	6101(6)	7465(6)	1805(4)	43(2)
N(4)	4448(6)	4839(6)	975(3)	33(2)
N(5)	6465(5)	4601(5)	415(3)	30(2)
Ni(1)	5000	5000	0	36(1)
O(1)	7192(5)	6998(5)	906(4)	55(2)
O(2)	6738(5)	5185(5)	1916(3)	43(2)
O(3)	4400(5)	4079(5)	2162(3)	51(2)

Table 3. Bond lengths [Å] and angles [°] for sad.

C(1)-Cl(6)	0.61(5)	C(1)-Cl(2)	0.85(2)
C(1)-Cl(1C)	1.28(4)	C(1)-Cl(3)	2.10(3)
C(2)-Cl(7)	1.36(7)	C(2)-Cl(9A)	1.54(3)
C(2)-Cl(8A)	1.63(3)	C(2)-Cl(9)	1.63(3)
C(2)-Cl(4)	1.78(2)	C(2)-Cl(8)	1.91(4)
C(2)-Cl(10)	1.88(4)	C(2)-Cl(5)	1.97(2)
C(2)-Cl(7A)	2.23(3)	C(3)-N(1)	1.368(12)
C(3)-C(4)	1.404(13)	C(3)-C(8)	1.422(11)
C(4)-C(5)	1.338(14)	C(5)-C(6)	1.430(14)
C(6)-C(7)	1.379(14)	C(7)-C(8)	1.390(13)
C(8)-N(2)	1.351(11)	C(9)-N(2)	1.299(10)
C(9)-C(10)	1.398(11)	C(9)-C(11)	1.491(13)
C(10)-N(1)	1.296(12)	C(11)-O(1)	1.243(10)
C(11)-N(3)	1.341(10)	C(12)-N(3)	1.462(11)
C(12)-C(13)	1.512(13)	C(13)-O(2)	1.436(9)
C(14)-O(2)	1.431(10)	C(14)-C(17)	1.521(10)
C(14)-C(15)	1.508(11)	C(14)-C(16)	1.547(12)
C(16)-O(3)	1.248(9)	C(16)-N(4)	1.333(10)
C(17)-N(5)	1.515(10)	C(18)-N(5)	1.485(9)
C(18)-C(19)	1.517(11)	C(19)-N(4)#1	1.473(10)
C(19)-C(21)	1.519(11)	C(19)-C(20)	1.538(12)
Cl(1)-Cl(1A)	1.458(16)	Cl(1)-Cl(1C)	1.81(4)
Cl(2)-Cl(1C)	1.74(5)	Cl(3)-Cl(1C)	1.65(4)
Cl(3)-Cl(4)	1.802(15)	Cl(4)-Cl(7)	2.29(7)
Cl(5)-Cl(9)	0.72(2)	Cl(5)-Cl(9A)	1.21(3)
Cl(6)-Cl(1C)	1.75(7)	Cl(6)-Cl(1A)#2	2.55(5)
Cl(7)-Cl(10)	0.65(9)	Cl(7)-Cl(8)	0.68(7)
Cl(7)-Cl(7A)	1.08(8)	Cl(7)-Cl(8A)	0.78(10)
Cl(7)-Cl(9A)	2.14(10)	Cl(7)-Cl(9)	2.49(10)
Cl(8)-Cl(7A)	0.60(4)	Cl(8)-Cl(10)	0.69(3)
Cl(8)-Cl(8A)	0.85(3)	Cl(8)-Cl(9A)	2.46(4)
Cl(8)-Cl(9)	2.81(4)	Cl(9)-Cl(9A)	0.54(3)
Cl(9)-Cl(8A)	2.19(3)	Cl(9)-Cl(1A)#3	2.63(3)
Cl(10)-Cl(7A)	0.71(4)	Cl(10)-Cl(8A)	1.27(4)
Cl(1A)-Cl(9)#4	2.63(3)	Cl(1A)-Cl(6)#5	2.55(5)
Cl(7A)-Cl(8A)	1.45(2)	Cl(8A)-Cl(9A)	1.75(3)
N(4)-C(19)#1	1.473(10)	N(4)-Ni(1)	1.935(6)
N(5)-Ni(1)	1.891(7)	Ni(1)-N(5)#1	1.891(7)
Ni(1)-N(4)#1	1.935(6)		

Cl(6)-C(1)-Cl(2)	24(4)	Cl(6)-C(1)-Cl(1C)	132(5)
Cl(2)-C(1)-Cl(1C)	107(3)	Cl(6)-C(1)-Cl(3)	170(5)
Cl(2)-C(1)-Cl(3)	154(3)	Cl(1C)-C(1)-Cl(3)	51.6(18)
Cl(7)-C(2)-Cl(9A)	95(5)	Cl(7)-C(2)-Cl(8A)	28(5)
Cl(9A)-C(2)-Cl(8A)	67.0(14)	Cl(7)-C(2)-Cl(9)	112(5)
Cl(9A)-C(2)-Cl(9)	19.4(12)	Cl(8A)-C(2)-Cl(9)	84.3(15)
Cl(7)-C(2)-Cl(4)	93(3)	Cl(9A)-C(2)-Cl(4)	109.8(15)
Cl(8A)-C(2)-Cl(4)	102.8(13)	Cl(9)-C(2)-Cl(4)	116.0(15)
Cl(7)-C(2)-Cl(8)	14(3)	Cl(9A)-C(2)-Cl(8)	90.5(18)
Cl(8A)-C(2)-Cl(8)	26.3(9)	Cl(9)-C(2)-Cl(8)	105.1(17)
Cl(4)-C(2)-Cl(8)	106.9(14)	Cl(7)-C(2)-Cl(10)	14(5)
Cl(9A)-C(2)-Cl(10)	108.7(18)	Cl(8A)-C(2)-Cl(10)	41.8(13)
Cl(9)-C(2)-Cl(10)	125.2(18)	Cl(4)-C(2)-Cl(10)	90.5(16)
Cl(8)-C(2)-Cl(10)	21.1(10)	Cl(7)-C(2)-Cl(5)	132(5)

Cl(9A)-C(2)-Cl(5)	37.8(11)	Cl(8A)-C(2)-Cl(5)	104.2(12)
Cl(9)-C(2)-Cl(5)	20.2(9)	Cl(4)-C(2)-Cl(5)	107.9(12)
Cl(8)-C(2)-Cl(5)	125.0(14)	Cl(10)-C(2)-Cl(5)	145.3(15)
Cl(7)-C(2)-Cl(7A)	21(3)	Cl(9A)-C(2)-Cl(7A)	103.0(15)
Cl(8A)-C(2)-Cl(7A)	40.5(11)	Cl(9)-C(2)-Cl(7A)	115.7(15)
Cl(4)-C(2)-Cl(7A)	107.8(12)	Cl(8)-C(2)-Cl(7A)	14.1(11)
Cl(10)-C(2)-Cl(7A)	17.5(11)	Cl(5)-C(2)-Cl(7A)	134.6(11)
N(1)-C(3)-C(4)	119.6(9)	N(1)-C(3)-C(8)	119.8(10)
C(4)-C(3)-C(8)	120.6(10)	C(5)-C(4)-C(3)	120.9(10)
C(4)-C(5)-C(6)	119.7(11)	C(7)-C(6)-C(5)	119.7(11)
C(6)-C(7)-C(8)	121.5(10)	N(2)-C(8)-C(7)	120.4(8)
N(2)-C(8)-C(3)	122.1(9)	C(7)-C(8)-C(3)	117.5(10)
N(2)-C(9)-C(10)	122.3(9)	N(2)-C(9)-C(11)	119.2(8)
C(10)-C(9)-C(11)	118.5(9)	N(1)-C(10)-C(9)	124.2(10)
O(1)-C(11)-N(3)	124.8(10)	O(1)-C(11)-C(9)	120.7(8)
N(3)-C(11)-C(9)	114.6(8)	N(3)-C(12)-C(13)	113.3(8)
O(2)-C(13)-C(12)	107.4(7)	O(2)-C(14)-C(17)	102.8(6)
O(2)-C(14)-C(15)	111.7(7)	C(17)-C(14)-C(15)	107.6(7)
O(2)-C(14)-C(16)	110.2(7)	C(17)-C(14)-C(16)	112.8(7)
C(15)-C(14)-C(16)	111.3(7)	O(3)-C(16)-N(4)	124.5(8)
O(3)-C(16)-C(14)	116.8(8)	N(4)-C(16)-C(14)	118.6(7)
C(14)-C(17)-N(5)	110.8(7)	N(5)-C(18)-C(19)	108.7(7)
N(4)#1-C(19)-C(18)	105.0(6)	N(4)#1-C(19)-C(21)	113.9(7)
C(18)-C(19)-C(21)	105.9(7)	N(4)#1-C(19)-C(20)	112.2(7)
C(18)-C(19)-C(20)	109.8(7)	C(21)-C(19)-C(20)	109.7(6)
Cl(1A)-Cl(1)-Cl(1C)	137.5(14)	C(1)-Cl(2)-Cl(1C)	45(2)
Cl(1C)-Cl(3)-Cl(4)	145.6(16)	Cl(1C)-Cl(3)-C(1)	37.6(14)
Cl(4)-Cl(3)-C(1)	143.8(8)	C(2)-Cl(4)-Cl(3)	162.0(10)
C(2)-Cl(4)-Cl(7)	36.4(18)	Cl(3)-Cl(4)-Cl(7)	161(2)
Cl(9)-Cl(5)-Cl(9A)	14(3)	Cl(9)-Cl(5)-C(2)	52(2)
Cl(9A)-Cl(5)-C(2)	51.1(12)	C(1)-Cl(6)-Cl(1C)	33(4)
C(1)-Cl(6)-Cl(1A)#2	123(6)	Cl(1C)-Cl(6)-Cl(1A)#2	148(3)
Cl(10)-Cl(7)-Cl(8)	63(8)	Cl(10)-Cl(7)-Cl(7A)	40(6)
Cl(8)-Cl(7)-Cl(7A)	30(7)	Cl(10)-Cl(7)-Cl(8A)	127(10)
Cl(8)-Cl(7)-Cl(8A)	71(9)	Cl(7A)-Cl(7)-Cl(8A)	101(8)
Cl(10)-Cl(7)-C(2)	136(10)	Cl(8)-Cl(7)-C(2)	136(10)
Cl(7A)-Cl(7)-C(2)	132(6)	Cl(8A)-Cl(7)-C(2)	96(10)
Cl(10)-Cl(7)-Cl(9A)	172(10)	Cl(8)-Cl(7)-Cl(9A)	110(10)
Cl(7A)-Cl(7)-Cl(9A)	132(7)	Cl(8A)-Cl(7)-Cl(9A)	50(7)
C(2)-Cl(7)-Cl(9A)	46(3)	Cl(10)-Cl(7)-Cl(4)	112(10)
Cl(8)-Cl(7)-Cl(4)	173(10)	Cl(7A)-Cl(7)-Cl(4)	147(8)
Cl(8A)-Cl(7)-Cl(4)	111(8)	C(2)-Cl(7)-Cl(4)	51(3)
Cl(9A)-Cl(7)-Cl(4)	76(3)	Cl(10)-Cl(7)-Cl(9)	165(9)
Cl(8)-Cl(7)-Cl(9)	112(10)	Cl(7A)-Cl(7)-Cl(9)	129(6)
Cl(8A)-Cl(7)-Cl(9)	59(7)	C(2)-Cl(7)-Cl(9)	37(3)
Cl(9A)-Cl(7)-Cl(9)	10.4(10)	Cl(4)-Cl(7)-Cl(9)	74(2)
Cl(7)-Cl(8)-Cl(7A)	115(10)	Cl(7)-Cl(8)-Cl(10)	56(8)
Cl(7A)-Cl(8)-Cl(10)	67(5)	Cl(7)-Cl(8)-Cl(8A)	60(10)
Cl(7A)-Cl(8)-Cl(8A)	174(4)	Cl(10)-Cl(8)-Cl(8A)	111(6)
Cl(7)-Cl(8)-C(2)	30(7)	Cl(7A)-Cl(8)-C(2)	115(3)
Cl(10)-Cl(8)-C(2)	77(4)	Cl(8A)-Cl(8)-C(2)	58.5(17)
Cl(7)-Cl(8)-Cl(9A)	55(10)	Cl(7A)-Cl(8)-Cl(9A)	147(3)
Cl(10)-Cl(8)-Cl(9A)	111(5)	Cl(8A)-Cl(8)-Cl(9A)	27.6(16)
C(2)-Cl(8)-Cl(9A)	38.7(10)	Cl(7)-Cl(8)-Cl(9)	55(10)
Cl(7A)-Cl(8)-Cl(9)	138(3)	Cl(10)-Cl(8)-Cl(9)	110(5)
Cl(8A)-Cl(8)-Cl(9)	36.6(16)	C(2)-Cl(8)-Cl(9)	34.0(10)
Cl(9A)-Cl(8)-Cl(9)	8.9(8)	Cl(9A)-Cl(9)-Cl(5)	148(7)
Cl(9A)-Cl(9)-C(2)	70(4)	Cl(5)-Cl(9)-C(2)	108(3)

Cl(9A)-Cl(9)-Cl(8A)	31(4)	Cl(5)-Cl(9)-Cl(8A)	155(3)
C(2)-Cl(9)-Cl(8A)	47.9(12)	Cl(9A)-Cl(9)-Cl(7)	45(4)
Cl(5)-Cl(9)-Cl(7)	138(3)	C(2)-Cl(9)-Cl(7)	30(2)
Cl(8A)-Cl(9)-Cl(7)	17.7(18)	Cl(9A)-Cl(9)-Cl(1A)#3	75(4)
Cl(5)-Cl(9)-Cl(1A)#3	118(2)	C(2)-Cl(9)-Cl(1A)#3	133.3(17)
Cl(8A)-Cl(9)-Cl(1A)#3	87.2(10)	Cl(7)-Cl(9)-Cl(1A)#3	104(2)
Cl(9A)-Cl(9)-Cl(8)	45(4)	Cl(5)-Cl(9)-Cl(8)	148(3)
C(2)-Cl(9)-Cl(8)	40.9(12)	Cl(8A)-Cl(9)-Cl(8)	13.4(6)
Cl(7)-Cl(9)-Cl(8)	12.9(18)	Cl(1A)#3-Cl(9)-Cl(8)	92.5(10)
Cl(7)-Cl(10)-Cl(7A)	105(9)	Cl(7)-Cl(10)-Cl(8)	61(7)
Cl(7A)-Cl(10)-Cl(8)	51(4)	Cl(7)-Cl(10)-Cl(8A)	29(8)
Cl(7A)-Cl(10)-Cl(8A)	89(3)	Cl(8)-Cl(10)-Cl(8A)	39(4)
Cl(7)-Cl(10)-C(2)	30(8)	Cl(7A)-Cl(10)-C(2)	110(3)
Cl(8)-Cl(10)-C(2)	82(4)	Cl(8A)-Cl(10)-C(2)	58.7(19)
Cl(1)-Cl(1A)-Cl(9)#4	133.5(10)	Cl(1)-Cl(1A)-Cl(6)#5	143.9(16)
Cl(9)#4-Cl(1A)-Cl(6)#5	82.0(15)	Cl(10)-Cl(7A)-Cl(8)	63(3)
Cl(10)-Cl(7A)-Cl(7)	35(5)	Cl(8)-Cl(7A)-Cl(7)	35(6)
Cl(10)-Cl(7A)-Cl(8A)	61(3)	Cl(8)-Cl(7A)-Cl(8A)	4(2)
Cl(7)-Cl(7A)-Cl(8A)	32(5)	Cl(10)-Cl(7A)-C(2)	52(3)
Cl(8)-Cl(7A)-C(2)	51(3)	Cl(7)-Cl(7A)-C(2)	27(3)
Cl(8A)-Cl(7A)-C(2)	47.0(9)	Cl(8)-Cl(8A)-Cl(7)	49(6)
Cl(8)-Cl(8A)-Cl(10)	31(3)	Cl(7)-Cl(8A)-Cl(10)	24(6)
Cl(8)-Cl(8A)-Cl(7A)	2.6(18)	Cl(7)-Cl(8A)-Cl(7A)	47(6)
Cl(10)-Cl(8A)-Cl(7A)	29.5(19)	Cl(8)-Cl(8A)-Cl(9A)	139(2)
Cl(7)-Cl(8A)-Cl(9A)	110(7)	Cl(10)-Cl(8A)-Cl(9A)	133(2)
Cl(7A)-Cl(8A)-Cl(9A)	137.0(13)	Cl(8)-Cl(8A)-C(2)	95.1(19)
Cl(7)-Cl(8A)-C(2)	56(6)	Cl(10)-Cl(8A)-C(2)	79.5(19)
Cl(7A)-Cl(8A)-C(2)	92.5(12)	Cl(9A)-Cl(8A)-C(2)	53.9(12)
Cl(8)-Cl(8A)-Cl(9)	130(2)	Cl(7)-Cl(8A)-Cl(9)	103(7)
Cl(10)-Cl(8A)-Cl(9)	126.2(19)	Cl(7A)-Cl(8A)-Cl(9)	127.8(11)
Cl(9A)-Cl(8A)-Cl(9)	9.3(12)	C(2)-Cl(8A)-Cl(9)	47.8(11)
Cl(9)-Cl(9A)-Cl(5)	18(4)	Cl(9)-Cl(9A)-Cl(8A)	139(5)
Cl(5)-Cl(9A)-Cl(8A)	148.9(17)	Cl(9)-Cl(9A)-C(2)	90(4)
Cl(5)-Cl(9A)-C(2)	91.1(17)	Cl(8A)-Cl(9A)-C(2)	59.1(13)
Cl(9)-Cl(9A)-Cl(7)	124(5)	Cl(5)-Cl(9A)-Cl(7)	130(2)
Cl(8A)-Cl(9A)-Cl(7)	20(2)	C(2)-Cl(9A)-Cl(7)	39(2)
Cl(9)-Cl(9A)-Cl(8)	126(5)	Cl(5)-Cl(9A)-Cl(8)	137.0(16)
Cl(8A)-Cl(9A)-Cl(8)	13.0(7)	C(2)-Cl(9A)-Cl(8)	50.9(13)
Cl(7)-Cl(9A)-Cl(8)	15(2)	C(1)-Cl(1C)-Cl(3)	91(2)
C(1)-Cl(1C)-Cl(2)	27.8(11)	Cl(3)-Cl(1C)-Cl(2)	117(2)
C(1)-Cl(1C)-Cl(1)	128(3)	Cl(3)-Cl(1C)-Cl(1)	112(2)
Cl(2)-Cl(1C)-Cl(1)	106.6(18)	C(1)-Cl(1C)-Cl(6)	15.1(19)
Cl(3)-Cl(1C)-Cl(6)	106(3)	Cl(2)-Cl(1C)-Cl(6)	12.8(17)
Cl(1)-Cl(1C)-Cl(6)	118(2)	C(10)-N(1)-C(3)	115.7(8)
C(9)-N(2)-C(8)	116.0(8)	C(11)-N(3)-C(12)	120.6(8)
C(16)-N(4)-C(19)#1	115.7(6)	C(16)-N(4)-Ni(1)	129.5(6)
C(19)#1-N(4)-Ni(1)	113.9(5)	C(18)-N(5)-C(17)	106.1(6)
C(18)-N(5)-Ni(1)	107.6(5)	C(17)-N(5)-Ni(1)	117.2(5)
N(5)#1-Ni(1)-N(5)	180.0(4)	N(5)#1-Ni(1)-N(4)	85.4(3)
N(5)-Ni(1)-N(4)	94.6(3)	N(5)#1-Ni(1)-N(4)#1	94.6(3)
N(5)-Ni(1)-N(4)#1	85.4(3)	N(4)-Ni(1)-N(4)#1	180.0(4)
C(14)-O(2)-C(13)	115.7(6)		

Symmetry transformations used to generate equivalent atoms:

#1 -x+1,-y+1,-z #2 -x,y+1/2,-z+1/2 #3 x,-y+3/2,z-1/2

#4 x,-y+3/2,z+1/2 #5 -x,y-1/2,-z+1/2

Table 5. Hydrogen coordinates (x 10^4) and isotropic displacement parameters ($Å^2$ x 10^3) for sad.

	x	y	z	U(eq)
H(4)	3820	9868	-1672	72
H(5)	2065	10292	-1491	94
H(6)	1410	9730	-338	105
H(7)	2597	8862	635	80
H(10)	6621	8053	-300	67
H(12A)	6772	7329	2935	63
H(12B)	7577	6940	2353	63
H(13A)	6864	5504	3056	61
H(13B)	5659	5747	2571	61
H(15A)	7333	3366	2536	82
H(15B)	6220	2702	2271	82
H(15C)	6240	3644	2892	82
H(17A)	6210	3117	869	44
H(17B)	7407	3595	1197	44
H(18A)	6670	3424	-362	45
H(18B)	7785	4078	-69	45
H(20A)	7331	6308	-1279	75
H(20B)	8264	5611	-759	75
H(20C)	7367	6239	-358	75
H(21A)	6366	3704	-1772	78
H(21B)	7666	3838	-1478	78
H(21C)	7016	4694	-2061	78

Table 4. Anisotropic displacement parameters [$Å^2$ x 10^3] for sad.

The anisotropic displacement factor exponent takes the form:

$-2\pi^2$ [$(ha^*)^2U_{11}$ + ... + $2hka^*b^*U_{12}$]

	U11	U22	U33	U23	U13	U12
C(3)	79(8)	25(6)	34(6)	-6(5)	11(6)	-16(6)
C(4)	89(9)	51(8)	36(6)	-3(5)	1(6)	-23(7)
C(5)	78(9)	95(10)	53(7)	29(7)	-17(6)	-42(9)
C(6)	42(7)	125(13)	89(9)	25(8)	-10(7)	-14(7)
C(7)	48(7)	98(10)	53(7)	18(7)	3(6)	-17(7)
C(8)	49(7)	40(6)	29(5)	-9(5)	4(5)	-14(5)
C(9)	51(7)	29(6)	32(5)	-11(4)	11(5)	-7(5)
C(10)	95(9)	28(7)	57(7)	3(5)	44(7)	5(6)
C(11)	48(7)	39(7)	53(6)	-21(5)	21(6)	-16(5)
C(12)	70(8)	49(7)	39(6)	-29(5)	6(5)	0(6)
C(13)	79(8)	52(8)	21(5)	-10(5)	5(5)	8(6)
C(14)	51(7)	29(6)	27(5)	-1(4)	6(4)	-2(5)
C(15)	89(8)	50(7)	28(5)	11(5)	20(5)	14(6)
C(16)	56(7)	25(6)	29(5)	-7(4)	13(5)	-13(5)
C(17)	56(6)	28(6)	29(5)	0(4)	11(4)	-1(5)
C(18)	52(6)	36(6)	26(5)	-2(4)	13(4)	-10(5)
C(19)	46(6)	35(6)	27(4)	-1(4)	15(4)	-8(5)
C(20)	65(7)	49(7)	40(5)	4(5)	20(5)	-11(6)
C(21)	70(7)	58(7)	32(5)	-4(5)	19(5)	4(6)
Cl(1)	73(5)	73(5)	117(6)	35(4)	53(4)	4(4)
Cl(2)	72(6)	98(9)	56(7)	38(7)	12(6)	-4(5)
Cl(3)	37(7)	106(12)	40(6)	15(7)	14(5)	41(7)
Cl(4)	48(4)	138(7)	70(4)	-57(4)	6(3)	-33(4)
Cl(5)	79(7)	63(7)	80(6)	-5(5)	1(4)	-12(5)
Cl(8A)	25(9)	40(12)	32(9)	-14(10)	4(8)	22(9)
N(1)	112(8)	37(6)	40(5)	3(4)	34(5)	-3(6)
N(2)	45(5)	45(6)	33(4)	-7(4)	11(4)	-11(4)
N(3)	59(5)	47(5)	22(4)	-10(4)	6(4)	-3(4)
N(4)	43(5)	33(5)	21(4)	1(4)	6(3)	2(4)
N(5)	43(5)	27(4)	26(4)	-3(3)	21(3)	-5(3)
Ni(1)	55(1)	32(1)	24(1)	-1(1)	11(1)	-7(1)
O(1)	58(5)	50(5)	64(4)	-7(4)	30(4)	0(4)
O(2)	60(4)	44(5)	26(3)	-8(3)	10(3)	-7(3)
O(3)	66(4)	56(5)	35(3)	15(3)	20(3)	-5(4)